

Biomechanical aspects of the pelvic bone and
design criteria for acetabular prostheses

Dalstra, Michel

Biomechanical aspects of the pelvic bone and design
criteria for acetabular prostheses / Michel Dalstra. -
[S.l. : s.n.] (Nijmegen : Drukkerij Leijn). - Ill.
Proefschrift Nijmegen. - Met lit. opg. - Met samenvatting
in het Nederlands.

ISBN 90-9006517-2

Trefw.: biomechanica / orthopedie / gewrichtsprothesen.

No part of this book may be reproduced in any form without
written permission of the author.

Druk: Drukkerij Leijn, Nijmegen

Publication of this dissertation was made possible by a grant from
"Het Wijbenga-Leen", Bolsward, The Netherlands

Additional support was received from:
AlloPro Nederland BV, Eindhoven, The Netherlands
DePuy, Warsaw IN, USA
Howmedica Nederland, Haarlem, The Netherlands
Mathys Ltd, Bettlach, Switzerland
Ortomed BV, Zwijndrecht, The Netherlands
Protek AG, Bern, Switzerland
West Meditec BV, Bilthoven, The Netherlands

Biomechanical aspects of the pelvic bone and design criteria for acetabular prostheses

Een wetenschappelijke proeve op het gebied van de
Medische Wetenschappen

Proefschrift ter verkrijging van de graad van doctor
aan de Katholieke Universiteit Nijmegen,
volgens het besluit van het College van Decanen
in het openbaar te verdedigen
op maandag 15 november 1993
des namiddags om 1.30 uur precies

door

Michel Dalstra

geboren op 15 november 1961 te Enschede

Promotor: Prof. Dr. Ir. R. Huiskes

..., ende voor alle tuestere secken dir verietten sijn ende naet voorclaert, ...
uit de stichtingsakte van het Wijbenga-leen (10 oktober 1452)

Voor mijn ouders

Dankwoord

Het is reeds menigmaal gezegd: "Promoveren doe je niet alleen!" Maar het is toch vaak pas bij het schrijven van het dankwoord van het proefschrift, dat je dit ten volste realiseert en apprecieert.

In de eerste plaats is daar mijn promotor Rik Huiskes. Beste Rik, ik ben jou erg dankbaar dat jij mij indertijd in staat hebt gesteld om na mijn afstuderen en militaire dienst terug te keren naar Nijmegen voor promotie onderzoek. Als leermeester had ik mij geen betere dan jou kunnen wensen. Jouw verblijf in Ann Arbor was voor mij zo in het laatste jaar van mijn onderzoek niet altijd even gemakkelijk, maar toch kon ik altijd rekenen op een vlotte en gedegen reactie op mijn manuscripten per fax. Juist nu ik binnenkort het honk ga verlaten, blijf ik jou beschouwen als mijn grote voorbeeld.

Voor de geweldige werksfeer tekenden mijn collega-(oud-)promovendi: Leendert Blankevoort, Jan Herman Kuiper, Dorethé Mommersteeg, Margriet Mullender, Bert van Rietbergen, Nico Verdonshot en Harrie Weinans. Jongens, bedankt voor jullie bijdrage, zij het groot of klein. Ik zal jullie straks missen.

Een deel van het werk voor Hoofdstuk I heb ik uitgevoerd bij het *Biomekanisk Laboratorium* van het *Ortopædisk Hospital* van de Universiteit van Aarhus. Ik wil speciaal Anders Odgaard en Prof. Sneppen bedanken voor de fijne samenwerking.

Voor het verkrijgen van de heupbeenderen voor de verschillende experimenten was ik aangewezen op de vakgroep Anatomie. Dank aan Prof. Kauer en zijn medewerkers, die behulpzaam zijn geweest bij het uitprepareren van de botten.

De CT-scans konden worden gemaakt dankzij de faciliteiten van de afdeling Radiodiagnostiek. Ik wil bij deze Leon van Erning bedanken voor het extra werk dat ik hem hiermee bezorgde.

Binnen de eigen gelederen gaat mijn dank uit naar Willem van de Wijdeven voor zijn technische assistentie bij de experimenten. Verder ben ik Huub Peeters en René van der Venne zeer erkentelijk voor hun hulp wanneer een computer het weer eens niet deed zoals ik wilde.

Wie ik ook niet onvernoemd wil laten zijn de leden van de manuscriptcommissie. Ik wil Prof. Gabreëls, Prof. Grootenboer (Universiteit Twente), Dr. Jansen en Prof. van der Linden (Rijks Universiteit Limburg) bedanken voor het nemen van de moeite om in hun vrije tijd mijn werk te bestuderen.

Tenslotte nog een woord aan al mijn vrienden. Ik realiseer mij dat ik jullie de afgelopen tijd niet de aandacht heb gegeven die jullie verdienen. Ik hoop dat wij de oude draad gauw weer op kunnen pakken.

Contents

	Introduction	11
Chapter I	Mechanical and textural properties of pelvic trabecular bone	17
Chapter II	Development and validation of a three-dimensional finite element model of the pelvic bone	37
Chapter III	Load transfer across the pelvic bone	53
Chapter IV	The effects of total hip replacement on pelvic load transfer	69
Chapter V	Prestresses around the acetabulum generated by screwed cups	83
Chapter VI	Differences in pelvic load transfer due to variations in acetabular cup design	97
Chapter VII	Towards a mechanically optimized acetabular cup?	111
	Summary and conclusion	125
	Samenvatting en conclusie	129
	Curriculum Vitae	135

Introduction

Since many years, replacement of the hip joint by a total hip arthroplasty has become a standard orthopaedic operation. For people suffering from osteoarthritis or rheumatoid arthritis a total hip arthroplasty offers pain relief, usually fully restores normal function and has only a small chance of failure of the implant. It is because of this that this type of operation is being considered to be one of the most successful operations of this century. Yet, the probability of implant failure is not entirely negligible. Roughly speaking about 10 percent of the implants need to be revised after 10 years postoperatively (Ahnfelt *et al.*, 1990). Whether or not failure occurs depends on patient-related factors, such as age, sex and loading history, on implant-related factors, such as design and type of fixation to the bone and on surgical factors, like cementing technique and positioning of the prosthesis. The design of the implant, the choice of materials and the manner in which the implant is fixated to the bone, have seen an enormous development over the last two decades in attempts to improve the quality of total hip arthroplasties. And although these attempts have not always proved to be successful, they have helped to enlarge our knowledge of the subject.

In particular the femoral part of the total hip arthroplasty has traditionally been a subject of study. This has arisen out of clinical demand as short- and medium-term follow-up studies (Stauffer, 1982; Sutherland *et al.*, 1982) showed that it were the stems which failed more often than the acetabular components. As a result of this somewhat unidirectional attention, we have now a fairly good idea of how the mechanics of a femoral stem *in situ* works and what the underlying causes for failure of these implants are. Whatever the individual design may look like, it is always some kind of compromise between a stiff stem, which is known to cause much proximal bone resorption and a flexible stem which generates high proximal interface stresses between implant and bone. These insights have also boosted the predictive power of pre-clinical testing methods for femoral stems (Huiskes, 1991). Stress analyses and computer models simulating adaptive bone remodeling around an implant (Weinans, 1991) can now supply information about the performance of a given design before it is actually used in clinical practice with a fair amount of certainty. In addition, computer optimization methods have been combined with traditional stress analyses to develop design guidelines for mechanically optimal femoral stems (Huiskes and Boeklagen, 1989; Kuiper, 1993).

Unfortunately much less is known about the basic mechanics of the pelvic bone and the acetabular component of a total hip arthroplasty. Unlike the simple, yet effective, mechanical paradigm for the femoral stem as a stiff rod in a hollow tube (Huiskes, 1980), the irregular outer geometry and complex inner architecture of the

pelvic bone make its mechanics and that of an acetabular cup more difficult to fathom.

The mature pelvic bone consists mainly of trabecular bone. Its outer surface is entirely covered with a thin layer of cortical bone. By this it resembles a so-called 'sandwich' construction, a structure which is used in engineering to combine high strength and low weight (Jacob *et al.*, 1976; Dalstra and Huiskes, 1990a). For the pelvic bone this means that the main load transfer takes place predominantly in the cortical shells, while the trabecular bone works as a spacer material keeping the shells from buckling. About the implications of this load transfer for the pelvic bone itself and the effect of an acetabular implant thereupon, little is known though. Pelvic stresses, strains and deformation patterns have been investigated in strain-gage experiments (Jacob *et al.*, 1976; Petty *et al.*, 1980; Lionberger *et al.*, 1985; Finlay *et al.*, 1986; Ries *et al.*, 1989; Dalstra and Huiskes, 1990a), photoelastic analyses (Holm, 1981; Yoshioka and Shiba, 1981; Miles and McNamee, 1989) and finite element modeling (Goel *et al.*, 1978; Vasu *et al.*, 1982; Carter *et al.*, 1982; Pedersen *et al.*, 1982; Oonishi *et al.*, 1983; Rapperport *et al.*, 1985; Huiskes, 1987; Koeneman *et al.*, 1989; Dalstra and Huiskes, 1990b; Landjerit *et al.*, 1992; Renaudin *et al.*, 1992). The results from most of these studies, however, should be interpreted with some reservations. *In vitro* loading of pelvic bones in strain-gage experiments is often restricted to just a substitute for the hip-joint force and the strain gages can only provide local data. Extrapolating this to actual stress distributions across the whole pelvic bone is difficult due to its irregular shape. Photoelastic analyses require considerable simplifications with regard to the realistic geometry and loading conditions. Apart from that, the results are difficult to interpret quantitatively. Potentially finite element modeling is the best candidate to study pelvic mechanics, but then a model prediction is only as good as the model itself. In most of the early pelvic finite element studies only the acetabulum and its immediate vicinity were considered, and two-dimensional or axisymmetric models were used to describe it. We know that for a femoral configuration this approach produces results which reasonably approximate the three-dimensional results (Verdonschot and Huiskes, 1990). But does this also hold true for a pelvic configuration? Results from these type of models are now often incompatible with clinical observations and this puts the adequacy of these models to question. Yet, three-dimensional modeling has hardly been used at all to study of pelvic load transfer or to evaluate acetabular prostheses. So, all in all the map of pelvic mechanics is still covered by large portions of *terra incognita*. Should the present acetabular prostheses perform satisfactorily, then this problem would not be so acute. However, more and more the opinion takes shape that the acetabular component will ultimately be the restrictive factor in the long-term endurance of total hip arthroplasty.

Clinical follow-up studies have shown that the primary cause for failure of acetabular prostheses is aseptic loosening (Charnley, 1979; Stauffer, 1982; Sutherland *et al.*, 1982). Survival rates suggest that the occurrence of implant loosening sharply increases after eight to ten years postoperatively resulting in a high number of late

acetabular failures (Sutherland *et al.*, 1982; Mulroy and Harris, 1990). The precise etiology of aseptic loosening for acetabular cups and the extent to which mechanical factors play a role in this process, however, are not well understood yet. Small polyethylene wear particles are seen as an important contributor to tissue reactions in the bone surrounding the implant (Wroblewski, 1986; Schmalzried *et al.*, 1992), but it is not known whether loosening is actually initiated by this polyethylene debris. Schmalzried *et al.* (1992) found a characteristic development in the loosening process of cemented cups. A front of bone resorption and soft tissue formation starts circumferentially at the edge of the cement mantle and then gradually progresses towards the dome of the cup. Their histologic analysis revealed that bone resorption is a result of macrophage inflammatory response to the polyethylene particles and they did not find evidence for mechanical failure of the cups, which led them to hypothesize that aseptic loosening of acetabular components and aseptic loosening of femoral components are in fact two different processes; the first being biological in nature, the second mechanical. However, Weinans *et al.* (1993) have shown that the development of a soft-tissue layer around an implant can very well be mechanically induced or regulated by mechanical stimuli. Therefore, mechanical aspects of acetabular cups should not be overlooked. Also the fact that some designs have a significant better performance than others (Carlson *et al.*, 1988; Ritter *et al.*, 1990) supports the hypothesis that the success of a particular acetabular implants is, at least partially, determined by mechanical factors.

The study which resulted in the present dissertation was set up about five years ago with the intention to enhance current views on pelvic mechanics and to catch up with the femoral lead. A proper insight in the basic mechanics of the pelvic bone will be the key to a better understanding of the mechanical behavior and performance of acetabular prostheses in general, and it may even provide information concerning the possible mechanisms underlying failure of acetabular cups.

Structure of the dissertation

In this dissertation several aspects of pelvic mechanics and acetabular implants will be discussed. Although both experimental methods and computer models have been used, the emphasis lies on the development and use of a three-dimensional finite element model of the pelvic bone.

Chapter I describes a study of the mechanical properties of pelvic trabecular bone. Trabecular bone is known to display a wide range of textures and densities throughout different locations in the skeleton, yet as it happened to be, virtually no quantitative data on the material properties of trabecular bone from pelvic origin existed. To be able to supply the finite element model with realistic input, elastic moduli and density distributions of the pelvic trabecular bone were determined, using both traditional mechanical testing and stereological measurements.

In Chapter II the development of the three-dimensional finite element model of the pelvic bone is described, whereby Quantitative Computer Tomography was used

to maximize a realistic representation of the material properties throughout the pelvic bone. Validation of this model was done by simulating an *in vitro* loading experiment and comparing the numerical and the experimental results.

The model is then used in Chapter III to study the load transfer in a natural pelvic bone under normal loading. Using physiological data for the hip-joint force and the most important muscle forces, stress distributions throughout the pelvic bone are analyzed for several phases of a walking cycle.

Chapter IV describes the mechanical consequences of the placement of an acetabular cup for the pelvic load transfer. The model is adjusted to account for both a relatively flexible and a relatively stiff acetabular reconstruction. The stress distributions in both implant and bone are investigated, as well as the changes in load transfer relative to the normal situation.

One of the possibilities for acetabular reconstruction is fixation with screwed cups. The prestresses these cups generate upon insertion are important for the initial stability of the implant, yet no quantitative data on these stresses exists. Chapter V describes *in vitro* experiments in which these prestresses are determined for two different designs of screwed cups. The effect of the prestresses on the stress distributions due to normal loading are assessed as well.

In Chapter VI the three-dimensional pelvic finite element model is used again, this time to study the influences of various design features of acetabular cups on the load transfer across the pelvic bone and on the stress distributions in the various materials. These design features include the presence of a metal backing, the use of bone cement and the thickness of the polyethylene liner.

Finally, in Chapter VII, the model is used in combination with a numerical optimization procedure. By varying the local stiffness of the backing of an acetabular cup, this procedure searches for the most optimal design for a cup with regard to loading of the cement mantle and the subchondral bone.

References

- Ahnfelt, L., Herberts, P., Malchau, H., Andersson, G.B.J. (1990) Prognosis of total hip replacement. A Swedish multicenter study of 4,664 revisions. *Acta Orthop. Scand.*, **61**, Suppl. 238.
- Carlson, A.S., Lindberg, H.O., Sanzén, L. (1988) Loosening of the socket in a 35-mm snap-fit prosthesis and the Charnley hip prosthesis. *Clin. Orthop. Rel. Res.*, **228**, 63-68.
- Carter, D.R., Vasu, R., Harris, W.H. (1982) Stress distributions in the acetabular region II: effects of cement thickness and metal backing of the total hip acetabular component. *J. Biomech.*, **15**, 165-170.
- Charnley, J. (1979) *Low friction arthroplasty of the hip.*, Springer-Verlag, New York, 1979.
- Dalstra, M., Huiskes, R. (1990a) Pre-stresses generated in acetabular bone by screwed-cup fixation in THA. *Proc. Europ. Soc. Biomech.*, **7**, A17.
- Dalstra, M., Huiskes, R. (1990b) The pelvic bone as a sandwich construction; a three dimensional finite element study. *Proc. Europ. Soc. Biomech.*, **7**, B32.
- Finlay, J.B., Bourne, R.B., Landsberg, P.D., Andreae, P. (1986) Pelvic stresses *in vitro* - I. malsizing of endoprostheses. *J. Biomech.*, **19**, 703-714.
- Goel, V.K., Valliappan, S., Svensson, N.L. (1978) Stresses in the normal pelvis. *Comput. Biol. Med.*, **8**, 91-104.

- Holm, N.J. (1981) The development of a two-dimensional stress-optical model of the os coxae. *Acta Orthop. Scand.*, **52**, 135-143.
- Huiskes, R. (1980) Some fundamental aspects of human joint replacement. *Acta Orthop. Scand.*, **51**, Suppl. 185.
- Huiskes, R. (1987) Finite element analysis of acetabular reconstruction. *Acta Orthop. Scand.*, **58**, 620-625.
- Huiskes, R., Boeklagen, R. (1989) Mathematical shape optimization of hip prosthesis design. *J. Biomech.*, **22**, 793-804.
- Huiskes, R. (1991) Biomechanics of artificial-joint fixation. In: *Basic orthopaedic biomechanics.*, eds. V.C. Mow, W.C. Hayes, Raven Press, New York.
- Jacob, H.A.C., Huggler, A.H., Dietschi, C., Schreiber, A. (1976) Mechanical function of subchondral bone as experimentally determined on the acetabulum of the human pelvis. *J. Biomech.*, **9**, 625-627.
- Koeneman, J.B., Hansen, T.M., Beres, K. (1989) Three dimensional finite element analysis of the hip joint. *Trans. Orthop. Res. Soc.*, **14**, 223.
- Kuiper, J.H. (1993) *Numerical optimization of artificial hip joint designs.*, dissertation, University of Nijmegen, Nijmegen, the Netherlands.
- Landjerit, B., Jacquard-Simon, N., Thourot, M., Massin, P.H. (1992) Physiological loadings on human pelvis: a comparison between numerical and experimental simulations. *Proc. Europ. Soc. Biomech.*, **8**, 195.
- Lionberger, D., Walker, P.S., Granholm, J. (1985) Effects of prosthetic acetabular replacement on strains in the pelvis. *J. Orthop. Res.*, **3**, 372-379.
- Miles, A.W., McNamee, P.B. (1989) Strain gauge and photoelastic evaluation of the load transfer in the pelvis in total hip replacement: the effect of the position of the axis of rotation. *Proc. Instn. Mech. Engrs.*, **203**, 103-107.
- Mulroy, R.D., Harris, W.H. (1990) The effect of improved cementing techniques on component loosening in total hip replacement - an 11-year radiographic review. *J. Bone Joint Surg.*, **72-B**, 757-760.
- Oonishi, H., Isha, H., Hasegawa, T. (1983) Mechanical analysis of the human pelvis and its application to the acetabular hip joint - by means of the three dimensional finite element method. *J. Biomech.*, **16**, 427-444.
- Pedersen, D.R., Crowninshield, R.D., Brand, R.A., Johnston, R.C. (1982) An axisymmetric model of acetabular components in total hip arthroplasty. *J. Biomech.*, **15**, 305-315.
- Petty, W., Miller, G.J., Piotrowski, G. (1980) In vitro evaluation of the effect of acetabular prosthesis implantation on human cadaver pelvis. *Bull. Pros. Res.*, **17**, 80-89.
- Rapperport, D.J., Carter, D.R., Schurman, D.J. (1985) Contact finite element stress analysis of the hip joint. *J. Orthop. Res.*, **3**, 435-446.
- Renaudin, F., Lavaste, F., Skalli, W., Pecheux, C., Schmitt, V. (1992) A 3D finite element model of pelvis in side impact. *Proc. Europ. Soc. Biomech.*, **8**, 194.
- Ries, M., Pugh, J., Au, J.C., Gurtowski, J., Dee, R. (1989) Cortical pelvic strains with varying size hemiarthroplasty in vitro. *J. Biomech.*, **22**, 775-780.
- Ritter, M.A., Keating, E.M., Faris, Ph.M., Brugo, G. (1990) Metal-backed acetabular cups in total hip arthroplasty. *J. Bone Joint Surg.*, **72-A**, 672-677.
- Schmalzried, Th.P., Kwong, L.M., Jasty, M., Sedlacek, R.C., Haire, T.C., O'Connor, D.O., Bragdon, Ch.R., Kabo, J.M., Malcolm, A.J., Path, M.R.C., Harris, W.H. (1992) The mechanism of loosening of cemented acetabular components in total hip arthroplasty. *Clin. Orthop. Rel. Res.*, **274**, 60-78.
- Stauffer, R.N. (1982) Ten year follow-up study of total hip replacement. *J. Bone Joint Surg.*, **64-A**, 983-990.
- Sutherland, Ch.J., Wilde, A.H., Borden, L.S., Marks, K.E. (1982) A ten-year follow-up of one hundred consecutive Müller curved-stem total hip-replacement arthroplasties. *J. Bone Joint Surg.*, **64-A**, 970-982.
- Vasu, R., Carter, D.R., Harris, W.H. (1982) Stress distributions in the acetabular region - I. before and after total joint replacement. *J. Biomech.*, **15**, 155-164.
- Verdonschot, N., Huiskes, R. (1990) FEM analyses of hip prostheses: validity of the 2-D side-plate model and the effects of torsion. *Proc. Europ. Soc. Biomech.*, **7**, A20.

- Weinans, H. (1991) *Mechanically induced bone adaptations around orthopaedic implants.*, dissertation, University of Nijmegen, Nijmegen, the Netherlands.
- Weinans, H., Huiskes, R., Grootenboer, H.J. (1993) Quantitative analysis of bone reactions to relative motions at implant-bone interfaces. *J. Biomech.* (in press).
- Wroblewski, B.M. (1986) 15-21-year results of the Charnley low-friction arthroplasty. *Clin. Orthop. Rel. Res.*, **211**, 30-35.
- Yoshioka, Y., Shiba, R. (1981) A study of the stress analysis of the pelvis by means of the three-dimensional photoelastic experiments. *J. Jap. Orthop. Ass.*, **55**, 63-76.

Chapter I

Mechanical and textural properties of pelvic trabecular bone

M. Dalstra, R. Huiskes, A. Odgaard*, L. van Erning[#]

Biomechanics Section, Institute of Orthopaedics, University of Nijmegen

*Biomechanics Laboratory, Orthopaedic Hospital, University of Aarhus

[#]Institute of Diagnostic Radiology, University Hospital Nijmegen St. Radboud

Published in the Journal of Biomechanics, Vol. 26, No.4/5, pp. 523-535, 1993.

Abstract: *So far, virtually nothing is known about the mechanical properties of pelvic trabecular bone. In this study, several techniques have been used to establish some insight in these properties. Dual Energy Quantitative Computer Tomography (DEQCT) was used to look at the distribution of bone densities throughout the pelvic bone and non-destructive mechanical testing was used to obtain Young's moduli and Poisson's ratios in three orthogonal directions for cubic specimens of pelvic trabecular bone. The same specimens were then used for stereological measurements to obtain volume fractions and the spatial orientations of the mean intercept lengths. The combined data of the mechanical tests and the stereological measurements made it possible to calculate the Young's moduli and Poisson's ratios for the specimens' principal material axes.*

DEQCT showed that bone densities within a pelvic bone are significantly higher in the superior part of the acetabulum, extending to the sacro-iliac joint area and secondly in the area of the pubic symphysis. Volume fractions found for the specimens did not exceed 20%. This may be considered rather low when compared to values reported in the literature for trabecular bone of femoral or tibial origin, but the values do lie in the same range as vertebral trabecular bone. With the volume fraction as its primary predictor, values of the Young's moduli were also low. For most specimens these values were not higher than 100 MPa, with an occasional peak of 250 MPa. Looking at the ratio of the highest and lowest Young's modulus or at the components of the fabric tensor, it can be concluded that pelvic trabecular bone is not highly anisotropic. On average, the Poisson's ratio was found to be closer to 0.2 rather than 0.3, which is in accordance with other studies on the Poisson's ratio of trabecular bone.

Introduction

Being part of the hip joint, the pelvic bone, like its femoral counterpart, frequently appears in finite element studies. However, apart from the obvious anatomical differences, there is another striking difference between the femur and the pelvic bone. Mechanical properties of femoral bone are well documented, but it is somewhat surprising that on the mechanical properties of pelvic bone virtually no data exist. The pelvic bone mainly consists of trabecular bone covered by a thin layer of cortical bone. The Young's moduli used in various finite element studies of pelvic trabecular bone, vary from 40 MPa to 3,000 MPa. For the most part, these values were based on experimental data of tibial and femoral origin. Only Vasu *et al.* (1982) and Rapperport *et al.* (1985) used density observations from roentgenograms to estimate the Young's moduli. In all studies, bone was assumed to be isotropic. Vasu *et al.* (1982), Pedersen *et al.* (1982) and Rapperport *et al.* (1985) made a differentiation in the values of the Young's modulus, based on density distributions, whereby near the acetabulum the density was found to be the highest and decreasing in value further away from the acetabulum. In most finite element studies, the Poisson's ratio for pelvic trabecular bone was taken as 0.2. Only Goel *et al.* (1978) and Pedersen *et al.* (1982) assumed a value of 0.3. Again, however, measurements for this value were never made.

Because of its sandwich construction, the overall mechanical behavior of the pelvic bone is to some extent insensitive to variations of the mechanical properties of its trabecular bone (Dalstra and Huiskes, 1990). However, if stresses and strains in the trabecular bone itself are the subject of study, accurate values of its material properties will be a pre-requisite. Therefore, the purpose of the present study was to obtain a better insight in the material properties of pelvic trabecular bone. To achieve this, three different techniques were used. With dual energy quantitative computer tomography, trabecular bone densities were quantified throughout the pelvic bone. This was necessary as the dimensions of the specimens used for mechanical testing limit harvesting to only those areas which have sufficient bone stock. Mechanical testing of pelvic trabecular bone specimens was performed in three orthogonal directions, thus not only providing values of Young's moduli and Poisson's ratios, but also information about the degree of anisotropy. Finally, using a 3-D reconstruction technique, stereological measurements were performed on the same specimens used for mechanical testing, in order to identify the material's principal directions and, together with the data from the mechanical tests, to calculate the elastic constants in those directions.

Materials and Methods

Material

For Dual Energy Quantitative Computer Tomography (DEQCT), six right pelvic bones were available; one of a 78 year old male and five of females, ranging from 77 to 87 years. Being embalmed, these bones were not used for mechanical testing. For

this purpose, two fresh right pelvic bones were used; one of a 82 years old female and one of a 72 year old male. None of the donors was known to have a history of bone or joint disease. From each bone, as many cubic specimens as possible were taken. Due to its lesser size, the bone of the female donor yielded no more than 18 specimens. From the other bone, 39 specimens could be obtained. Due to insufficient bone stock in both bones, no specimens could be taken from the superior iliac crest, nor from the connection between ischial and pubic bone. All cubes were cut according to a Cartesian coordinate system defined by a plane over the rim of the acetabulum (xy-plane, the x-axis bisecting the angle between the ischial and pubic bones) and the z-axis as the normal to this plane, pointing into the acetabulum. The cubes were machined on a cutting-grinding system (EXAKT Cutting-Grinding System). Different colors of dye were used to mark the orientation of the faces of the bone cubes. These cubes had sides of about 6.5 mm; the exact dimensions of each individual specimen were measured with a caliber. After cutting, the specimens were stored in a wet state at -18°C until testing.

Quantitative computer tomography

The bones were scanned with a CT-scanner (Siemens, SOMATOM DR3) using dual energy mode, i.e. at 85 and 125 kVp. Using the same definition of the coordinate axes as mentioned above, scans were taken parallel to the yz-plane. Slice thickness was 8 mm and the distance between two consecutive scans was 10 mm. This resulted in twenty-one or twenty-two scans per bone, depending on the size. Together with the bones, a calibration phantom (Kalender and Suess, 1987) was scanned in order to be able to relate the X-ray absorption values with their Ca-equivalents. Postprocessing the CT-data, calcium-images were reconstructed, which were used for further evaluation. Via a network, the digital images were transferred to a PC. Using a PC-based image-analysis system (TIM, Difa Measuring Systems, Breda, the Netherlands), the areas of trabecular bone in each scan were marked and the average Ca-equivalents for those areas were calculated, thus providing a global mapping of trabecular bone densities throughout a pelvic bone. Furthermore, Ca-equivalents were measured locally at the same places where the cubic specimens had been harvested, which should give information about the relation between apparent density and Ca-equivalent density.

Mechanical testing

Unconstrained compressive mechanical testing was performed on a 4302 model Instron materials testing machine (INSTRON Ltd., High Wycombe, Bucks., U.K.). As several tests had to be performed on one specimen in order to obtain the material properties in the three directions of the cube, a non-destructive test procedure was used (Linde *et al.*, 1988). All tests were performed at a strain rate of $0.1\% \text{ s}^{-1}$ up to a maximal strain of 0.8%. Before the actual test cycle, the bone samples were conditioned to viscoelastic steady state by uniaxial cyclic compression between preloads of 2 N (defined as 0% strain) and 0.8% strain. Usually five to ten cycles were necessary

to reach steady state. During the actual test, the longitudinal deformation was recorded by an extensometer, fixed to the anvils as close to the specimen as possible, and the deformation in one of the transverse directions was recorded by a pair of LVDT's, placed opposite to one another. In measuring the transverse deformation, the surfaces were covered by a plastic foil. After one test cycle, the specimen was rotated 90° around its longitudinal axis and tested once more to measure the other transverse deformation. This procedure was repeated for the longitudinal axis set to each of the three directions, resulting in a total of six test cycles for each specimen. The order in which each axis was chosen to be the longitudinal axis (xyz) was the same for each specimen, although this does not seem to have a major effect on the stiffness values (Linde *et al.*, 1990b).

Load and deformation data were recorded during testing and sent to a PC, where they were converted into stress and strain values. A 5th degree polynomial fitting routine was performed on the stress data as a function of the longitudinal strain and on the transverse strain data as a function of the stress. Then the stress and the accompanying transverse strain were calculated at a longitudinal strain of 0.7%. The elastic modulus was defined as the tangent of the stress curve at a longitudinal strain of 0.7% and the Poisson's ratio as the ratio between the transverse strain and the longitudinal strain. For the second test in the same longitudinal direction, the same routine was followed and then the two elastic moduli were averaged. This was performed for all three directions of the cube, finally resulting in three elastic moduli and six Poisson's ratios for a single specimen.

After testing, the marrow was removed from the specimens by air jet and subsequently specimens were submerged in an alcohol/acetone solution for two days. After a final air jet cleansing and a one day evaporation time, the specimens were weighed. The apparent density of a specimen was then calculated from the weight of the specimen and its volume.

Stereological measurements

Data from the mechanical tests, by itself, are not sufficient to calculate all elastic constants, as beforehand, unlike for the trabecular bone in the proximal tibia, no information is available on the direction of the material's principal axes. However, assuming that the axes of the Mean Intercept Length (MIL) ellipsoid coincide with the principal axes of the material (Harrigan and Mann, 1984), it becomes possible to reconstruct the elasticity (or compliance) matrix in its principal directions. The only flaw in this assumption is that if the principal axes should happen to coincide with the directions in which mechanical testing was performed, the calculated values for the shear moduli will not be very good.

To be able to perform true three-dimensional MIL measurements, a three-dimensional serial reconstruction technique was used (Odgaard *et al.*, 1990). Due to technical reasons, only the specimens of the male pelvic bone were used for the MIL measurements. Of the original 39, six cubes failed during the embedding process, leaving 33 cubes for stereological analysis. Figure 1 shows the locations on the pelvic bone from

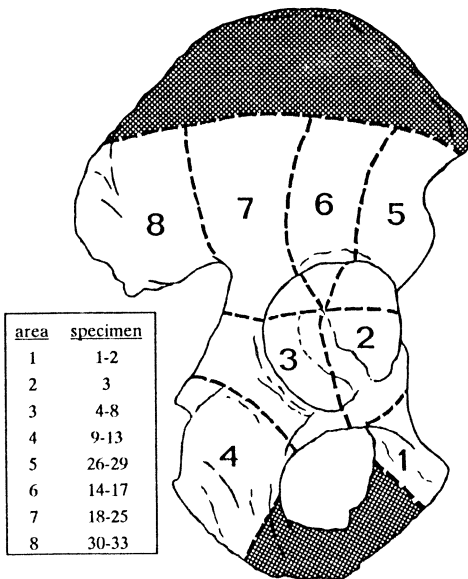


Fig. 1: Locations on the pelvic bone where the 33 specimens, used for combined mechanical testing and MIL measurements, were taken. The dotted areas denote the locations from which no specimens could be obtained due to lack of bone stock.

where these specimens were taken. The specimens were imbedded in a black epoxy resin under vacuum. Using a standard hard tissue microtome, the specimens were sectioned, whereby an image of the section was digitized by a CCD-camera mounted on the microtome. Depending on the exact size of the specimen, around 300 images of the individual sections were thus obtained and their binary information was stored after segmentation. From these files, a 3-D array consisting of voxels representing either bone or 'air', could then be reconstructed.

The volume fraction of bone was calculated simply by dividing the number of voxels representing bone by the total number of voxels. The MIL was measured by defining 222 uniformly random sets of equally-spaced parallel lines passing through the reconstructed specimen. For each set of lines, the number of intersections were counted, and the MIL was defined as the total line length divided by the number of intersections. Using multiple regression, the components of the MIL matrix \mathbf{M} , describing the MIL ellipsoid (Harrigan and Mann, 1984), were found. Assuming that the eigenvalues of the MIL matrix have the same standard deviation as its components, classification of the material was done by putting either a 90%, 95% or a 99% confidence interval around the middle eigenvalue of the MIL matrix. The presence of the other two eigenvalues in the confidence interval decided whether orthotropy, transverse isotropy or isotropy was assumed. The eigenvectors of \mathbf{M} give the directions of the axes of the ellipsoid, relative to the original coordinate system and thereby the assumed principal directions of the material were known.

Calculation of the elastic constants

Tensor transformation was performed on the stress and strain tensors obtained from the mechanical test procedure to the principal directions obtained from the stereological measurement. As mentioned above, depending on the statistical uniqueness of the eigenvalues of \mathbf{M} , orthotropy, transverse isotropy or isotropy was assumed, which set the restrictions for the twelve non-zero components of the compliance matrix \mathbf{S} . In case of orthotropy, the following equation should apply:

$$\begin{bmatrix} \varepsilon_1 \\ \varepsilon_2 \\ \varepsilon_3 \\ \varepsilon_4 \\ \varepsilon_5 \\ \varepsilon_6 \end{bmatrix} = \begin{bmatrix} S_{11} & S_{12} & S_{13} & 0 & 0 & 0 \\ S_{12} & S_{22} & S_{23} & 0 & 0 & 0 \\ S_{13} & S_{23} & S_{33} & 0 & 0 & 0 \\ 0 & 0 & 0 & S_{44} & 0 & 0 \\ 0 & 0 & 0 & 0 & S_{55} & 0 \\ 0 & 0 & 0 & 0 & 0 & S_{66} \end{bmatrix} \begin{bmatrix} \sigma_1 \\ \sigma_2 \\ \sigma_3 \\ \sigma_4 \\ \sigma_5 \\ \sigma_6 \end{bmatrix}$$

For each specimen, three mechanical tests had been performed, so, for each ε_i and σ_i in the equation above, three values were known. In order to force-fit these data to a thermodynamically sound compliance matrix, separate singular value decompositions were then applied to the stress sub-matrices of the systems, given (in case of orthotropy) by the first three, the fourth, the fifth and the sixth rows of the above equation respectively. The obtained pseudo-inverse stress matrices were multiplied by the respective strain sub-matrices, yielding the nine independent components of S . For isotropy and transverse isotropy, similar calculations were made, taking into account that for those cases, S contains only two and five independent components respectively. A more detailed description of the above procedure is given in Appendix I.

Depending on the type of material behavior, Young's moduli, shear moduli and Poisson's ratios were calculated from the data of the mechanical tests and the MIL measurements according to Appendix I. Finally, for each confidence level considered to determine uniqueness of the eigenvalues of the MIL matrix, the calculated Young's and shear moduli were correlated to both the apparent density alone and a combination of apparent density and fabric components (Cowin, 1985), using nonlinear curve-fitting.

Results

Dual Energy Quantitative Computer Tomography

Ca-equivalents for pelvic trabecular bone found with DEQCT varied between 0.04 and 0.22 g/cm³. It appeared that the average Ca-equivalent value of the male bone was slightly, yet significantly ($p=0.05$) higher than the values of the female bones (0.13 g/cm³ vs. 0.09 to 0.11 g/cm³). Figure 2 shows the average Ca-equivalents at the respective scan levels, averaged over the six pelvic bones. Statistical analysis (ANOVA) of this data revealed four areas where Ca-equivalents were significantly different ($p=0.05$) from each other; these being the ala of the iliac bone (1), the superior part of the acetabulum and the corpus of the iliac bone (2), the inferior part of the acetabulum, the ischial bone and the pubic-ischial junction (3) and finally the crista and the superior ramus of the pubic bone (4) (Figure 2).

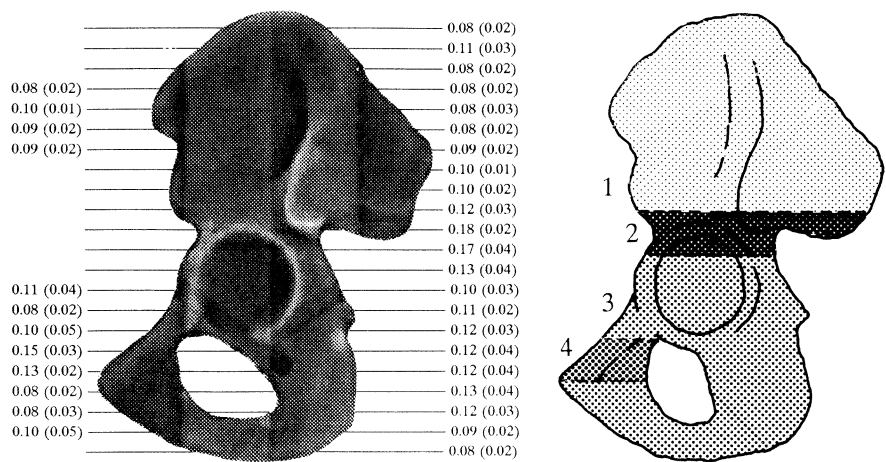


Fig. 2: Average Ca-equivalent densities and standard deviations (in g cm^{-3}) at every scan level and the identification of the areas between which the average Ca-equivalent densities were significantly different, based on six pelvic bones. (Those slices for which Ca-equivalent densities are indicated on the left as well, had such a thin connection between the anterior and posterior trabecular bone mass (or even none) that separate anterior and posterior measurements were made.)

Average values and standard deviations of the Ca-equivalents in these four areas are summarized in Table 1.

area	mean Ca-equiv. (g/cm^3)	s.d. Ca-equiv. (g/cm^3)
1	0.09	0.02
2	0.17	0.03
3	0.10	0.04
4	0.14	0.03

Table 1: The mean values and standard deviations of the Ca-equivalents in the four areas with statistically different bone densities of a pelvic bone.

Mechanical testing

The average values of the apparent densities of the specimens were 0.345 g/cm^3 (s.d.: 0.219 g/cm^3) in a range from 0.109 to 0.959 g/cm^3 for the female bone and 0.195 g/cm^3 (s.d.: 0.054 g/cm^3) in a range from 0.114 to 0.314 g/cm^3 for the male bone. It may seem surprising that the female bone displayed a higher average bone density. This was mainly due to four of the female specimens with an apparent density of over 0.5 g/cm^3 , which were taken from the superior acetabular area. When these four specimens were excluded as being subchondral bone rather than trabecular

bone, the average apparent density for the female bone decreased to 0.248 g/cm^3 (s.d.: 0.105 g/cm^3). Although still higher, this average density is not significantly different from the one found for the male bone. For both bones, the highest densities were found in the anterosuperior region of the acetabular wall, while the lowest densities were found in the ischial bone.

Although, for the combination with the results of the MIL-measurements, only the stress and transverse strains at a longitudinal strain of 0.7% were needed, the elastic moduli in x-, y- and z-direction were calculated. In Figure 3, these properties are represented as functions of the apparent density. The average elastic moduli in the x- and y-directions were not statistically different between both bones, the average elastic modulus in the z-direction for the female bone was slightly higher.

Stereological measurements

The low density of the specimens was reflected in the volume fractions (V_V), found by voxel counting. The average volume fraction was 10.8 percent (s.d.: 3.6 percent). Correlating the apparent density to the volume fraction resulted in $\rho_{\text{app}} = 1.75 V_V$ ($R^2 = 0.99$). Visual representation of the 3-D specimen reconstructions showed a wide range of trabecular structures. There were specimens with an apparently direction-independent strut configuration, but also specimens with a well defined texture of parallel plates (Figure 4). A plate-like structure could be identified in about 70 percent of the cases. In none of these cases were the plates positioned parallel to the x/y-plane, meaning that the plates were always found to be more or less perpendicular to the cortical shells.

Calculation of the elastic constants

Calculation of the elastic constants is dependent on the type of material behavior. Table 2 shows the distribution of the types of material behavior depending on the confidence level used to determine statistical uniqueness of the eigenvalues of the MIL matrix found for the 33 specimens.

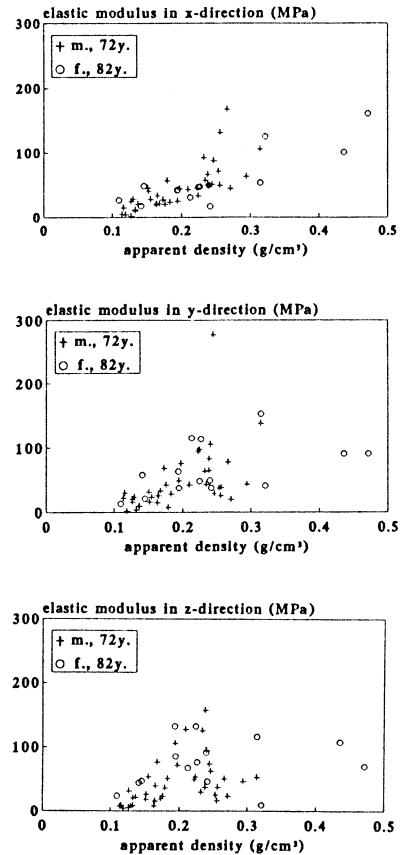


Fig. 3: Elastic moduli of the specimens from both the male and female donors in the x-, y- and z-directions as functions of the apparent density.

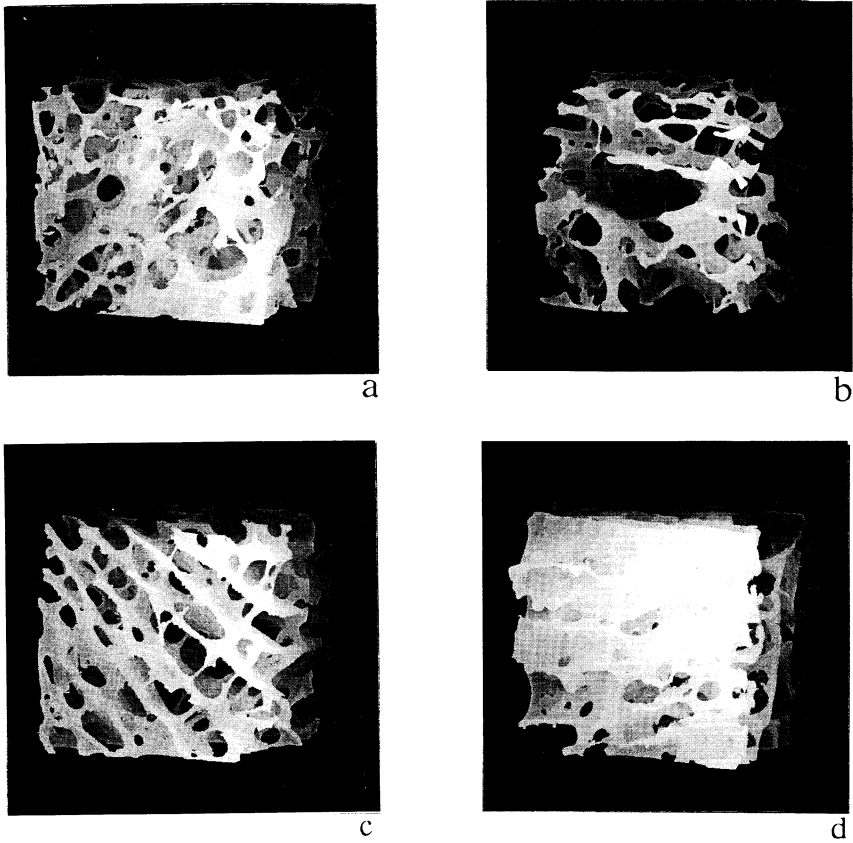


Fig. 4: Different appearances of pelvic trabecular structure in specimen no. 3 (a), specimen no. 4 (b), specimen no. 17 (c) and specimen no. 33 (d).

	Confidence level		
	90%	95%	99%
Orthotropy, $E_1 > E_2 > E_3$	16	9	2
Prolate transverse isotropy, $E_1 > E_2 = E_3$	5	3	3
Oblate transverse isotropy, $E_1 = E_2 > E_3$	9	13	15
Isotropy, $E_1 = E_2 = E_3$	3	8	13

Table 2: Occurrence of the various types of material behavior, depending upon the confidence level used to determine uniqueness of the eigenvalues of the MIL matrix for the 33 specimens.

It is obvious that a wider confidence interval implies that more specimens will be classified as isotropic. One of the specimens (no. 14) was actually classified differently at each of the three considered confidence levels. For this particular specimen, the actual procedure of calculating its elastic constants is worked out in Appendix II. Values of the elastic moduli, the Poisson's ratios, the components of the fabric tensor and the ratio between the maximal and minimal Young's moduli (this being a measure for the degree of anisotropy) averaged over all 33 specimens together with the respective standard deviations are given in Table 3.

	Confidence level		
	90%	95%	99%
E_1	61.6 (48.2)	59.8 (45.2)	59.8 (44.9)
E_2	42.4 (29.1)	50.1 (41.5)	57.3 (44.6)
E_3	31.0 (22.5)	38.3 (39.1)	43.2 (39.9)
G_{23}	18.4 (12.9)	20.8 (17.1)	22.6 (17.2)
G_{31}	23.4 (17.8)	23.5 (18.3)	22.6 (17.1)
G_{12}	25.7 (19.8)	25.2 (17.8)	26.0 (19.1)
ν_{21}	0.17 (0.12)	0.17 (0.10)	0.17 (0.10)
ν_{12}	0.24 (0.17)	0.20 (0.12)	0.18 (0.11)
ν_{31}	0.14 (0.07)	0.15 (0.08)	0.16 (0.07)
ν_{13}	0.27 (0.17)	0.26 (0.16)	0.24 (0.14)
ν_{32}	0.20 (0.14)	0.19 (0.13)	0.14 (0.09)
ν_{23}	0.28 (0.21)	0.27 (0.21)	0.21 (0.16)
H_1	0.390 (0.035)	0.377 (0.038)	0.365 (0.035)
H_2	0.334 (0.024)	0.341 (0.026)	0.346 (0.029)
H_3	0.276 (0.031)	0.282 (0.036)	0.346 (0.040)
E_1/E_3	2.0 (1.0)	1.7 (0.8)	1.4 (0.6)

Table 3: Mean values and standard deviations (between brackets) of the Young's moduli E_i (MPa), shear moduli G_{ij} (MPa), Poisson's ratios ν_{ij} , fabric components H_i and ratio between E_1 and E_3 depending upon the confidence level used to determine uniqueness of the eigenvalues of the MIL matrix for all specimens.

Returning to the four specimens shown in Figure 4, their material behavior was

classified respectively as oblatelly transversely isotropic ($E_1 = E_2 = 43.8$ MPa, $E_3 = 20.7$ MPa), isotropic ($E_1 = E_2 = E_3 = 23.6$ MPa), orthotropic ($E_1 = 167.0$ MPa, $E_2 = 64.6$ MPa, $E_3 = 58.9$ MPa) and prolately transversely isotropic ($E_1 = 96.0$ MPa, $E_2 = E_3 = 49.7$ MPa) at a confidence level of 95%.

Having information about the magnitudes and the directionality of the elastic properties of the tested specimens, it becomes possible to transpose this data back to the pelvic bone. Again for a confidence level of 95%, Figure 5 shows the projections of the eigenvectors of the MIL matrix together with the calculated Young's moduli for a number of specimens at their original locations in the pelvic bone.

Correlating the Young's and shear moduli to apparent density and fabric components resulted in the following set of relations:

confidence level 90%:

$$\begin{aligned} E_i &= 2017.3 \rho_{app}^{2.46} & (R^2=0.58), & G_{ij} = 1012.1 \rho_{app}^{2.44} & (R^2=0.62), \\ E_i &= 15098.5 \rho_{app}^{2.46} H_i^{1.80} & (R^2=0.69), & G_{ij} &= 2049.1 \rho_{app}^{2.44} (H_i + H_j)^{1.72} & (R^2=0.65), \end{aligned}$$

confidence level 95%:

$$\begin{aligned} E_i &= 1751.0 \rho_{app}^{2.32} & (R^2=0.54), & G_{ij} &= 938.8 \rho_{app}^{2.38} & (R^2=0.61), \\ E_i &= 12261.9 \rho_{app}^{2.33} H_i^{1.73} & (R^2=0.64), & G_{ij} &= 1534.0 \rho_{app}^{2.39} (H_i + H_j)^{1.17} & (R^2=0.62), \end{aligned}$$

confidence level 99%:

$$\begin{aligned} E_i &= 1958.6 \rho_{app}^{2.33} & (R^2=0.57), & G_{ij} &= 919.4 \rho_{app}^{2.35} & (R^2=0.61), \\ E_i &= 9162.7 \rho_{app}^{2.34} H_i^{1.37} & (R^2=0.62), & G_{ij} &= 1084.2 \rho_{app}^{2.35} (H_i + H_j)^{0.39} & (R^2=0.61). \end{aligned}$$

Looking at the values of R^2 , it can be seen that using only the apparent density as its predictor, the shear modulus shows a slightly better correlation than the Young's modulus. However, adding the fabric components results in the opposite.

Discussion

The purpose of this study was to find values for the elastic properties of pelvic trabecular bone. Assuming orthotropy as the highest degree of anisotropy, multiple tests on a single specimen would be required. This dictated the use of cubic specimens, even though the authors were well aware of the disadvantages and inaccuracies associated with this approach (Evans and King, 1961; Ashman *et al.*, 1989; Linde *et al.*, 1990a; Odgaard and Linde, 1991), causing an underestimation of the Young's modulus relative to specimens with a larger length-to-area ratio. Bearing this in mind, non-destructive compressive tests were performed in three directions. However, it is not possible to obtain the shear moduli from these data. A solution for this could be to cut a smaller cube from the original under different angles and test this as well. Transformation of this second set of data into the directions of the first, makes it possible to find the values for the shear moduli (Snyder *et al.*, 1989). However, in

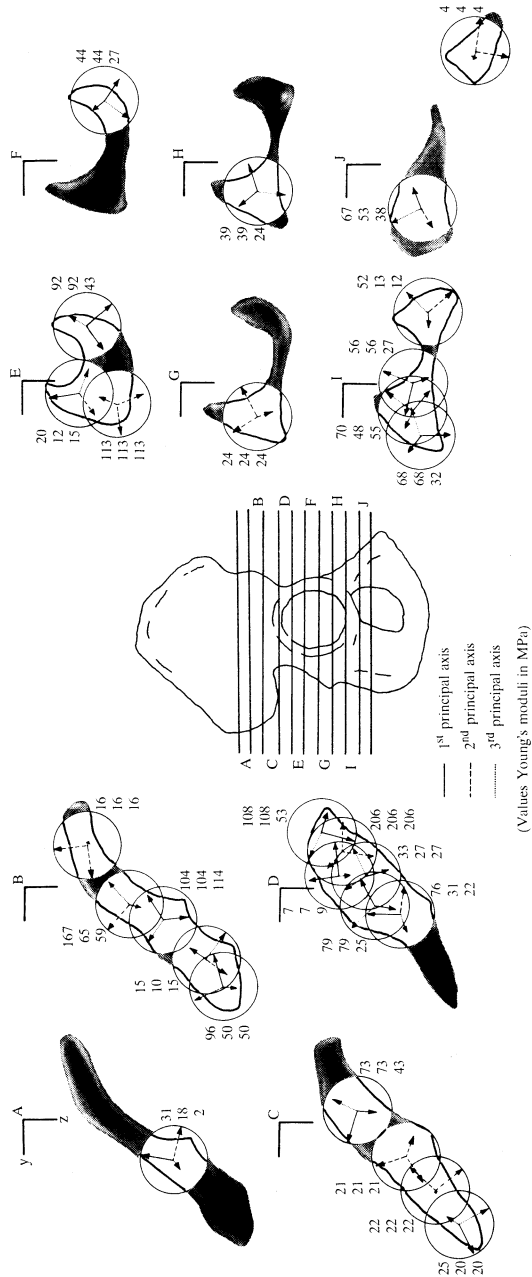


Fig. 5: Projections of the principal material directions in the yz-plane (the out-of-plane components are directed in the positive x-direction) and magnitudes of Young's moduli in those directions for a number of specimens at their original locations in the pelvic bone (confidence level 95%).

our case an additional problem was the fact that the material's principal axes were not known beforehand. Cutting one smaller cube from the original would therefore not be sufficient and at least a third cube would be needed as well. But this would mean that the original specimens should be rather big. In fact, too big for trabecular bone specimens to be taken from the pelvic bone. Therefore another approach was chosen. MIL measurements were performed on a digitized three-dimensionally reconstructed geometry of the specimens after mechanical testing. The axes of the MIL ellipsoid were assumed to be the same as the material's principal axes and the data from the mechanical tests were transformed in these directions. Using singular value decomposition on the relations for either orthotropic, transversely isotropic or isotropic behavior yielded three Young's moduli, three shear moduli and six Poisson's ratios.

Although none of the donors was known to have any history of bone or joint disease, their ages (72-87 yrs.) alone contribute to the fact that low bone densities and consequently low elastic constants were found. However, as a part of the purpose of this study was to compare pelvic trabecular bone with trabecular bone from femoral and tibial origin, this aspect should have no effect. For the two pelvic bones used in this study for mechanical testing, trabecular bone with relatively low apparent densities was found. To support this finding, six other pelvic bones were used for bone densitometry measurements with a DEQCT method. The average Ca-equivalent densities at each scan-level did not vary much between these six bones. The variation within a bone per scan-level was such that four areas could be identified where Ca-equivalents were significantly different from adjacent areas (Figure 2). The fact that the two high density areas (upper part of the acetabulum to the sacro-iliac joint area and the middle part of the pubic bone) coincide with the areas of major load transfer may, from a bone remodeling point of view, not come as a surprise. The apparent densities found for the two other bones, which were used for mechanical testing, suited well with these findings. Relating these apparent densities to the average Ca-equivalent densities locally measured at the six other bones, resulted in a positive correlation: $\rho_{\text{Ca-eq}} = 0.626 \rho_{\text{app}}$ ($R^2 = 0.87$).

The values of the Ca-equivalent densities found in this study (0.04 - 0.22 g/cm³) are quite similar to values of vertebral Ca-equivalent densities found by Lang *et al.* (1988) and Kalender *et al.* (1989). Other evidence for the resemblance between pelvic and vertebral trabecular bone are the values of the apparent densities of vertebral trabecular bone found by McBroom *et al.* (1985), lying in a range of 0.10 to 0.25 g/cm³. These kind of values were also found in this study for the two pelvic bones used for mechanical testing. The average densities found for both male and female donors were not statistically different. These are indications that the densities found in this study are not exceptionally low, at least for donors in the age range used in this study (72-87 yrs.).

With apparent density (or volume fraction) as their primary predictor, the elastic constants that were found were low as well. For the majority of the specimens, the highest Young's modulus did not exceed 100 MPa. To some extent, this may be attributed to the methodology of mechanical testing. In the first place, cubic compres-

sion is known to underestimate Young's modulus, as already mentioned above. Furthermore, the fact that the specimens were tested unconstrained does also result in lower stiffnesses, but constrained testing would only have increased the stiffness by about 20 percent (Linde and Hvid, 1989). Multiple testing of the specimens, however, should not have had any major effect on the stiffness (Linde *et al.*, 1990b). But even taking these aspects into account, the elastic constants were significantly lower than values reported for specimens from the femoral head (Snyder *et al.*, 1989) or from the proximal tibia (Turner *et al.*, 1990), although it must be stated that in these studies the average age of the donors was lower (65 and 55 yrs. respectively). However, our values for the Young's moduli are again similar to values for vertebral trabecular bone (Lang *et al.*, 1988).

Looking back at the values assumed for Young's moduli for cancellous bone in various pelvic FE models, it appears that in most cases the values were too high. Pedersen *et al.* (1982) and Huiskes (1987) used values ranging from 1,000 to 3,000 MPa. Oonishi *et al.* (1983) used 1,000 MPa in one study, while in another study 300 MPa was used (Oonishi *et al.*, 1986). Goel *et al.* (1978) also used a value of around 300 MPa. Only Vasu *et al.* (1982) and Rappoport *et al.* (1985) have used values which correspond to our findings, although their upper limits (1,025 and 600 MPa respectively) were high as well. It is worth noting that they were the only ones to base their Young's moduli on density distributions of actual pelvic bone (roentgenograms). The assumed value of 0.2 for the Poisson's ratio of trabecular bone in nearly all studies mentioned above was shown by our study to be a good estimate. A Poisson's ratio of 0.2 was also found in other studies of trabecular bone from locations other than the pelvic bone.

Visual representation of the specimens that underwent the 3-D serial reconstruction, revealed a wide range of trabecular structures. In more than half of the specimens, a plate-like trabecular structure could be observed, whereby the plates were always more or less oriented perpendicular to the cortical shells. From a mechanical point of view, this is quite understandable, because as core material in a sandwich construction, pelvic trabecular bone will predominantly have to withstand shear-loading modes, against which a plate-like structure is the best resistance. Quantifying the degree of anisotropy depended on the statistical uniqueness of the eigenvalues of the MIL matrix. The smaller the confidence limit, the more specimens were classified as orthotropic. A rise in confidence level from 90% to 99% showed a decrease from 48 percent to 6 percent occurrence of orthotropic specimens. In case of transverse isotropy, the variant with two high-level moduli and one low-level modulus (oblate) was seen more often than the variant with one high-level modulus and two low-level moduli (prolate). This confirms the visual observation of the frequent occurrence of the plate-like structures. The two high-level moduli lie in the plane of the plate, while the low-level modulus is found in the connecting rods. With this, pelvic trabecular bone distinguishes itself from direct weight bearing (*e.g.* tibial) trabecular bone, where prolate transverse isotropy is found (high-level modulus in the weight bearing direction and the low-level moduli in the transverse directions). The ratio between the

maximal and minimal Young's moduli (Table 3) reveals that pelvic trabecular bone is not highly anisotropic. This is confirmed by a minimal value of 0.315 for the second invariant of the fabric tensor, a measure of the degree of textural anisotropy, suggesting a maximal ratio of 1.9 : 1 between the major and minor orientation axes.

The statistical correlations between mechanical and textural properties are not as strong as reported in other studies (Turner *et al.*, 1988 & 1990; Snyder *et al.*, 1989; Hodgskinson and Currey, 1990; Turner, 1992). The exponent of the apparent density in the relations with both the Young's modulus and the shear modulus varies between 2.3 and 2.5. With regard to the work of Gibson (1985), these values may be considered somewhat high. She points out that for low density bone (open-celled structure) this relationship should be quadratic. In this study, however, despite the low densities, plate-like structures (closed-celled structure with a cubic relationship) were found relatively often, which might be the reason that the exponent lies between 2 and 3. For the fabric components this exponent shows a much broader range (0.4 to 1.8) and is strongly dependent on the confidence level used to determine uniqueness of the eigenvalues of the MIL matrix. This is plausible as a higher confidence level implies relatively much isotropic behavior and for perfect isotropy the fabric components can not provide anymore relevant information. This can also be seen by the decreasing portion added to the R^2 when the fabric components are added in the correlations at increasing confidence levels. At a confidence level of 90%, adding H_i explains an extra 11 percent of the variance in the Young's modulus, while at a level of 99% this percentage is reduced to 5 percent. For the shear modulus at 99%, even nothing seems to be gained by adding fabric components in the correlation. The fact that pelvic trabecular bone is not highly anisotropic and therefore does not show much variance in its fabric components, is the reason why, unlike Turner (1992), no higher exponents for the fabric components than 1.8 were found. The relatively high variances in the values of the elastic properties itself in combination with the wide range of observed bone structures seem to suggest that other textural properties than fabric or MIL are also needed in order to improve relations between elastic and textural properties.

Not having a direct weight bearing function, it can be concluded that pelvic trabecular bone consists of lower density bone than trabecular bone in the femoral head or the proximal tibia. Consequently, the mechanical stiffness and strength (although the latter was not investigated here) will be lower. Its architecture displays a wide range of structures, although the predominant appearance is one of parallel plates. This accounts for the fact that transverse isotropic behavior with two high-level moduli and one low-level modulus is found relatively often.

References

- Ashman, R.B., Rho, J.Y., Turner, C.H. (1989) Anatomical variation of orthotropic elastic moduli of the proximal human tibia. *J. Biomech.*, **22**, 895-900.
- Cowin, S.C. (1985), The relationship between the elasticity tensor and the fabric tensor. *Mech. Mat.*, **4**, 137-147.

- Cowin, S.C., Van Buskirk, W.C. (1986) Thermodynamic restrictions on the elastic constants of bone. *J. Biomech.*, **19**, 85-87.
- Dalstra, M., Huiskes, R. (1990) The pelvic bone as a sandwich construction; a three dimensional finite element study. *Proc. Europ. Soc. Biomech.*, **7**, B32.
- Evans, F.G., King, A. (1961) Regional differences in some physical properties of human spongy bone. In: *Biomechanical studies of the musculo-skeletal system.*, ed. F.G. Evans, Charles C. Thomas Publisher, Springfield, IL, pp. 19-67.
- Gibson, J.L. (1985) The mechanical behaviour of cancellous bone. *J. Biomech.*, **18**, 317-328.
- Goel, V.K., Valliappan, S., Svensson, N.L. (1978) Stresses in the normal pelvis. *Comput. Biol. Med.*, **8**, 91-104.
- Harrigan, T.P., Mann, R.W. (1984) Characterization of microstructural anisotropy in orthotropic materials using a second rank tensor. *J. Mat. Sci.*, **19**, 761-767.
- Hodgskinson, R., Currey, J.D. (1990) Effects of structural variation on Young's modulus of non-human cancellous bone. *Proc. Instn. Mech. Engrs.*, **204**, 43-52.
- Huiskes, R. (1987) Finite element analysis of acetabular reconstruction - Noncemented threaded cups. *Acta Orthop. Scand.*, **58**, 620-625.
- Kalender, W.A., Suess, C. (1987) A calibration phantom for quantitative computed tomography. *Med. Phys.*, **14**, 863-866.
- Kalender, W.A., Felsenberg, D., Louis, O., Lopez, P., Klotz, E., Osteaux, M., Fraga, J. (1989) Reference values for trabecular and cortical vertebral bone density in single and dual-energy quantitative computed tomography. *Europ. J. Radiol.*, **9**, 75-80.
- Lang, S.M., Moyle, D.D., Berg, E.W., Detorie, N., Gilpin, A.T., Pappas, N.J., Reynolds, J.C., Tkacik, M., Waldron, R.L. (1988) Correlation of mechanical properties of vertebral trabecular bone with equivalent mineral density as measured by computed tomography. *J. Bone Joint Surg.*, **70-A**, 1531-1538.
- Linde, F., Gøthgen, C.B., Hvid, I., Pongsoipetch, B. (1988) Mechanical properties of trabecular bone by a non-destructive testing approach. *Engng. Med.*, **17**, 23-29.
- Linde, F., Hvid, I. (1989) The effect of constraint on the mechanical behaviour of trabecular bone specimens. *J. Biomech.*, **22**, 485-490.
- Linde, F., Hvid, I., Madsen, F. (1990a) The effect of specimen size and geometry on the mechanical behaviour of trabecular bone. *Proc. Europ. Soc. Biomech.*, **7**, A25.
- Linde, F., Pongsoipetch, B., Frick, L.H., Hvid, I. (1990b) Three-axial strain controlled testing applied to bone specimens from the proximal tibial epiphysis. *J. Biomech.*, **23**, 1167-1172.
- McBroom, R.J., Hayes, W.C., Edwards, W.T., Goldberg, R.P., White, A.A. (1985) Prediction of vertebral body compressive fracture using quantitative computed tomography. *J. Bone Joint Surg.*, **67-A**, 1206-1214.
- Odgaard, A., Andersen, K., Melsen, F., Gundersen, H.J.G. (1990) A direct method for fast three-dimensional serial reconstruction. *J. Microsc.*, **159**, 335-342.
- Odgaard, A., Linde, F. (1991) The underestimation of Young's modulus in compressive testing of cancellous bone specimens. *J. Biomech.*, **24**, 691-698.
- Oonishi, H., Isha, H., Hasegawa, T. (1983) Mechanical analysis of the human pelvis and its application to the articular hip joint - by means of the three dimensional finite element method. *J. Biomech.*, **16**, 427-444.
- Oonishi, H., Tatsumi, M., Kawaguchi (1986) Biomechanical studies on fixations of an artificial hip joint acetabular socket by means of 2D-FEM. In: *Biological and biomechanical performance of biomaterials.*, eds. P. Christel, A. Meunier, A.J.C. Lee, Amsterdam: Elsevier Science Publishers B.V., pp. 513-518.
- Pedersen, D.R., Crowninshield, R.D., Brand, R.A., Johnston, R.C. (1982) An axisymmetric model of acetabular components in total hip arthroplasty. *J. Biomech.*, **15**, 305-315.
- Rapperport, D.J., Carter, D.R., Schurman, D.J. (1985) Contact finite element stress analysis of the hip joint. *J. Orthop. Res.*, **3**, 435-446.
- Snyder, B.D., Cheal, E.J., Hipp, J.A., Hayes, W.C. (1989) Anisotropic structure - Property relations for trabecular bone. *Trans. Orthop. Res. Soc.*, **14**, 265.

- Strang, G. (1986) *Introduction to applied mathematics.*, Cambridge, MA: Wellesley-Cambridge Press.
- Turner, C.H., Rho, J.Y., Ashman, R.B., Cowin, S.C. (1988) The dependence of the elastic constants of cancellous bone upon structural density and fabric. *Trans. Orthop. Res. Soc.*, **13**, 74.
- Turner, C.H., Cowin, S.C., Rho, J.Y., Ashman, R.B., Rice, J.C. (1990) The fabric dependence of the orthotropic elastic constants of cancellous bone. *J. Biomech.*, **23**, 549-561.
- Turner, C.H. (1992) On Wolff's Law of trabecular architecture. *J. Biomech.*, **25**, 1-9.
- Vasu, R., Carter, D.R., Harris, W.H. (1982) Stress distributions in the acetabular region - I. before and after total joint replacement. *J. Biomech.*, **15**, 155-164.

Appendix I

One of the general descriptions of Hooke's Law can be written as: $\epsilon = \mathbf{S} \sigma$, with \mathbf{S} being the material's compliance matrix. From this, \mathbf{S} can be solved if sufficient sets of ϵ and σ are available. Singular value decomposition is a standard means to calculate the pseudo-inverse of a non-square matrix (Strang, 1986), in this case σ . Multiplying ϵ and σ^{-1} should yield \mathbf{S} . However, in this particular case, only three sets of stresses and strains are available, which is not enough to solve the 21 unknown components of \mathbf{S} . But, assuming the anisotropic material behavior to be either orthotropic, transverse isotropic or isotropic, already a lot of \mathbf{S} is known, namely:

$$\mathbf{S}_{\text{ortho}} = \begin{bmatrix} S_{11} & S_{12} & S_{13} & 0 & 0 & 0 \\ S_{12} & S_{22} & S_{23} & 0 & 0 & 0 \\ S_{13} & S_{23} & S_{33} & 0 & 0 & 0 \\ 0 & 0 & 0 & S_{44} & 0 & 0 \\ 0 & 0 & 0 & 0 & S_{55} & 0 \\ 0 & 0 & 0 & 0 & 0 & S_{66} \end{bmatrix}, \quad \mathbf{S}_{\text{tr. iso}} = \begin{bmatrix} S_{11} & S_{12} & S_{12} & 0 & 0 & 0 \\ S_{12} & S_{22} & S_{23} & 0 & 0 & 0 \\ S_{12} & S_{23} & S_{22} & 0 & 0 & 0 \\ 0 & 0 & 0 & S_{44} & 0 & 0 \\ 0 & 0 & 0 & 0 & S_{55} & 0 \\ 0 & 0 & 0 & 0 & 0 & S_{55} \end{bmatrix} \text{ or}$$

$$\mathbf{S}_{\text{tr. iso}} = \begin{bmatrix} S_{11} & S_{12} & S_{13} & 0 & 0 & 0 \\ S_{12} & S_{11} & S_{13} & 0 & 0 & 0 \\ S_{13} & S_{13} & S_{33} & 0 & 0 & 0 \\ 0 & 0 & 0 & S_{44} & 0 & 0 \\ 0 & 0 & 0 & 0 & S_{44} & 0 \\ 0 & 0 & 0 & 0 & 0 & S_{66} \end{bmatrix} \text{ and } \mathbf{S}_{\text{iso}} = \begin{bmatrix} S_{11} & S_{12} & S_{12} & 0 & 0 & 0 \\ S_{12} & S_{11} & S_{12} & 0 & 0 & 0 \\ S_{12} & S_{12} & S_{11} & 0 & 0 & 0 \\ 0 & 0 & 0 & S_{44} & 0 & 0 \\ 0 & 0 & 0 & 0 & S_{44} & 0 \\ 0 & 0 & 0 & 0 & 0 & S_{44} \end{bmatrix}$$

For transverse isotropy, two separate cases are considered. In the first, the material is supposed to have one high-level Young's modulus and two equal low-level Young's moduli (prolate). In the second one, it is just the other way around, namely two equal high-level moduli and one low-level modulus (oblate).

In the following, only the orthotropic case will be worked out further. For transverse isotropy and isotropy similar equations can easily be derived, which will be less elaborate, because in these cases, \mathbf{S} has less independent components. As already stated above, singular value decomposition will not be used on

the total system, but instead on four sub-systems, these being

$$\begin{bmatrix} \varepsilon_1 \\ \varepsilon_2 \\ \varepsilon_3 \end{bmatrix} = \begin{bmatrix} S_{11} & S_{12} & S_{13} \\ S_{12} & S_{22} & S_{23} \\ S_{13} & S_{23} & S_{33} \end{bmatrix} \begin{bmatrix} \sigma_1 \\ \sigma_2 \\ \sigma_3 \end{bmatrix} \quad \text{and}$$

$\varepsilon_i = S_{ii} \sigma_i$ for $i = 4$ to 6 .

The first can be rewritten as:

$$\begin{bmatrix} \varepsilon_1 \\ \varepsilon_2 \\ \varepsilon_3 \end{bmatrix} = \begin{bmatrix} \sigma_1 & \sigma_2 & \sigma_3 & 0 & 0 & 0 \\ 0 & \sigma_1 & 0 & \sigma_2 & \sigma_3 & 0 \\ 0 & 0 & \sigma_1 & 0 & \sigma_2 & \sigma_3 \end{bmatrix} \begin{bmatrix} S_{11} \\ S_{12} \\ S_{13} \\ S_{22} \\ S_{23} \\ S_{33} \end{bmatrix}$$

In this equation, the 'extra' two sets of ε and σ are added row-wise, in the three other equations, the extra sets are added column-wise. Labeling the three sets of ε and σ with a, b and c respectively, the following sets of equations remain to be solved:

$$\begin{bmatrix} \varepsilon_{1a} \\ \varepsilon_{2a} \\ \varepsilon_{3a} \\ \varepsilon_{1b} \\ \varepsilon_{2b} \\ \varepsilon_{3b} \\ \varepsilon_{1c} \\ \varepsilon_{2c} \\ \varepsilon_{3c} \end{bmatrix} = \begin{bmatrix} \sigma_{1a} & \sigma_{2a} & \sigma_{3a} & 0 & 0 & 0 \\ 0 & \sigma_{1a} & 0 & \sigma_{2a} & \sigma_{3a} & 0 \\ 0 & 0 & \sigma_{1a} & 0 & \sigma_{2a} & \sigma_{3a} \\ \sigma_{1b} & \sigma_{2b} & \sigma_{3b} & 0 & 0 & 0 \\ 0 & \sigma_{1b} & 0 & \sigma_{2b} & \sigma_{3b} & 0 \\ 0 & 0 & \sigma_{1b} & 0 & \sigma_{2b} & \sigma_{3b} \\ \sigma_{1c} & \sigma_{2c} & \sigma_{3c} & 0 & 0 & 0 \\ 0 & \sigma_{1c} & 0 & \sigma_{2c} & \sigma_{3c} & 0 \\ 0 & 0 & \sigma_{1c} & 0 & \sigma_{2c} & \sigma_{3c} \end{bmatrix} \begin{bmatrix} S_{11} \\ S_{12} \\ S_{13} \\ S_{22} \\ S_{23} \\ S_{33} \end{bmatrix} \quad \text{and} \quad [\varepsilon_{ia} \ \varepsilon_{ib} \ \varepsilon_{ic}] = S_{ii} [\sigma_{ia} \ \sigma_{ib} \ \sigma_{ic}] \quad \text{for } i = 4 \text{ to } 6.$$

Singular value decomposition applied to the matrices, containing the stress components in the above equations, will give their pseudo-inverses. Multiplying these by the respective strain matrices will yield the components of S_i based on a multi-dimensional least-square fit. In Appendix II, a numerical example of the above exercises will be given, using actual data of one of the specimens.

Appendix II

The calculation of the Young's and shear moduli and Poisson's ratios in the material's principal directions from the data of the mechanical tests and the MIL measurements for specimen no. 14 will be shown here as an example. This specimen happens to be classified as orthotropic at a 90% confidence level, transversely isotropic at 95% and isotropic at 99%. From the mechanical tests of this particular specimen follow the three pairs of stress and strain tensors (see note on page 36) (σ in MPa and ε in microstrain):

$$\sigma_x = \begin{bmatrix} -0.172 \\ 0 \\ 0 \\ 0 \\ 0 \\ 0 \end{bmatrix}, \epsilon_x = \begin{bmatrix} -7000 \\ 890 \\ 193 \\ 0 \\ 0 \\ 0 \end{bmatrix}, \sigma_y = \begin{bmatrix} 0 \\ -0.344 \\ 0 \\ 0 \\ 0 \\ 0 \end{bmatrix}, \epsilon_y = \begin{bmatrix} 1868 \\ -7000 \\ 1286 \\ 0 \\ 0 \\ 0 \end{bmatrix}, \sigma_z = \begin{bmatrix} 0 \\ 0 \\ -0.741 \\ 0 \\ 0 \\ 0 \end{bmatrix}, \epsilon_z = \begin{bmatrix} 1428 \\ 647 \\ -7000 \\ 0 \\ 0 \\ 0 \end{bmatrix}.$$

The MIL measurements and subsequent ellipsoid-fitting produced the following material anisotropy tensor \mathbf{M} :

$$\mathbf{M} = \begin{bmatrix} 0.912 & 0.016 & -0.126 \\ 0.016 & 1.002 & -0.026 \\ -0.126 & -0.026 & 1.160 \end{bmatrix}.$$

The standard deviation in its components was 0.017. Eigenvalues and eigenvectors of \mathbf{M} are:

$$\lambda_1 = 0.859, \mathbf{v}_1 = \begin{bmatrix} -0.923 \\ 0.033 \\ -0.384 \end{bmatrix}, \lambda_2 = 0.998, \mathbf{v}_2 = \begin{bmatrix} 0.023 \\ -0.990 \\ -0.140 \end{bmatrix}, \lambda_3 = 1.217, \mathbf{v}_3 = \begin{bmatrix} -0.385 \\ -0.138 \\ 0.913 \end{bmatrix}.$$

With a 90% confidence interval based on a standard deviation of 0.017 around λ_2 all three eigenvalues are distinct, so then orthotropy is assumed. With a 95% confidence interval, λ_1 becomes trapped, so here transverse isotropy with two high-level moduli and one low-level modulus is assumed. Finally, with a 99% confidence interval also λ_3 is trapped and now isotropy is assumed.

The material's principal directions are defined by the eigenvectors of \mathbf{M} . Transforming the above stress and strain tensors into these directions, results in:

$$\sigma_{x'} = \begin{bmatrix} -0.026 \\ -0.000 \\ -0.146 \\ 0.004 \\ -0.061 \\ 0.002 \end{bmatrix}, \epsilon_{x'} = \begin{bmatrix} -859 \\ 873 \\ -5930 \\ 256 \\ -5114 \\ 316 \end{bmatrix}, \sigma_{y'} = \begin{bmatrix} -0.007 \\ -0.337 \\ -0.000 \\ 0.011 \\ 0.002 \\ -0.047 \end{bmatrix}, \epsilon_{y'} = \begin{bmatrix} 1216 \\ -6835 \\ 1772 \\ 518 \\ 488 \\ -2266 \end{bmatrix}, \sigma_{z'} = \begin{bmatrix} -0.617 \\ -0.014 \\ -0.109 \\ -0.040 \\ 0.260 \\ 0.094 \end{bmatrix}, \epsilon_{z'} = \begin{bmatrix} -5608 \\ 499 \\ 184 \\ -852 \\ 5915 \\ 1934 \end{bmatrix}.$$

In case of orthotropy, these tensors are substituted in the appropriate equations as given in Appendix I. For the transverse isotropic and isotropic cases, similar sets of equations can be derived. Applying singular value decomposition to obtain the pseudo-inverses of the stress sub-matrices, and multiplying these to the respective strain sub-matrices yield the values of S_{ij} . Having these values, the Young's and shear moduli and the Poisson's ratios are easily found using the relations worked out by Cowin and van Buskirk (1986). Their values are given in Table 4.

Despite the fact that the equations describing the material behavior were thermodynamically correct, it is due to the nature of the solution process using pseudo-inverse matrices (multi-dimensional least squares) that anomalies like $G_{23} > G_{12}$ may occur.

	Confidence level		
	90%	95%	99%
E_1	96.4	79.2	75.4
E_2	49.1	79.2	75.4
E_3	25.2	25.4	75.4
G_{23}	42.3	38.6	32.1
G_{31}	38.5	38.6	32.1
G_{12}	38.4	37.1	32.1
ν_{21}	0.06	0.07	0.18
ν_{12}	0.12	0.07	0.18
ν_{31}	0.17	0.16	0.18
ν_{13}	0.64	0.51	0.18
ν_{32}	0.12	0.16	0.18
ν_{23}	0.24	0.51	0.18

Table 4: Values of the Young's moduli E_i (MPa), shear moduli G_{ij} (MPa) and Poisson's ratios ν_{ij} , depending on the confidence level used to determine uniqueness of the eigenvalues of the MIL matrix for specimen no. 14.

Note: In case of orthotropy or transverse isotropy, the three shear components in the strain tensors are not actually zero. However, this 'isotropic simplification' is needed to obtain feasible values for the elastic moduli and Poisson's ratios. (Alternative methods to process the present data, like the one described by Cowin *et al.* (J. Biomech., **24**, 637-641, 1991), lead to unrealistic results.) Although the order of magnitude will not change, the actual values of the elastic moduli and Poisson's ratios may be affected by this assumption, though. Thanks to Prof. S.C. Cowin (City University of New York) for drawing attention to this problem.

Development and validation of a three-dimensional finite element model of the pelvic bone

M. Dalstra, R. Huiskes, L. van Erning*

Biomechanics Section, Institute of Orthopaedics, University of Nijmegen

*Institute of Diagnostic Radiology, University Hospital Nijmegen St. Radboud

Accepted for the Journal of Biomechanical Engineering

Abstract: *Due to both its shape and its structural architecture, the mechanics of the pelvic bone are complex. In Finite Element (FE) models, these aspects have often been (over)simplified, sometimes leading to conclusions which did not bear out in reality. The purpose of this study was to develop a more realistic FE model of the pelvic bone. This not only implied that the model had to be three-dimensional, but also that the thickness of the cortical shell and the density distribution of the trabecular bone throughout the pelvic bone had to be incorporated in the model in a realistic way. For this purpose, quantitative measurements were performed on computer tomography scans of several pelvic bones, after which the measured quantities were allocated to each element of the mesh individually. To validate this FE model, two fresh pelvic bones were fitted with strain gages and loaded in a testing machine. Stresses calculated from the strain data of this experiment were compared to the results of a simulation with the developed pelvic FE model.*

Introduction

The pelvic bone forms the upper part of the hip, and therefore plays an important role in the load transfer across this joint. During normal walking, the hip-joint force reaches values up to three or four times bodyweight. Also a number of powerful muscles are attached to the pelvic bone. Unlike long bones, which have to withstand similar loads and therefore have developed thick cortical shafts, the pelvic bone consists mainly of low-density trabecular bone, and is only covered by a thin cortical layer. In this, it resembles a so-called 'sandwich' construction (Jacob *et al.*, 1976; Dalstra and Huiskes, 1990), used in engineering to combine low weight and high strength. For the pelvic bone, this means that the bulk of the load is carried by and transferred through the cortical shell, while the trabecular bone acts as a spacer, keeping the shells from collapsing.

Having this complex geometry and structure, the basic mechanics of the pelvic bone are still not quite as well understood as, for example that of the femur. In studying the mechanics of the pelvic bone, strain-gage experiments (Jacob *et al.*, 1976; Petty *et al.*, 1980; Lionberger *et al.*, 1985; Finlay *et al.*, 1986; Ries *et al.*, 1989) and finite element analyses (Goel *et al.*, 1978; Vasu *et al.*, 1982; Carter *et al.*, 1982; Pedersen *et al.*, 1982; Oonishi *et al.*, 1983; Rapperport *et al.*, 1985; Huiskes, 1987; Koeneman *et al.*, 1989; Dalstra and Huiskes, 1990; Renaudin *et al.*, 1992; Landjerit *et al.*, 1992) have been the two most frequently used methods, although photoelastic models (Holm, 1981; Yoshioka and Shiba, 1981; Miles and McNamee, 1989) and thermoelastic emission techniques are occasionally being used as well. Potentially, the Finite Element Method (FEM) offers the most possibilities, as the other methods are surface techniques, which can only measure and describe phenomena taking place on the outside of the bone. However, the other methods normally use actual pelvic bones on which the measurements are performed, while for the FEM a computer model of the bone has to be constructed. The quality of FE results, therefore, is dependent on the quality of the model. The mechanics of the femur, for example, can well be analyzed using two-dimensional (2-D) models (Verdonschot and Huiskes, 1990), but for the pelvic bone this is entirely different. The first pelvic FE models with spin-off in designing acetabular prostheses, were either 2-D (Vasu *et al.*, 1982; Carter *et al.*, 1982; Rapperport *et al.*, 1985) or axisymmetric semi 3-D (Pedersen *et al.*, 1982; Huiskes, 1987) approximations of the real geometry. From a mechanical point of view, though, neither of these two approaches can adequately describe the mechanical situation around the acetabulum and throughout the rest of the pelvic bone. A 2-D model cannot account for the out-of-plane part of the acetabular wall and will therefore be too flexible. Vasu and co-workers (1982) found stresses exceeding 30 percent of the yield stress (appr. 120 MPa) and therefore they concluded that their 2-D model must overestimate the stresses. With an axisymmetric model just the opposite occurs, for in this case it is inherently assumed that the acetabular wall is present around the full 360 degrees. The opening between the pubic and ischial bones (the incisura acetabuli), however, shows that in reality this is not the case. These models, therefore, overestimate the real stiffness. So did Pedersen and

co-workers (1982) find stresses in the cortical shell due to a physiological value of the hip-joint force in the order of 0.5 MPa, which is improbably low. This gap between stresses of 40 MPa in a 2-D model and 0.5 MPa in an axisymmetric model suggest that by its shape and architecture, the pelvic bone is so typically three-dimensional by nature, that a FE analysis of the pelvic bone has to be done with a 3-D model. However, these models have negative aspects too. For a 3-D FE model of a complex structure like the pelvic bone to be accurate, many elements are required. This not only makes the computer analyses more time consuming and therefore more expensive, but also the pre- and postprocessing becomes much more cumbersome. In the last few years, however, increased computer capabilities have made 3-D models more accessible and because of this, the most recent pelvic FE studies have only made use of 3-D models (Koeneman *et al.*, 1989; Dalstra and Huiskes, 1990; Renaudin *et al.*, 1992; Landjerit *et al.*, 1992). Allocation of the material properties to the elements of a pelvic mesh is a problem, as well. In most, if not all, studies of the mechanics of the pelvic bone by means of a 3-D FE model, homogeneously distributed Young's moduli of trabecular bone and a uniform thickness of the cortical shell were assumed. Because of its 'sandwich' behavior, the load transfer across a pelvic bone will be relatively insensitive to changes in the material properties of the trabecular bone (Dalstra and Huiskes, 1990). The thickness of the cortical layer, however, is directly coupled to its stiffness and load-transmitting capability and, therefore, it is to be expected that variations in this parameter will certainly influence the overall load-transfer mechanism of the pelvic bone.

The purpose of this study was to develop and validate a realistic 3-D finite element model of the pelvic bone. Quantitative computer tomography scanning of several pelvic bones, together with data from an earlier study on the mechanical properties of pelvic trabecular bone (Dalstra *et al.*, 1993), were used to supply data for the FE mesh concerning the distribution of the density of the trabecular bone (and thus its Young's modulus) and the thickness of the cortical shell. This FE model was then verified by simulating a loading experiment with fresh pelvic bones fitted with strain gages, and comparing the numerical and experimental output. As a control, a 3-D FE model with homogeneous material properties and a cortical shell with uniform thickness was also included in this comparison.

Materials and Methods

Finite Element Mesh

A left pelvic bone of a 87 year old male donor was submerged in polyester resin. Fixed to the bone was a set of three small brass bars, which had been added for orientation purposes; originating in the center of the acetabulum, the first was aligned with the pubic bone, the second with the ischial bone and the third with the iliac bone. After hardening of the resin, the pelvic bone was sectioned by cutting 6 mm slices perpendicular to the brass bars. This meant that the pubic, the ischial and the iliac bones were sectioned perpendicular to their 'longitudinal' axes. The contours of

the sectioned bones were then digitized and, because the relative positions of the brass bars were known relative to one another, the spatial position of the contours could be reconstructed. This reconstruction was done in a Cartesian coordinate system defined by a plane over the rim of the acetabulum (xy-plane, the x-axis bisecting the angle between the ischial and pubic bones) and the z-axis as the normal to this plane, pointing into the acetabulum. The area within a contour was divided into 4-node elements and using a computer program, the respective elements in the subsequent contours were then connected to each other, forming the basic mesh consisting of 8-node brick elements. Some additional adjustments to the nodes and elements were necessary to make the sub-meshes of the iliac, pubic and ischial bone fit to one another at the acetabulum. Several views of the basic mesh are shown in Figure 1.

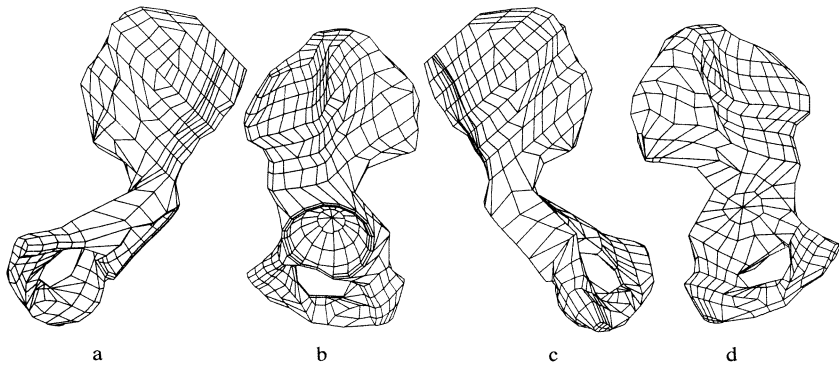


Fig. 1: The FE mesh of the left pelvic bone, seen from an anterior (a), a lateral (b), a posterior (c) and a medial (d) view.

The brick elements in the basic mesh only represent the trabecular and the subchondral bone. Given the dimensions of these elements, the cortical shell is so thin, that it could not be modeled by brick elements, since the thickness to length ratio (aspect ratio) of the elements would have been too small. In analogy with other 3-D pelvic studies (Oonishi *et al.*, 1983; Koeneman *et al.*, 1989; Renaudin *et al.*, 1992), membrane elements were chosen to represent the cortical layer, as these elements are compatible with brick elements. Keeping in mind the role of the cortical shell in the pelvic sandwich construction, it is not to be expected that the cortical bone will be heavily loaded perpendicular to the shell, and therefore membrane elements, which can only be submitted to in-plane loading, will be sufficient to describe the mechanical situation within the cortical shell. With another computer program, all the faces of the brick elements on the outer surface of the basic mesh were covered by 4-node membrane elements. Finally, the contralateral pelvic bone was added by mirroring the mesh in the sagittal plane. This final mesh consisted of 2,602 elements with a total of 1,862 nodes.

Quantitative Computer Tomography

Both pelvic bones of a 89 year old male donor were available. After being stripped of soft tissues, the bones were stored at -18°C until scanning and subsequent testing. The bones were scanned with a CT-scanner (Siemens, SOMATOM DR3) operating in dual-energy mode (85 and 125 kVp). Using the coordinate system as mentioned above, scans were taken parallel to the yz-plane. The slice thickness of a scan was 4 mm and the distance between two consecutive scans was 4 mm as well. Given the dimension of the bones, this resulted in a total of 57 scans per bone. A calibration phantom was included in the scans in order to be able to relate the X-ray absorption values for bone to a Ca-equivalent density, a quantity expressing the amount of hydroxyapatite per volume (Kalender and Suess, 1987). Postprocessing the CT-data, so-called water-equivalent and calcium-equivalent images were reconstructed, of which only the latter were used for further evaluation. Via a network, the digital images were transferred to a PC, equipped with an image-analysis system (TIM, Difa Measuring Systems, Breda, the Netherlands). This system was basically used to obtain two quantities. The first was the thickness of the cortical shell, which was directly measured as the distance between two points marked by the user on the outside and inside of the cortical shell. Owing to the calcium-equivalent images, the cortical shell was clearly distinguishable with a sharp contour and therefore it posed no problem defining two points on both sides of the shell. The second quantity was the Ca-equivalent density of the trabecular and subchondral bone, which was more elaborate to measure. First, an area-of-interest had to be defined by the user and in this area the grey values of all pixels were averaged. Then, an area on both sides of the calibration phantom had to be marked as well. By interpolating the average grey value of the area-of-interest between the grey values (with known Ca-equivalents) of the areas on the phantom, the Ca-equivalent density in the area-of-interest was found.

These measurements were performed twice over. At first instance, they were done to examine the differences between the left and the right bone. For this purpose, only the maximal cortical thickness and the average Ca-equivalent density for the entire trabecular bone area from each scan were recorded and compared to the respective values of the contralateral scan. After this, the measurements were repeated in order to allocate the quantities to the elements of the FE mesh. To do this as accurately as possible, mappings of cross-sections through the FE mesh were made in order to be able to transpose the exact locations of the individual elements to an area-of-interest in the scans. Figure 2 shows an example of a scan through the lower half of the acetabulum, with the accompanying cross-section through the FE mesh. At each location of an element, the thickness (for the membrane elements) or the Ca-equivalent density (for the brick elements) were measured and allocated to this element. If a particular element appeared in more than one scan, its values of the density or thickness were averaged after the measurements in all scans had been completed.

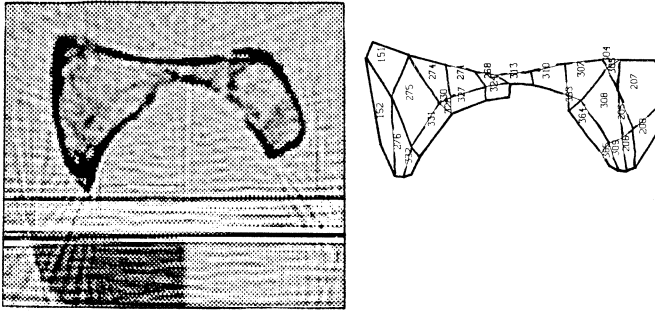


Fig. 2: A CT-scan from the lower acetabular region with the accompanying section through the FE mesh.

Mechanical Testing

The two bones, which had been used for the QCT measurements, were also used in the strain-gage experiment. Each bone was fitted with eight 90° rosette strain gages (FRA-1-11; Tokyo Sokki Kenkyujo Co., Japan). The locations of the gages were chosen both on the lateral and medial cortical shell (Figure 3). The bones were placed next to each other with the iliac crests submerged in a bed of acrylic cement. A physiological position of the bones relative to one another was maintained and contact at the pubic symphysis was restored. The angle of placement was such that the direction of a vertically downward applied load would correspond to that of the hip-joint force during one-legged stance. This position had been found by applying a coordinate transformation to telemetry data by Bergmann and co-workers (1990) from their femur-based coordinate system to the present acetabulum-based coordinate system.

After hardening of the cement, the bones were placed in an MTS-based testing machine (DSTS Engineering & Electronics, Zoetermeer, the Netherlands). The load was applied through a femur-shaped lever arm, attached to the force transducer. Each bone was loaded separately by applying forces of 150, 300, 450 and 600 N and at each load increment, the strains in the gages were recorded and stored in a PC. From these data, the principal strains and stresses, the Von Mises stresses and the maximal shear stresses were calculated afterwards. For the calculations of stresses, a Young's modulus of 17 GPa and a

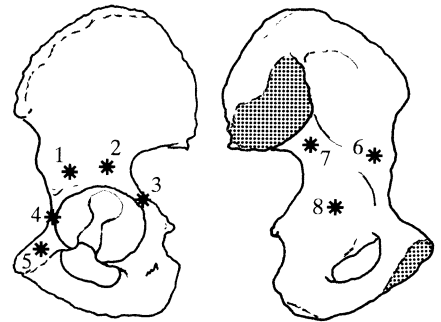


Fig. 3: The locations of the eight rosette strain gages.

Poisson's ratio of 0.3 were assumed for the cortical bone.

Finite Element Analyses

The mesh described above was used in two FE analyses. The first model had material properties according from the results of the CT-measurements. The Ca-equivalent density and the cortical thickness measured at the respective locations of each brick and membrane element were used as input for these elements. The relationship between Ca-equivalent density (ρ_{Ca-eq}), apparent density (ρ_{app}) and Young's modulus (E) of both trabecular and subchondral bone was based on two relations which were established in an earlier study: $\rho_{Ca-eq} = 0.626 \rho_{app}$ and $E = 2017.3 \rho_{app}^{2.46}$ (Dalstra *et al.*, 1993). This study also showed that pelvic trabecular bone can be assumed as isotropic and that its Poisson's ratio is close to 0.2. Furthermore, based on current values reported in literature, the Young's modulus and Poisson's ratio of cortical bone were assumed to be 17 GPa and 0.3, respectively. For the second FE model, the same mesh was used, but in this case material properties were assumed to be homogeneous. Young's modulus and Poisson's ratio for trabecular, subchondral and cortical bone were taken to be 70 MPa and 0.2, 2 GPa and 0.3, and 17 GPa and 0.3, respectively. In accordance with other 3-D pelvic models (Goel *et al.*, 1978; Oonishi *et al.*, 1983), a cortical thickness of 1 mm was used. As the sub-mesh of the right side pelvic bone merely had an auxiliary function, in both models its elements were given the same material properties as used for the homogeneous model.

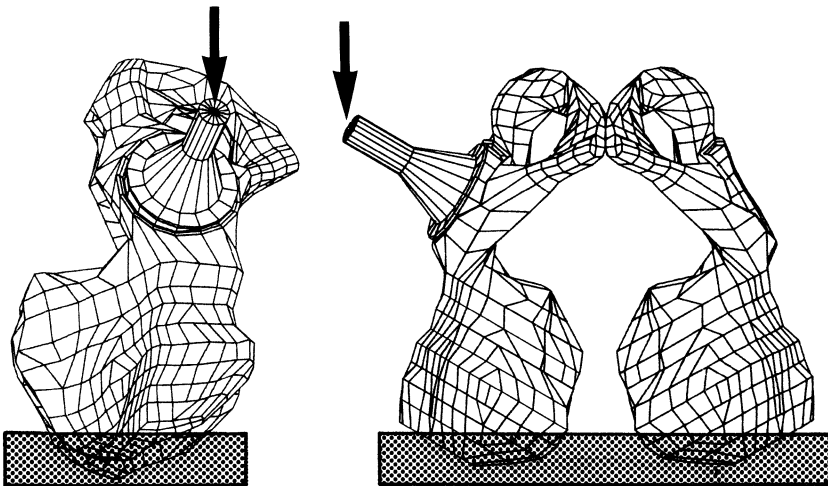


Fig. 4: FE simulation of the loading experiment (lateral and frontal view).

Both the 'realistic' and the homogeneous model were supported by keeping the nodes on the superior iliac crest fixed, which corresponded to the boundary conditions of the experimental set-up. To simulate the exact loading conditions from the experiment, a part of the femur-shaped lever arm had to be included in the

model, which, in correspondence to the experiment, was only allowed to move vertically. The actual loading was applied by a vertically directed point load at the back of the lever arm, which had a magnitude of 600 N. Figure 4 shows a lateral and a frontal view of the experimental set-up of the FE model. Contact between the ball-shaped head and the acetabular surface was modelled by 60 gap elements, thus ensuring that only compressive forces could be transferred onto the acetabulum.

The analyses were performed using the MARC/MENTAT FEM and pre- and postprocessing codes (MARC Analysis Corporation, Palo Alto, CA, USA) running on the EX-60 mainframe computer (Hitachi Data Systems, Japan) of the University of Nijmegen.

Results

Dual Energy Quantitative Computer Tomography

The results of the CT-measurements showed a very close resemblance between the left and the right bone. In Figure 5, it can be seen that both the maximal cortical thickness and the average Ca-equivalent density per scan have a high degree of similarity between left and right. Apart from the close resemblance of the curves, it also shows that the highest values for the cortical thickness (just over 3 mm) are found at the level of the superior acetabular rim. Here, also the average trabecular density is highest. The increase of the Ca-equivalent density at both ends of the curves is an anomaly and is caused by 'cortical interference'; in the first and last two scans, the trabecular bone could not be identified separately from the cortical shell, thus yielding the higher absorption values.

Having this good agreement in material properties between the left and the right bone, only the left pelvic bone was used for the CT-measurements to allocate the material properties to the individual elements. In Figure 6 and 7, the distribution of both the thickness of the cortical bone and the Young's modulus (calculated directly from the Ca-equivalent density) of the trabecular bone are shown. The values are already transposed onto their respective elements in the FE mesh.

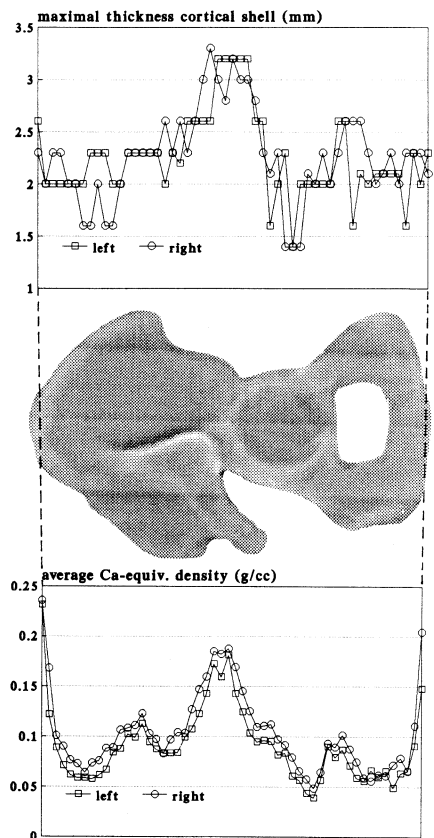


Fig. 5: Values of the maximal cortical thickness (top) and the average Ca-equivalent density (bottom) for the left and the right bone.

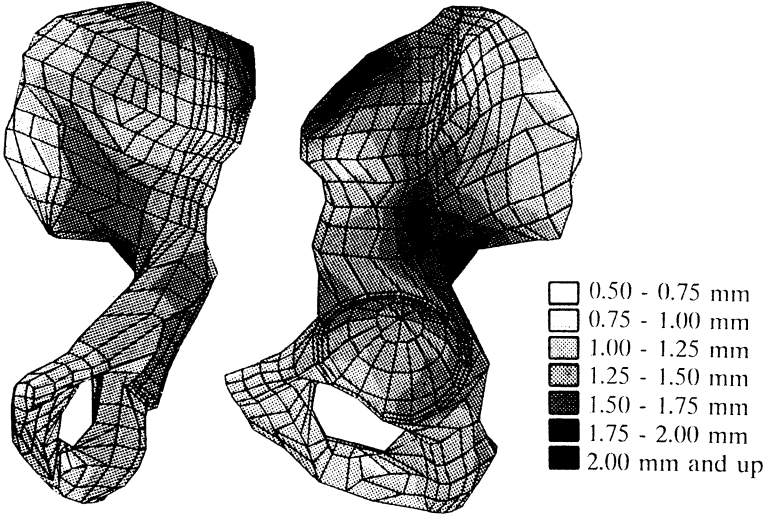


Fig. 6: Distribution of the thickness of the cortical shell, as measured from the CT-scans and transposed onto the FE mesh (frontal and lateral view).

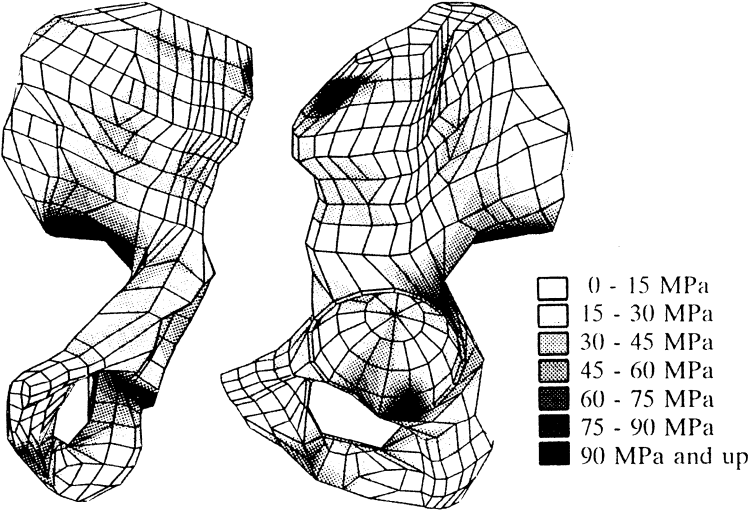


Fig. 7: Distribution of the Young's modulus of the underlying trabecular bone, as measured from the CT-scans and transposed onto the FE mesh (frontal and lateral view).

Cortical thicknesses of 2 mm and up are found at the incisura ischiadaca major region extending up the iliac bone. Also the top of the iliac bone has a relatively thick cortex. At the articular surfaces of the sacro-iliac joint and the pubic symphysis, cortical thickness is less than 1 mm. For the trabecular Young's modulus the average value lies around 40 MPa. Areas with relatively high densities are found around the acetabulum extending to the sacro-iliac joint, where values of around 100 MPa are

found. However, the highest value was only 186 MPa. It should be noted that the Young's moduli for the subchondral bone are not included in Figure 7. For this type of bone, the Young's modulus was found to be one order of magnitude higher than for the trabecular bone, with values ranging between 132 and 2,155 MPa.

Mechanical Testing

The applied loads had been relatively low to ensure that the strains and stresses measured at the strain-gage locations were linearly related to the magnitude of that

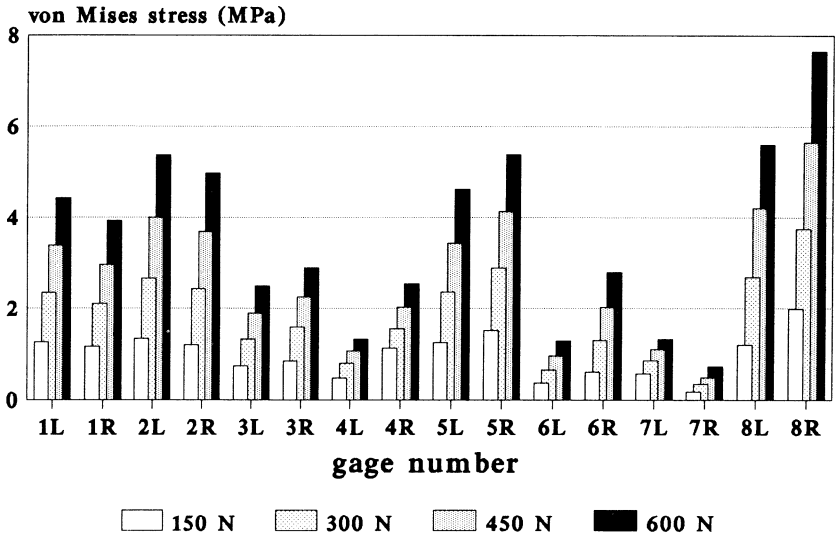


Fig. 8: Von Mises stresses at the eight strain gages for both left and right pelvic bone as a function of the applied load.

load. Figure 8 shows the Von Mises stresses at the strain-gage locations for both left and right bones as a function of the load applied in the test.

When correlating these values to the magnitude of the applied load, the lowest value for R^2 was still 0.954 (gage 7 of the left bone; Figure 3). The highest stresses occurred at location 8, the medial cortical shell right underneath the acetabular dome. Also the locations 1, 2 (the superior acetabular rim) and 5 (the pubic bone) showed relatively high stresses. The least-stressed area was location 7, lying in the incisura ischiadaca major region. As mentioned above, in this region the

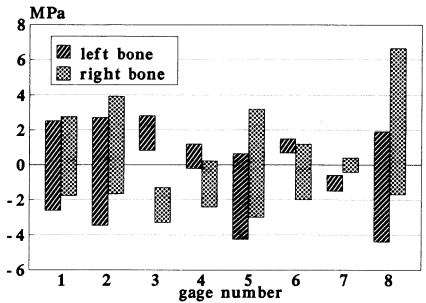


Fig. 9: Ranges between the maximal and minimal principal stresses at the eight strain-gage locations found in the experiment for both left and right pelvic bones at a load of 600 N.

cortical shell had been found to be relatively thick and therefore the local resistance against deformation is higher. In Figure 9, the range between the maximal and minimal principal stresses is given for each strain gage. This shows that at some gages, the similarity between left and right is less consistent as Figure 8 suggests. At gage 3 of the left bone, for instance, only tensile stresses occur, while at the same location on the right bone only compressive stresses are found. However, the Von Mises stresses at both gages are almost the same, as can be seen in Figure 8.

Finite Element Analyses

Given the differences between the stresses in the left and right bone in the experiment, the numerical and experimental results were very well comparable.

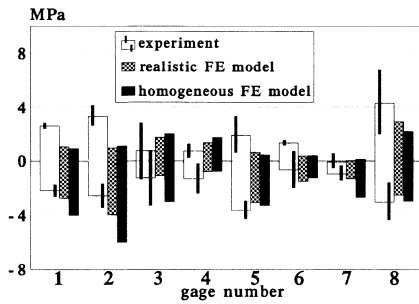


Fig. 10: Ranges between the maximal and minimal principal stresses at the strain-gage locations found in the experiment (averaged for the left and right bone; the bars denote the standard deviations), the 'realistic' FE model and the homogeneous FE model.

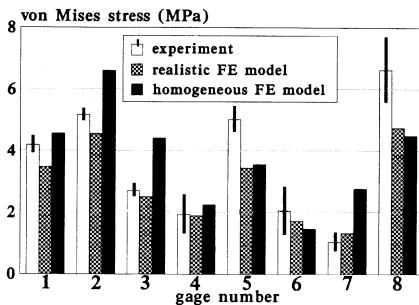


Fig. 11: The Von Mises stresses found in the experiment (averaged for the left and right bone; the bars denote the standard deviations), the 'realistic' FE model and the homogeneous FE model.

Figure 10 shows a comparison between the ranges set by the principal stresses at the locations of the strain gages for the experiment, the 'realistic' FE model and the homogeneous FE model. The minimal principal stresses predicted by the 'realistic' FE model agree very well with the experimental findings. At locations 1, 2, 5 and 6, the maximal principal stresses are somewhat lower than the experimental results. The stresses predicted by the homogeneous model are generally higher than the ones predicted by the 'realistic' model. This becomes clear in Figure 11, which shows the Von Mises stresses at the strain-gage locations. At locations 2, 3 and 7, the homogeneous model predicts stresses, which exceed both the 'realistic' and the experimental results. These increases are caused by increased compressive stresses at these locations, as can be seen in Figure 10. The differences in the stresses at the strain-gage locations between the two FE models indicate that the overall load transfer between the two models is different, as well. This is illustrated in Figure 12, where the distributions of the Von Mises stresses in the cortical shell are given for both the 'realistic' model and the homogeneous model. The overall load transfer is governed by the hip-joint force, of which a major part is transferred from the acetabulum to the area of support at the iliac

crest and a minor part is transferred onto the contralateral pelvic bone through the pubic bone. The highest stresses, therefore, are found at the superior acetabular rim, extending through the central part of the iliac bone towards the iliac crest and also at the pubic bone (Figure 12).

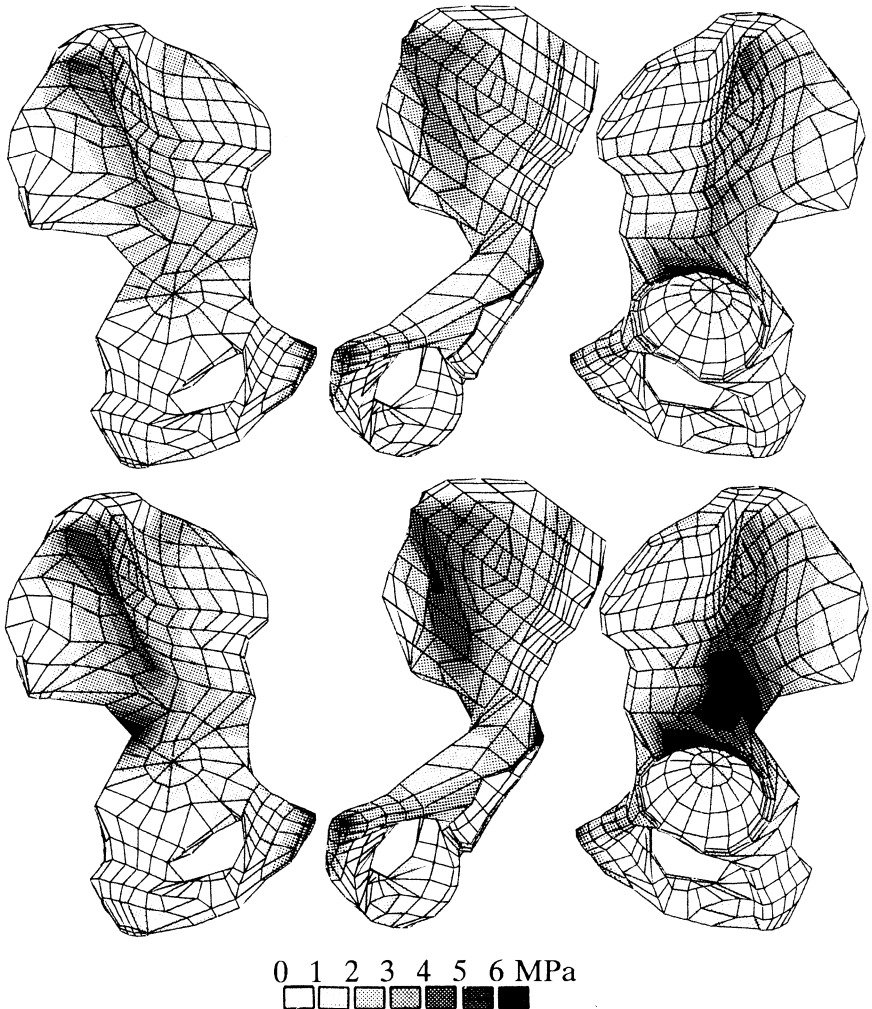


Fig. 12: Distribution of the Von Mises stresses in the cortical shell of the 'realistic' model (top) and the homogeneous model (bottom).

The stresses in this 'central column' of the iliac bone are predominantly compressive and are directed parallel to the line of action of the applied load. In this particular loading mode, with no muscles present, the ischial bone and the anterior and posterior parts of the iliac bone remain virtually unloaded. As already stated above,

the stress intensity is generally higher for the homogeneous model; especially in the areas of primary load transfer, like the superior acetabular rim and the incisura ischiadaca major region.

Discussion

From a mechanical point of view, the pelvic bone is a complex structure. Not only due to its three-dimensional character, but also by the distribution of different types of bone. The bulk of its material is low-density trabecular bone, which is covered by a thin cortical shell. The thickness of this layer is not uniformly distributed over the bone and is adjusted to the load transfer across the pelvic bone. To take this into account when analyzing pelvic mechanics by means of the finite element method, a mere 3-D model of the pelvic bone is not enough. We have tried to develop a physiological pelvic FE model in which the material properties of the trabecular bone and the thickness of the cortical shell were based on quantitative measurements from dual-energy CT-scans of an actual pelvic bone. It might be argued that the values obtained from only one bone of one individual (♂, 89 yrs.) will limit the applicability of the model. However, comparative measurements performed on the contralateral bone of the same donor showed that the distributions of trabecular density and cortical thickness between the left and the right bone were virtually symmetrical (Figure 5). Furthermore, the densities measured were compared to values found for a series of eight other pelvic bones of both male and female donors of the same age group (Dalstra *et al.*, 1993), and were found to be in the same range. It can therefore be assumed that the measured values of this particular bone were neither exceptionally low nor high. And as one of the future uses for this FE model will be to assess acetabular prostheses, the allocation of material properties of bone from elderly people may not be considered to be a problem.

The Young's moduli for trabecular bone calculated from the measured Ca-equivalent densities varied between 1 and 186 MPa. This shows that pelvic trabecular bone is much less stiff as, for instance, trabecular bone of femoral or tibial origin, for which values of 1500 MPa are not exceptional. Yet, it were these higher values, which have often been used in pelvic FE studies (Goel *et al.*, 1978; Oonishi *et al.*, 1983; Pedersen *et al.*, 1982; Rappoport *et al.*, 1985; Huiskes, 1987). For the Young's modulus of the subchondral bone layer in the acetabulum, higher values were found, ranging between 132 and 2,155 MPa. The thickness of the cortical shell varied between 0.7 and 3.2 mm (Figure 6). The highest values were found in the regions of primary load transfer (the superolateral part of the acetabular rim and the incisura ischiadaca major area leading to the sacroiliac joint). The articulating surfaces of the cortical shell at the sacro-iliac joint and pubic symphysis displayed thicknesses below 1 mm. From these measurements it appears that 3-D models with a uniform cortical thickness of 1 mm (Goel *et al.*, 1978; Oonishi *et al.*, 1983) may be somewhat unrealistic. Goel and co-workers found stresses of 0.82 times bodyweight (57.4 MPa for a bodyweight of 70 kg) in the cortical shell. Oonishi and co-workers, on the other

hand, reported very low stresses; from their results it appears that the Von Mises stresses in the cortex are well below 1 MPa. However, they made a mistake in calculating the magnitude of the load from kgf to N (instead of multiplying by 9.8, they divided by 9.8, which would mean that their results are almost a factor 100 too small!). If this is the case, their results become comparable again to those of Goel and co-workers. Stresses of this magnitude are indeed much too high to occur in cortical bone during normal walking and would in reality lead to rapid fatigue failure. It must, therefore, be concluded that both models are too flexible.

To verify our FE model, the bones which had been used for the CT-measurements were also used for strain-gage measurements in a loading machine. In this testing procedure, the only load applied to the pelvic bones was a force directed into the acetabulum, simulating the hip-joint force at one-legged stance. Because no muscle forces were simulated and due to the unnatural fixation of the pelvic bones at the top of the iliac crest, instead of at the articulating surface of the sacro-iliac joint area, this set-up cannot be considered particularly physiological. However, this was not the intention in the first place, as its sole purpose was just to obtain data which could be directly compared to the results from the analyses with the FE model.

It is difficult to compare the experimental stresses with values from the literature, because in the various reported pelvic strain-gage studies, different aspects of pelvic mechanics were examined. Jacob and co-workers (1976) did not use actual bones for their experiment, but epoxy models. Furthermore, they included muscle forces. Petty and co-workers did use actual bones, but they were only interested in the strains in a particular region at the medial cortex (Petty *et al.*, 1980), where in our case no strain gage was present. Finlay and co-workers (1986) reported on stresses in the cortical shell of a normal pelvic bone. However, when calculating stresses from the strains, they assumed a Young's modulus of 6.2 GPa for cortical bone, which seems rather low and besides that, both the magnitude and the direction of the load in their study differ from the present case. Although the magnitude of the stresses are of the same order of magnitude as our findings, their results are somewhat lower due to the lower cortical Young's modulus. Ries and co-workers (1989) looked at the strains in the pelvic cortical shell as a function of the size of the head of a hemiarthroplasty. The results of this study can neither be compared to the present ones, as they give no absolute values of these strains. Miles and McNamee (1989) looked at the load transfer in the pelvic bone being affected by the position of the axis of rotation. However, like Ries and co-workers, they neither gave absolute values of the strains they measured.

When comparing the strain-gage results with the FE results, one should realize that strain-gage measurements supply only local data, which is in fact an average of the real strains occurring underneath the gage. The outcome of a FE analysis provides a continuous field of strains or stresses, and if sharp gradients in these quantities are present, it will be virtually impossible to find a perfect match between experiment and FE model. Beside the stress/strain gradients, another reason for experimental and numerical mismatch might be the use of the membrane elements for the cortical shell. For the 'realistic' model, relatively high values for the thickness of the membrane

elements had to be allocated at some locations. It was unknown, how this would affect the performance of these membrane elements. Therefore, benchtesting of these elements with increasing thicknesses was done and this showed that an element with a thickness of 50 percent of its length overestimated the actual results by only 10 percent. Therefore, this can be considered a minor effect. Finally, there was a difference in the diameter of the head of the femur-shaped lever arm between the experiment and the FE model. In correspondence to the size of the acetabula of the bones used in the experiment, a diameter of 45 mm had to be used, while due to the larger acetabulum of the bone on which the FE mesh had been based, a femoral head with a diameter of 62 mm was needed in the FE model. This difference will certainly affect the stresses within the acetabulum and at its close surroundings, but most strain-gage locations were located in the periphery. Taking all this and the differences between the experimental results from the left and the right bone into account, it appeared that, on the whole, the stresses from the FE models showed a reasonable agreement to the experimental ones. As to be expected, the results from the 'realistic' model were better than the homogeneous model, although the results from the latter were not that far off, either. However, the homogeneous model overestimated the stresses by an average 30 percent, particularly in the areas of primary load transfer, where the 'realistic' model had a thicker cortical shell to compensate for the higher loads.

It can therefore be concluded that the presently developed FE model has the basic ability to describe the stress and strain distributions in the pelvic bone realistically. For comparative studies, a less elaborate model with homogeneously distributed material properties may be used, but if absolute values of mechanical quantities are to be examined, it will certainly pay off to use a more detailed model.

References

- Bergmann, G., Graichen, F., Rohlmann, A. (1990) Instrumentation of a hip joint prosthesis. In: *Implantable telemetry in orthopaedics.*, eds. G. Bergmann, F. Graichen, A. Rohlmann, Freie Universität Berlin, pp. 35-63.
- Carter, D.R., Vasu, R., Harris, W.H. (1982) Stress distributions in the acetabular region II: effects of cement thickness and metal backing of the total hip acetabular component. *J. Biomech.*, **15**, 165-170.
- Dalstra, M., Huiskes, R. (1990) The pelvic bone as a sandwich construction; a three dimensional finite element study. *Proc. Europ. Soc. Biomech.*, **7**, B32.
- Dalstra, M., Huiskes, R., Odgaard, A., van Erning, L. (1993) Mechanical and textural properties of pelvic trabecular bone. *J. Biomech.*, **26**, 523-535.
- Finlay, J.B., Bourne, R.B., Landsberg, P.D., Andreae, P. (1986) Pelvic stresses *in vitro* - I. malsizing of endoprostheses. *J. Biomech.*, **19**, 703-714.
- Goel, V.K., Valliappan, S., Svensson, N.L. (1978) Stresses in the normal pelvis. *Comput. Biol. Med.*, **8**, 91-104.
- Holm, N.J. (1981) The development of a two-dimensional stress-optical model of the os coxae. *Acta Orthop. Scand.*, **52**, 135-143.
- Huiskes, R. (1987) Finite element analysis of acetabular reconstruction. *Acta Orthop. Scand.*, **58**, 620-625.
- Jacob, H.A.C., Huggler, A.H., Dietschi, C., Schreiber, A. (1976) Mechanical function of subchondral bone as experimentally determined on the acetabulum of the human pelvis. *J. Biomech.*, **9**, 625-627.

- Kalender, W.A., Suess, C. (1987) A calibration phantom for quantitative computed tomography. *Med. Phys.*, **14**, 863-866.
- Koenenman, J.B., Hansen, T.M., Beres, K. (1989) Three dimensional finite element analysis of the hip joint. *Trans. Orthop. Res. Soc.*, **14**, 223.
- Landjerit, B., Jacquard-Simon, N., Thourot, M., Massin, P.H. (1992) Physiological loadings on human pelvis: a comparison between numerical and experimental simulations. *Proc. Europ. Soc. Biomech.*, **8**, 195.
- Lionberger, D., Walker, P.S., Granholm, J. (1985) Effects of prosthetic acetabular replacement on strains in the pelvis. *J. Orthop. Res.*, **3**, 372-379.
- Miles, A.W., McNamee, P.B. (1989) Strain gauge and photoelastic evaluation of the load transfer in the pelvis in total hip replacement: the effect of the position of the axis of rotation. *Proc. Instn. Mech. Engrs.*, **203**, 103-107.
- Oonishi, H., Isha, H., Hasegawa, T. (1983) Mechanical analysis of the human pelvis and its application to the articular hip joint - by means of the three dimensional finite element method. *J. Biomech.*, **16**, 427-444.
- Pedersen, D.R., Crowninshield, R.D., Brand, R.A., Johnston, R.C. (1982) An axisymmetric model of acetabular components in total hip arthroplasty. *J. Biomech.*, **15**, 305-315.
- Petty, W., Miller, G.J., Piotrowski, G. (1980) In vitro evaluation of the effect of acetabular prosthesis implantation on human cadaver pelves. *Bull. Pros. Res.*, **17**, 80-89.
- Rapperport, D.J., Carter, D.R., Schurman, D.J. (1985) Contact finite element stress analysis of the hip joint. *J. Orthop. Res.*, **3**, 435-446.
- Renaudin, F., Lavaste, F., Skalli, W., Pecheux, C., Scmitt, V. (1992) A 3D finite element model of pelvis in side impact. *Proc. Europ. Soc. Biomech.*, **8**, 194.
- Ries, M., Pugh, J., Au, J.C., Gurtowski, J., Dee, R. (1989) Cortical pelvic strains with varying size hemiarthroplasty in vitro. *J. Biomech.*, **22**, 775-780.
- Vasu, R., Carter, D.R., Harris, W.H. (1982) Stress distributions in the acetabular region - I. before and after total joint replacement. *J. Biomech.*, **15**, 155-164.
- Verdonschot, N., Huiskes, R. (1990) FEM analyses of hip prostheses: validity of the 2-D side-plate model and the effects of torsion. *Proc. Europ. Soc. Biomech.*, **7**, A20.
- Yoshioka, Y., Shiba, R. (1981) A study of the stress analysis of the pelvis by means of the three-dimensional photoelastic experiments. *J. Jap. Orthop. Ass.*, **55**, 63-76.

Chapter III

Load transfer across the pelvic bone

M. Dalstra, R. Huiskes

Biomechanics Section, Institute of Orthopaedics, University of Nijmegen

Submitted to the Journal of Biomechanics

Abstract: *Earlier experimental and finite element studies notwithstanding, the load transfer and stress distribution in the pelvic bone and the acetabulum in normal conditions are not well understood. This hampers the development of orthopaedic reconstruction methods. The present study deals with more precise finite element analyses of the pelvic bone, which are used to investigate its basic load transfer and stress distributions under physiological loading conditions. For this purpose, a three-dimensional model of two bilateral pelvic bones was used. Material properties of the elements were based on quantitative computer tomography measurements of actual pelvic bones. For loading conditions, eight different phases of a normal walking cycle were considered, accounting for the hip-joint force and twenty one muscle forces.*

Acting as a 'sandwich construction', the major part of the load is transferred through the cortical shell. Although the magnitude of the hip-joint force varies considerably, its direction during normal walking remains pointed into the anterosuperior quadrant of the acetabulum. Combined with the fact that the principal areas of support for the pelvic bone are the sacro-iliac joint and the pubic symphysis, this causes the primary areas of load transfer to be found in the superior acetabular rim, the incisura ischiadaca region and, to a lesser extent, the pubic bone. Due to the 'sandwich' behavior of the pelvic bone, stresses in the cortical shell are about 50 times higher than in the underlying trabecular bone. Muscle forces have a stabilizing effect on the pelvic load transfer. Analyses without muscle forces show that at some locations stresses are actually higher than when muscle forces are included.

Introduction

A mature pelvic bone is an osseous integration of three separate parts, the iliac, the ischial and the pubic bones. These three merge, forming the acetabulum, the socket of the hip joint, through which the pelvic bone interacts with the femoral head. The primary task of the pelvic bone in this interaction is to support the weight of the upper body and transfer it onto the lower extremities. In doing so, the pelvic bones have to withstand forces which are a multitude of that weight. Within the limits of the anatomical boundary conditions, the pelvic bone has evolved into a very efficient structure, which is well able to carry these large forces. Consisting mainly of low-density trabecular bone (Dalstra *et al.*, 1992), which by itself is not strong enough by far to withstand such high loads, it is totally covered by a thin layer of cortical bone. In this way, it resembles a so-called 'sandwich construction', used in engineering to combine high strength and low weight (Jacob *et al.*, 1976). However, besides this 'sandwich behavior', little is known about the basic mechanics of the pelvic bone. Strain-gage techniques (Jacob *et al.*, 1976; Petty *et al.*, 1980; Lionberger *et al.*, 1985; Finlay *et al.*, 1986; Ries *et al.*, 1989) and finite element (FE) analyses (Goel *et al.*, 1978; Vasu *et al.*, 1982; Carter *et al.*, 1982; Pedersen *et al.*, 1982; Oonishi *et al.*, 1983; Rapperport *et al.*, 1985; Oonishi *et al.*, 1986; Huiskes, 1987; Koeneman *et al.*, 1989; Dalstra and Huiskes, 1990; Renaudin *et al.*, 1992; Landjerit *et al.*, 1992) are the two methods most frequently used for studying pelvic mechanics. But most of the studies on pelvic mechanics reported in the literature deal with certain aspects of acetabular implants rather than the basic mechanics of the pelvic bone itself.

Due to the highly irregular geometry of a pelvic bone, FE analyses are required to obtain a proper insight in the strain distributions throughout the whole bone. Two-dimensional and axisymmetric finite element models each have their specific shortcomings which make them less suitable to describe pelvic mechanics in a realistic way.

The purpose of this study was to evaluate the load-transfer mechanism and the stress patterns in the natural pelvic bone, using an experimentally validated sophisticated three-dimensional (3-D) finite element model and new information about the hip-joint force and muscle loads.

Method

In this 3-D FE analysis, a bilateral pelvic mesh was used consisting of 2,602 isoparametric elements. Figure 1 gives a frontal view of the mesh. Brick elements were used to form the trabecular and the subchondral bone. The Young's moduli allocated to these elements were based on the results of quantitative computer tomography measurements (Dalstra and Huiskes, 1992). For the trabecular bone, the Young's moduli ranged from 1 MPa to 132 MPa; for the subchondral bone, the range was 186 MPa to 2,155 MPa. Examination of the material properties of pelvic trabecular bone has shown that it is not highly anisotropic (Dalstra *et al.*, 1993). Therefore, assuming isotropy for these elements seems justified. The same study

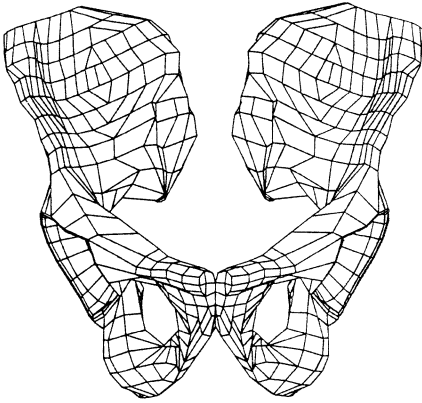


Fig. 1: Frontal view of the 3-D mesh of the two pelvic bones.

showed that 0.2 is a good approximation for the Poisson's ratio of pelvic trabecular bone. In the FE model, the thin cortical shell of the pelvic bones is represented by membrane elements. The thickness of these elements was based on computer tomography measurements as well (Dalstra and Huiskes, 1992) and ranged from 0.7 to 3.2 mm with an average value of about 1.5 mm. Young's modulus and Poisson's ratio for these elements were assumed to be 17 GPa and 0.3 respectively. Furthermore, a part of the femoral head was included as well to ensure smooth and realistic introduction of the hip-joint force into the acetabulum (Huiskes, 1987). Contact between

this head and the acetabulum was modeled by 60 gap elements, ensuring that only compressive forces could be transmitted from the femoral head onto the acetabulum. This contact was assumed to be frictionless, but articular cartilage was not included in this model, so that the femoral head was in direct contact with the subchondral bone. The model described has previously been verified in a simulation of a strain-gage experiment and its results have shown satisfying agreement with the experimental findings (Dalstra and Huiskes, 1992).

As kinematic boundary conditions for the FE model, the nodes situated in the sacro-iliac joint areas on both bones were kept fixed to simulate sacral support of both pelvic bones. The loading conditions for the model were based on walking activities. The hip-joint force and the forces of twenty one muscles attached to the pelvic bone were taken into account at eight characteristic phases of a normal walking cycle (Table 1). The magnitudes and directions of the hip-joint force at these eight phases were based on data by Bergmann *et al.* (1990). By means of prostheses fitted with telemetry devices, they performed *in-vivo* measurements of the hip-joint force during all kinds of activities. The direction of the hip-joint force in their measurements was given in a coordinate system relative to the femur and had to be transformed accordingly into a direction relative to the coordinate system of the present pelvic model. The relative position of the pelvic bone and the femur changes during walking. For the transformation calculations, the angle between the pelvic bone (longitudinal body axis) and the femur in the A/P plane (flexion/extension) was taken into account. Values for this angle were measured with a SELSPOT motion-analysis system (Selspot AB, Mölndal, Sweden) on one of the authors (M.D.) and are also given in Table 1. Furthermore, Bergmann and co-workers express the magnitude of the hip-joint force as a percentage of the total body weight. In our particular case, a body weight of 650 N was assumed. The magnitudes of the hip-joint forces in which this resulted are given in Table 2. In the FE model, the hip-joint force was applied as a distributed load on the head/neck section of the femoral head.

Case	Description	% Walking Cycle	Flexion Angle
1	Double support, beginning left stance phase	2	22° (fl.)
2	Beginning left single support phase	13	18° (fl.)
3	Halfway left single support phase	35	4° (ext.)
4	End left single support phase	48	12° (ext.)
5	Double support, end left stance phase	52	14° (ext.)
6	Beginning left swing phase	63	2° (fl.)
7	Halfway left swing phase	85	31° (fl.)
8	End left swing phase	98	21° (fl.)

Table 1: Description of the load cases with respect to their occurrence within a walking cycle and the flexion/extension angle between the pelvic bone and the femur.

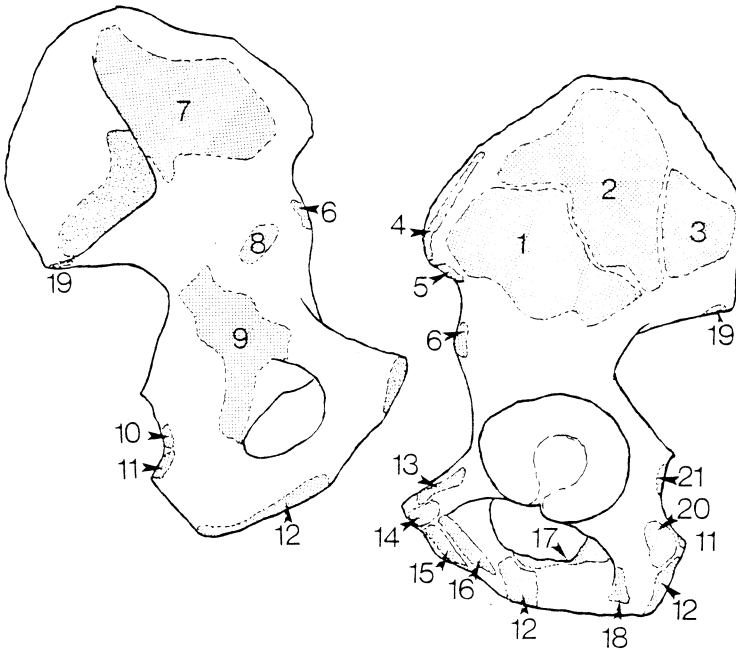


Fig. 2: Identification of the insertion areas of the various muscles used in the model; 1. gluteus minimus, 2. gluteus medius, 3. gluteus maximus, 4. tensor fascia lata, 5. sartorius, 6. rectus femoris, 7. iliacus, 8. psoas, 9. obturator internus, 10. gemellus inferior, 11. semitendinosus, 12. adductor magnus, 13. pectineus, 14. adductor longus, 15. gracilis, 16. adductor brevis, 17. obturator externus, 18. quadratus femoris, 19. piriformis, 20. semimembranosus, 21. gemellus superior.

	Load Cases							
	1	2	3	4	5	6	7	8
hip-joint force	426	2158	1876	1651	1180	187	87	379
gluteus maximus	842	930	167	377	456	491	114	482
gluteus medius	1018	1053	1474	1509	1412	982	105	421
gluteus minimus	228	140	263	228	175	123	114	219
tensor fasciae latae	0	132	88	158	149	88	70	96
iliacus	0	0	0	228	307	272	0	0
psoas	149	0	316	175	88	175	105	140
gracilis	0	0	0	0	88	158	70	140
sartorius	0	88	0	0	35	158	88	88
semimembranosus	579	368	333	368	421	298	61	421
semitendinosus	0	140	105	246	316	368	105	0
biceps femoris longus	298	202	88	70	123	114	79	377
adductor longus	0	88	0	0	88	158	70	140
adductor magnus	0	0	0	0	132	263	0	0
adductor brevis	0	114	0	0	0	202	0	114
obturator externus	0	0	0	0	123	167	132	123
obturator internus	167	123	0	61	61	149	123	0
pectineus	0	0	175	96	0	149	0	0
piriformis	202	175	0	0	0	0	123	228
quadratus femoris	61	96	0	0	88	184	0	0
superior gemellus	140	88	123	79	0	0	158	202
inferior gemellus	0	0	0	0	0	140	79	149
rectus femoris	0	123	0	0	0	175	105	96

Table 2: Magnitudes (in Newton) of the hip-joint force and muscle forces for the considered eight load cases.

Apart from the hip-joint force, twenty two muscles inserting onto the pelvic bone were incorporated in the model. Figure 2 shows the areas of attachment of these muscles. The directions of the muscles were found by subtracting the coordinates of their distal and proximal insertions (Dostal and Andrews, 1981), whereby the same

rotation of the pelvic bone relative to the femur in the A/P-plane as mentioned above was taken into account. Because of their multiple lines of action, it was necessary to make a differentiation in ventral, central and dorsal parts for the gluteus minimus, the gluteus medius and the adductor magnus muscle. The magnitudes of the muscle forces were based on EMG-data by Crowninshield and Brand (1981). A mapping of the physiological areas of insertion of each of the muscles was made onto the finite element mesh and muscle forces were applied as distributed loads on the surfaces of those elements which were located in these respective areas of insertion. The magnitudes of the muscle forces during the eight considered phases of the walking cycle are given in Table 2 as well.

The various stress components and the Von Mises stresses in the various materials were calculated, as well as first-order approximations of the strain rates. The latter was done by subtracting the strains from two consecutive load cases and dividing the result by the elapsed time between these phases (assuming one step to last 1.1 s). Because the load cases are static and no accelerations are taken into account, these strain rates are only first-order approximations, but they do give some indication where large changes in stresses may be expected.

To determine the influence of the muscle forces on the stress distributions in the pelvic bone, two additional cases were analyzed. Firstly, all muscle forces were omitted, leaving the hip-joint force as the only external load. The hip-joint force being the largest of all forces acting on the pelvic bone, this analysis should give insight in how this force is transferred through the pelvic bone and it will disclose whether including muscle forces is necessary at all when analyzing implants. Secondly, the assumed body weight was increased from 650 N to 800 N, resulting in a higher hip-joint force, while the muscle forces were kept at their original level.

For the analyses, the MARC/MENTAT FEM and pre- and postprocessing codes (MARC Analysis Corporation, Palo Alto, CA, USA) running on the EX-60 main-frame computer (Hitachi Data Systems, Bells Hill, Bucks., U.K.) of the University of Nijmegen were used.

Results

As a sandwich construction, the cortical shell takes the bulk of the load. In Figure 3, the distributions of the Von Mises stress intensities in the cortical shell are shown for the eight phases of the walking cycle considered. Figure 4 shows the same for the stresses in the underlying trabecular bone. Here, the stresses are about 50 times smaller than in the cortical shell. The locations of the highest stresses in the cortical shell and the underlying trabecular bone do not coincide. In the cortical shell, the highest stresses are found in the attachment area of the gluteus major muscle and the incisura ischiadaca major region, while in the trabecular bone, the highest stresses occur in the thin central area of the iliac wing and in the acetabulum. The accompanying strain rates were found to be between the orders of 0.001 to 0.1 s^{-1} . The highest strain rate (based on the Von Mises strain, defined as the square root of two-

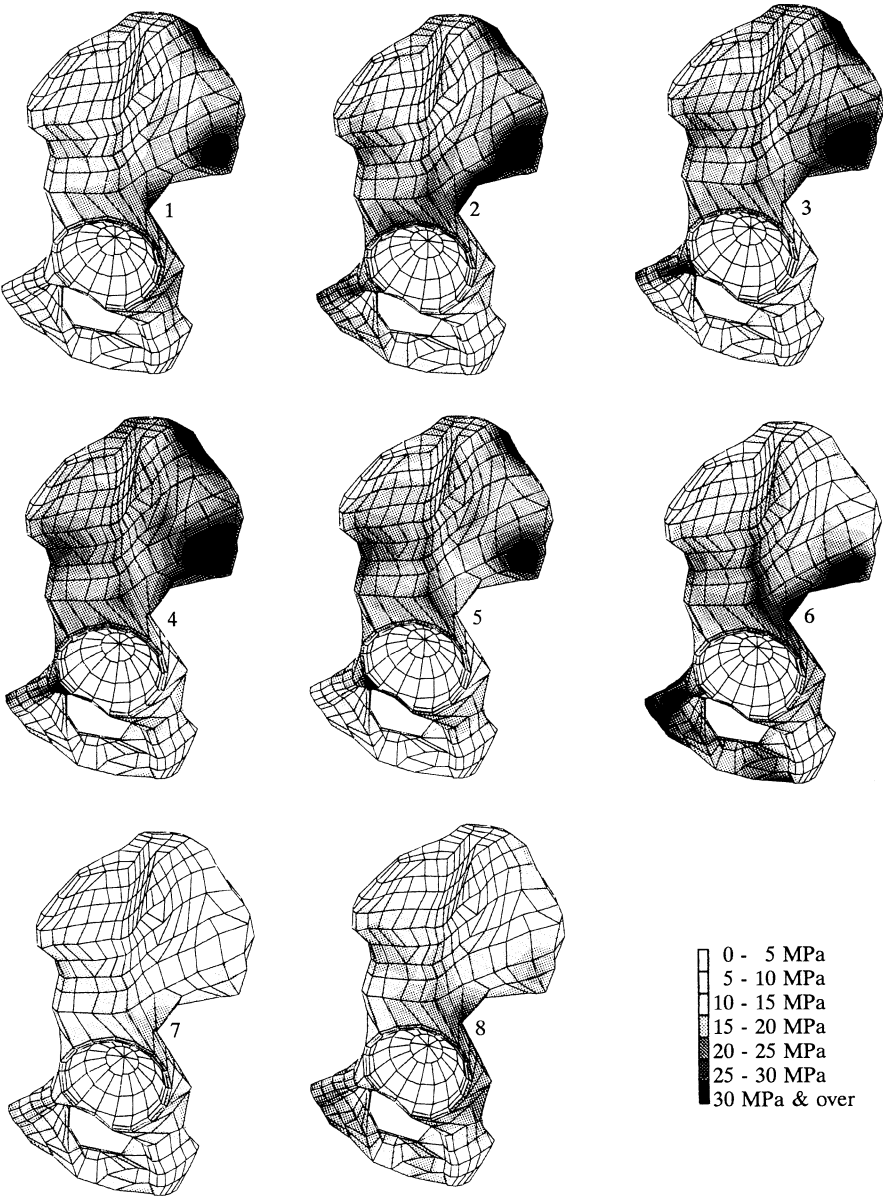


Fig. 3: Lateral views of the Von Mises stress distribution in the cortical shell for the eight load cases.

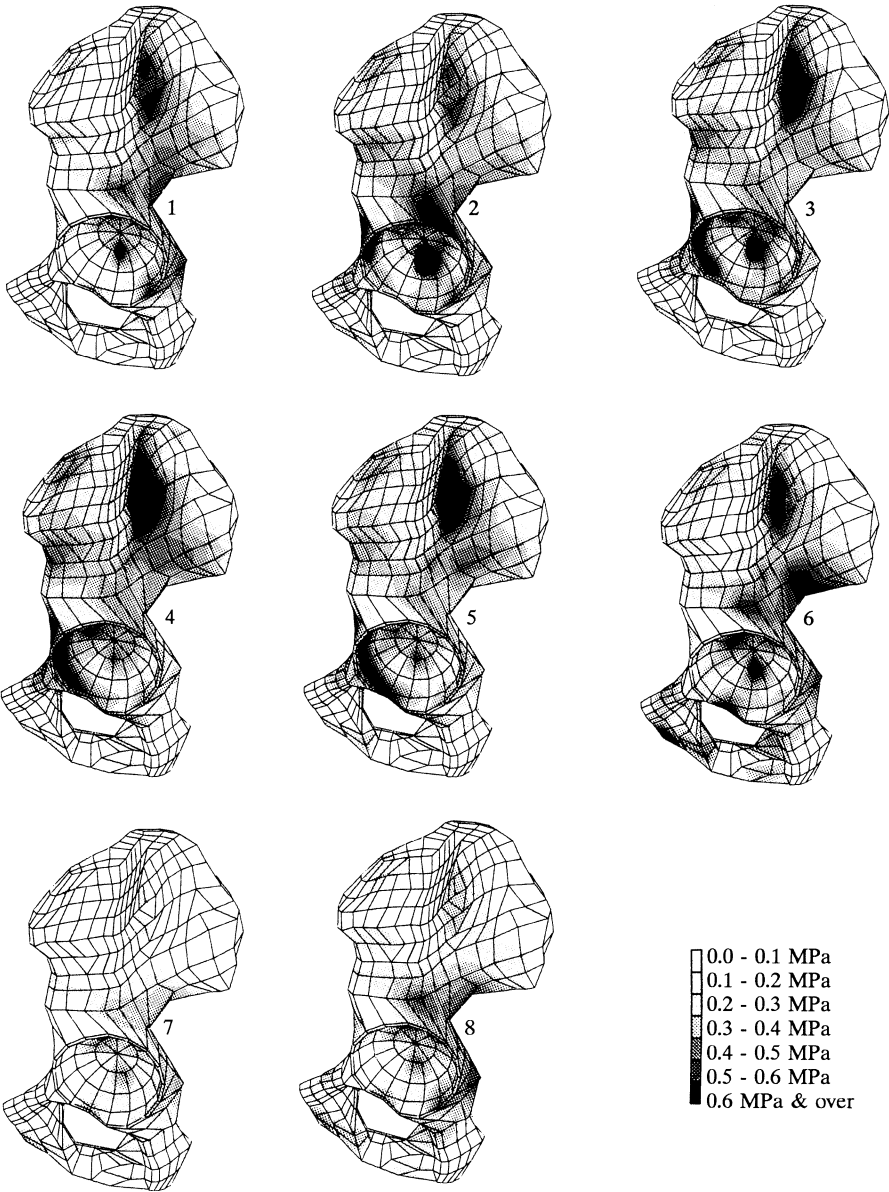


Fig. 4: Lateral views of the Von Mises stress distribution in the underlying trabecular bone for the eight load cases.

thirds of the sum of the squared principal strains) occurred in the trabecular bone between the phases 8 and 1, and had a value of 0.4 s^{-1} . In Figure 5, the distribution of the strain rates throughout the trabecular bone are displayed for this particular moment. At the end of the single leg stance (between phases 5 and 6) high strain rates occurred also at the anterior acetabular rim in the subchondral bone (0.35 s^{-1}). In general, strain rates in the cortical shell were found to be lower than in the subchondral and trabecular bone.

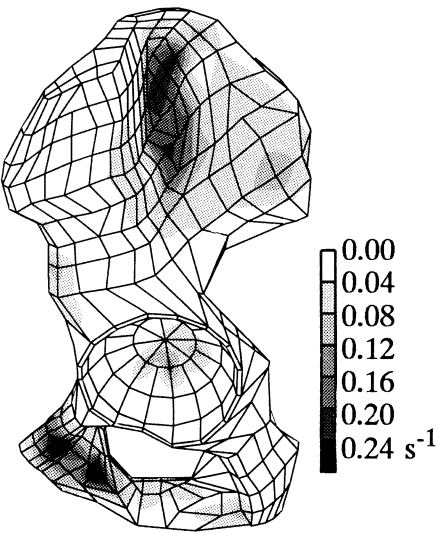


Fig. 5: Distribution of the momentary strain rates in the trabecular bone between cases 8 and 1.

the acetabulum in all eight loading cases considered, while the main area of support (the sacro-iliac joint) is located more posteriorly. Due to this, the cortical bone at the anterosuperior wall is still considerably stressed, while in the underlying trabecular bone the areas of high stresses have shifted more to posterior and anterior.

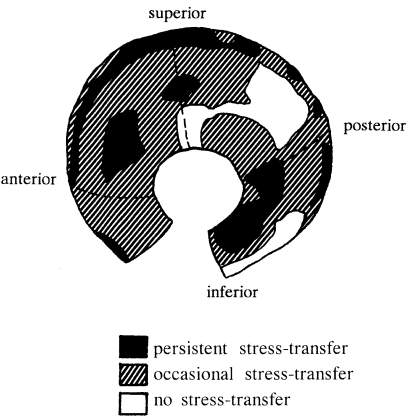


Fig. 6: The nature of stress transfer between the femoral head and the pelvic bone during a complete walking cycle.

In and closely around the acetabulum, the highest stresses occur in the superior acetabular wall and from there they are transferred to either the sacro-iliac joint or the pubic symphysis. As can be seen in Figures 3 and 4, the pubic bone is loaded most heavily at the beginning of the swing phase of the leg (phase 6). At this particular moment, the reaction force at the pubic symphysis reaches its maximal value of 750 N (115% body weight). The reaction force at the sacro-iliac joint, however, is still more than four times as high. The hip-joint force is pointing into the anterosuperior quadrant of the acetabulum in all eight loading cases considered, while the main area of support (the sacro-iliac joint) is located more posteriorly. Due to this, the cortical bone at the anterosuperior wall is still considerably stressed, while in the underlying trabecular bone the areas of high stresses have shifted more to posterior and anterior.

The hip-joint force itself is not being distributed evenly over the acetabulum. In Figure 6 those areas are identified, where during the eight phases considered compressive normal stresses in the subchondral bone occurred persistently (load-transferring contact) and where normal stresses were persistently zero (no load-transferring contact). From this it can be concluded that the load transfer between femoral head and acetabulum takes place predominantly along the antero-superior edge of the acetabulum. The highest (compressive) normal stress

occurs during one-legged stance (phase 3) and has a magnitude of 8.7 MPa. In Figure 7, the peak values of this stress component are plotted against the respective values of the hip-joint force, and this shows that even for relatively low values of the hip-joint force high compressive normal stresses in the subchondral bone may occur.

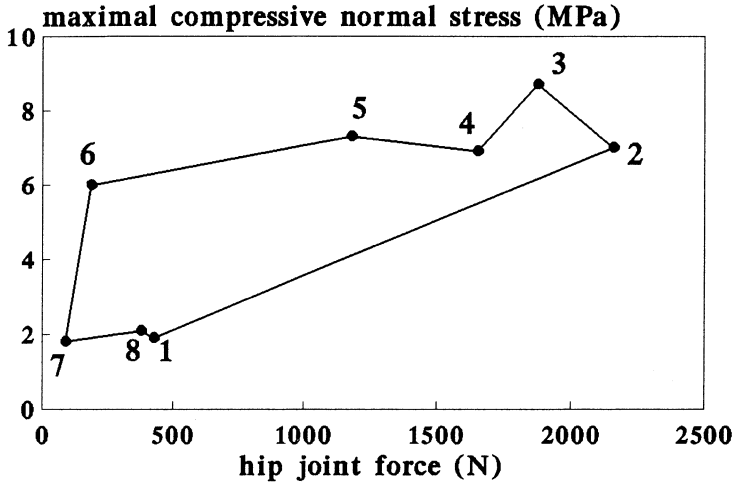


Fig. 7: Peak values of the compressive normal stresses in the subchondral bone layer versus the respective magnitude of the hip joint force.

The muscle forces have a considerable influence on the stress patterns in the pelvic bone. Figure 8 shows the Von Mises stresses during one-legged stance in the cortical shell when only the hip-joint force is taken into account. Comparing this to the corresponding stress distribution in Figure 3 (phase 2), the load transfer is entirely directed along the axis from the sacro-iliac joint to the pubic symphysis. The ischial bone and the superior part of the iliac bone remain virtually unloaded, while the pubic bone is much higher stressed than in the case that muscle forces are included.

The increase in the hip-joint force (by increasing the bodyweight from 650 to 800 N) affected only the stresses in the direct vicinity of the acetabulum. The stresses in the subchondral bone responded almost linearly to the change. Figure 9 shows the compressive

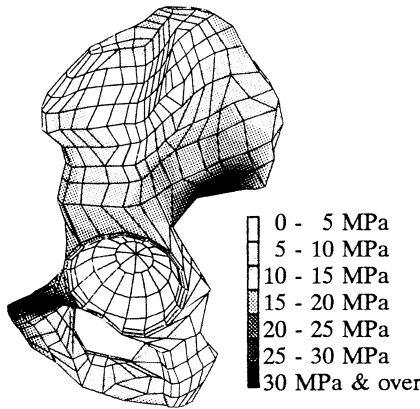


Fig. 8: Lateral view of the Von Mises stress distribution in the cortical shell during one-legged stance if only the hip joint force is applied.

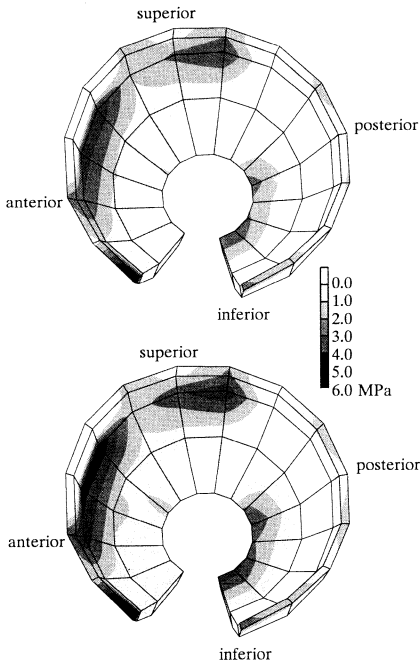


Fig. 9: Compressive normal stress at the articular surface of the subchondral bone during one-legged stance for the basic model (top) and the model with the increased hip-joint force (bottom); in the white areas, normal stresses are tensile.

normal stresses at the articular surface of the subchondral bone for both the initial value and the increased value of the hip-joint force. Qualitatively, both patterns are similar. The peak value for the latter, however, has increased from 7.0 to 9.3 MPa, which is more than the 23 percent rise in the hip-joint force.

Discussion

Finite element stress analyses of the normal pelvic bone have been described in only a few cases. Vasu *et al.* (1982) and Rapperport *et al.* (1985) based their respective models on two-dimensional sections through the pelvic bone. These kind of models, however, lack the ability to describe the three-dimensional aspects of pelvic mechanics adequately. Obviously, two-dimensional models are restricted to the plane of modeling, which in case of the pelvic bone is usually a cross section through the pubic bone, the acetabulum and the sacro-iliac joint. Because of this, a two-dimensional model lacks the reinforcement of the out-of-plane part of the acetabular wall, thus making these models inherently too flexible. Loading is also

restricted to the plane of modeling, which is a serious shortcoming. Due to its circumferential geometry, an axisymmetric pelvic model has to be restricted to the immediate vicinity of the acetabulum. Furthermore, it assumes that the acetabular wall is present around the full 360 degrees, which is not the case in reality. Therefore, axisymmetric models are structurally too stiff. In comparative studies, two-dimensional and axisymmetric models may be able to indicate certain trends, but for more detailed evaluations, a three-dimensional model will be required. Goel *et al.* (1978) and Oonishi *et al.* (1983) did use three-dimensional models, but since then additional data concerning pelvic loading and material properties of bone have become available. We have aimed at making the present model as sophisticated as possible by using a three-dimensional mesh with material properties taken from quantitative computer tomography measurements, and applying realistic loads, which not only consisted of the hip-joint force, but also included twenty one muscle forces. With this model, the load transfer in the normal pelvic bone was evaluated and for this purpose, several phases in a walking cycle were considered as loading conditions.

The pelvic bone is usually characterized as a so-called sandwich construction, in

which the bulk of the load is carried by thin shells of a high-modulus material, while a low-weight core material acts as a spacer (Jacob *et al.*, 1976; Dalstra and Huiskes, 1990). In this study, this phenomenon has been confirmed; the stress levels in the cortical shell were found to be about 50 times higher than in the underlying trabecular bone. For the load cases in the first half of the walking cycle (the stance phase), the average Von Mises stress in the cortical shell lies between 15 and 20 MPa, while in the underlying trabecular bone, this value lies between 0.3 and 0.4 MPa. Distributions of the strain rates indicate that during walking the highest gradients of the stresses occur in the pubic bone, the subchondral bone in the acetabulum and in the posterior part of the iliac bone. In general, strain rates were lower in the cortical shell than in the underlying trabecular bone. The magnitudes of these strain rates were found in the range of 10^{-3} to 10^{-1} s^{-1} . According to Carter and Hayes (1977) no significant hydraulic effect of the marrow will be found for strain rates lower than 10 s^{-1} . Linde *et al.* (1991) measured the strength and stiffness of trabecular bone for a wide range of strain rates (10^{-4} to 10 s^{-1}). Based on their findings, in the present range of strain rates increases up to 40 percent for the strength and 20 percent for the stiffness of the bone may be expected due to visco-elastic effects.

The hip-joint force is the most important force for the load transfer across the pelvic bone. During normal walking, it remains directed towards a relatively small area in the anterosuperior quadrant of the acetabulum, according to the measurements of Bergmann *et al.* (1990). Its line of action does not intersect the line between the iliac and the pubic support areas and therefore, the hip-joint force tends to tilt the acetabulum upward. This is countered by the muscle forces acting on the iliac and the ischial bones and it is because of this muscle action that the pelvic bone is stress-relieved in the cases with full loading assumed compared to the cases with only the hip-joint force included (Figures 3 and 8). Due to the muscle forces, the stress distributions in the bone remain fairly constant during a walking cycle (Figures 3 and 4), even though the hip-joint force varies considerably (from almost 200 to 2,200 N). Only halfway through the swing phase the pelvic bone is clearly less stressed. So, apparently the muscle forces help to keep changes in the stress distribution to a minimum, which is supposedly favorable with regard to fatigue failure of the bone material.

The transfer of the hip-joint force takes place predominantly in a narrow strip along the anterosuperior edge of the acetabulum. Depending on its precise direction, deeper areas in the acetabulum also transfer a part of the hip-joint force. Because of this load transfer at the edge of the acetabulum, the lateral shell of the iliac cortex, just above the acetabulum and extending towards the incisura ischiadaca major region, is heavily stressed, which is qualitatively confirmed by results from strain-gage measurements by Finlay *et al.* (1986). The absolute values of the stresses which they reported were smaller, due to the lower value they assumed for the Young's modulus of cortical bone. Pauwels (1973) argued that for a normal configuration of the hip joint the stress distribution in the acetabulum is uniform. This, however, is based on the assumption that the acetabulum can transfer loads in all directions. Our

results indicate however that loads are mainly transferred from the acetabulum through the lateral cortical shell to the sacro-iliac joint and the pubic symphysis. The actual stress distribution in the acetabulum is affected by this load-transfer mechanism and the deeper parts of the acetabulum are stress-shielded. The high stresses at the superior acetabular wall demonstrate its importance in the natural load-transfer mechanism of the hip joint. In dysplastic acetabula, where this part of the wall is underdeveloped or even lacking, an alternative load-transfer mechanism with higher stresses to compensate for this will be the result, which is shown by Schüller *et al.* (1993) in case of reconstructed acetabula. Therefore, a dysplastic acetabulum can definitely be considered as a considerable risk factor for wear of the hip joint.

The stress component which actually transfers the hip-joint force onto the pelvic bone, is the normal or radially directed component of the contact stress between acetabulum and femoral head. Its highest value was found to have a magnitude of around 9 MPa and occurred during the one-legged stance phase. Even during the swing phase, the compressive normal stress still has a peak value of nearly 2 MPa (Figure 7). In the present model, no cartilage was taken into account and as a result, these stress values may be exaggerated. It is, therefore, interesting to compare these values to experimental results. Hodge and co-workers (1989) reported on pressures between prosthesis and acetabular cartilage in the acetabulum for walking, stair climbing and rising from a chair, which had been measured *in-vivo* by pressure transducers in the head of a telemetrically instrumented femoral prosthesis. During walking, they found peak values of 5.5 MPa shortly after the operation, but when gait had normalized after two or three years, these peaks reduced to 4 MPa. The superiorly directed stress peak during the stance phase of walking, found by Hodge and co-workers, corresponds well to our findings. Contact stresses within the acetabulum have also been measured by Brown and Shaw (1983) and they reported values of 8.8 MPa for local stress peaks in the region of the acetabular dome. This indicates that the magnitude of the contact stresses predicted by the present finite element model are indeed somewhat high, but still lie within a realistic range.

As mentioned in the introduction, most pelvic or acetabular finite element studies deal with acetabular implants rather than with mechanics of the pelvic bone itself. The 3-D models of Goel *et al.* (1978) and Oonishi *et al.* (1983), however, do represent natural pelvic bones. Goel and co-workers (1978) found values up to 40 MPa for the principal stresses (both tensile and compressive) in the acetabular region. These values are probably too high, because with the strength of cortical bone around 120 MPa (Carter *et al.*, 1981), this would make the pelvic bone very vulnerable to fatigue failure. Stresses within the acetabulum, found by Oonishi and co-workers (1983) with their pelvic FE model, had a magnitude of around 0.01 MPa. Compared to the present results, this is improbably low, and therefore we fear an error has been made in their calculations or conversions. In their model, the highest stresses in the subchondral bone are found near the bottom of the acetabulum, while in our case the stress peaks occur near the edge of the acetabulum. When comparing the stresses calculated in the rest of the pelvic bone, Oonishi and co-workers also report high stresses in the ilium, above the superior edge of the acetabulum, extending to the

incisura ischiadaca major region. The area of high stresses at the posterior part of the ilium due to the gluteus major muscle did not occur in their model.

We may conclude that the pelvic bone behaves like a sandwich construction. The most important force for the pelvic bone, the hip-joint force, is predominantly transferred along the superior edge of the acetabulum onto the rest of the pelvic bone towards the sacroiliac joint and the pubic symphysis. Transformation of the data by Bergmann and co-workers (1990) into an acetabular orientation, showed that the hip-joint force remains pointed into the anterosuperior quadrant of the acetabulum during walking. When external loading only includes the hip-joint force, very high stresses are found in the pubic bone. The muscle forces have a stabilizing effect on the pelvic load transfer and largely compensate for changes in the magnitude of the hip-joint force. Because of this the stress distributions in the pelvic bone are not subject to large variations during a walking cycle. Within the acetabulum itself, changes are more substantial, as here the stress distributions are more directly dependent on the magnitude of the hip-joint force.

References

- Bergmann, G., Graichen, F., Rohlmann, A. (1990) Instrumentation of a hip joint prosthesis. In: *Implantable telemetry in orthopaedics*, eds. G. Bergmann, F. Graichen, A. Rohlmann, Freie Universität Berlin, pp. 35-63.
- Brown, Th.D., Shaw, D.T. (1983) In vitro contact stress distributions in the natural human hip. *J. Biomech.*, **16**, 373-384.
- Carter, D.R., Hayes, W.C. (1977) The compressive behaviour of bone as a two-phase porous structure. *J. Bone Joint Surg.*, **59-A**, 954-962.
- Carter, D.R., Caler, W.E., Sprengler, D.M., Frankel, V.H. (1981) Fatigue behavior of adult cortical bone: the influence of mean strain and strain range. *Acta Orthop. Scand.*, **52**, 481-490.
- Carter, D.R., Vasu, R., Harris, W.H. (1982) Stress distributions in the acetabular region - II. Effects of cement thickness and metal backing of the total hip acetabular component. *J. Biomech.*, **15**, 165-170.
- Crowninshield, R.D., Brand, R.A. (1981) A physiologically based criterion of muscle force prediction in locomotion. *J. Biomech.*, **14**, 793-801.
- Dalstra, M. and Huiskes, R. (1990) The pelvic bone as a sandwich construction; a three dimensional finite element study. *Proc. Europ. Soc. Biomech.*, **7**, B32.
- Dalstra, M., Huiskes, R. (1992) Development of a pelvic finite element model. *Trans. Europ. Orthop. Res. Soc.*, **2**, 23.
- Dalstra, M., Huiskes, R., Odgaard, A., van Erning, L. (1993) Mechanical and textural properties of pelvic trabecular bone. *J. Biomech.*, **26**, 523-535.
- Dostal, W.F., Andrews, J.G. (1981) A three-dimensional biomechanical model of hip musculature. *J. Biomech.*, **14**, 802-812.
- Finlay, J.B., Bourne, R.B., Landsberg, P.D., Andreae, P. (1986) Pelvic stresses in vitro - I. malsizing of endoprostheses. *J. Biomech.*, **19**, 703-714.
- Goel, V.K., Valliappan, S., Svensson, N.L. (1978) Stresses in the normal pelvis. *Comput. Biol. Med.*, **8**, 91-104.
- Hodge, W.A., Carlson, K.L., Fijan, R.S., Burgess, R.G., Riley, P.O., Harris, W.H., Mann, R.W. (1989) Contact pressures from an instrumented hip endoprosthesis. *J. Bone Joint Surg.*, **71-A**, 1378-1386.
- Huiskes, R. (1987) Finite element analysis of acetabular reconstruction. *Acta Orthop. Scand.*, **58**, 620-625.
- Jacob, H.A.C., Huggler, A.H., Dietschi, C., Schreiber, A. (1976) Mechanical function of subchondral bone as experimentally determined on the acetabulum of the human pelvis. *J. Biomech.*, **9**, 625-627.

- Koeneman, J.B., Hansen, T.M., Beres, K. (1989) Three dimensional finite element analysis of the hip joint. *Trans. Orthop. Res. Soc.*, **14**, 223.
- Landjerit, B., Jacqard-Simon, N., Thourot, M., Massin, P.H. (1992) Physiological loadings on human pelvis: a comparison between numerical and experimental simulations. *Proc. Europ. Soc. Biomech.*, **8**, 195.
- Linde, F., Nørgaard, P., Hvid, I., Odgaard, A., Soballe, K. (1991) Mechanical properties of trabecular bone. Dependency on strain rate. *J. Biomech.*, **24**, 803-809.
- Lionberger, D., Walker, P.S., Granholm, J. (1985) Effects of prosthetic acetabular replacement on strains in the pelvis. *J. Orthop. Res.*, **3**, 372-379.
- Oonishi, H., Isha, H., Hasegawa, T. (1983) Mechanical analysis of the human pelvis and its application to the articular hip joint - by means of the three dimensional finite element method. *J. Biomech.*, **16**, 427-444.
- Oonishi, H., Tatsumi, M., Kawaguchi (1986) Biomechanical studies on fixations of an artificial hip joint acetabular socket by means of 2D-FEM. In: *Biological and biomechanical performance of biomaterials.*, eds. P. Christel, A. Meunier and A.J.C. Lee, Amsterdam, Elsevier Science Publishers B.V., pp. 513-518.
- Pauwels, F. (1973) *Atlas zur Biomechanik der gesunden and kranken Hüfte.*, Berlin, Springer Verlag.
- Pedersen, D.R., Crowninshield, R.D., Brand, R.A., Johnston, R.C. (1982) An axisymmetric model of acetabular components in total hip arthroplasty. *J. Biomech.*, **15**, 305-315.
- Petty, W., Miller, G.J., Piotrowski, G. (1980) In vitro evaluation of the effect of acetabular prosthesis implantation on human cadaver pelvis. *Bull. Pros. Res.*, **17**, 80-89.
- Rapperport, D.J., Carter, D.R., Schurman, D.J. (1985) Contact finite element stress analysis of the hip joint. *J. Orthop. Res.*, **3**, 435-446.
- Renaudin, F., Lavaste, F., Skalli, W., Pecheux, C., Scmitt, V. (1992) A 3D finite element model of pelvis in side impact. *Proc. Europ. Soc. Biomech.*, **8**, 194.
- Ries, M., Pugh, J., Au, J.C., Gurtowski, J., Dee, R. (1989) Cortical pelvic strains with varying size hemiarthroplasty in vitro. *J. Biomech.*, **22**, 775-780.
- Rohlmann, A., Bergmann, G., Graichen, F. (1990) Hip joint forces measured in a patient with two instrumented joint prostheses. *Proc. First World Congress of Biomechanics*, **II**, 220.
- Schüller, H.M., Dalstra, M., Huiskes, R., Marti, R.K. (1993) Total hip reconstruction in acetabular dysplasia; a finite element study. *J. Bone Joint Surg.* **75-B**, 468-478.
- Vasu, R., Carter, D.R., Harris, W.H. (1982) Stress distributions in the acetabular region - I. before and after total joint replacement. *J. Biomech.*, **15**, 155-164.

Chapter IV

The effects of total hip replacement on pelvic load transfer

M. Dalstra, R. Huiskes

Biomechanics Section, Institute of Orthopaedics, University of Nijmegen

Submitted to the Journal of Orthopaedic Research

Abstract: *Compared to the femoral side, only little is known about the effects of a total hip arthroplasty on acetabular mechanics. The changes in load transfer in the femur after placement affect the performance of the implant and may ultimately decide whether the implant fails or not. For the acetabular component, however, such insights are still practically non-existent, even though the acetabular component is gradually being recognized as the restrictive factor for the life-span of a total hip arthroplasty in the long run. To develop a better understanding of the etiology of the failure mechanisms for acetabular prostheses, it is therefore important to know how the natural mechanical situation in the pelvic bone is altered after placement of an acetabular prosthesis.*

The present study investigates the changes in pelvic load transfer after a hip joint has been reconstructed with a total hip arthroplasty. For this purpose, comparisons were made between three-dimensional finite element analyses simulating a normal pelvic bone and a pelvic bone with an acetabular reconstruction. Changes in the stress patterns due to the reconstruction were only found to occur in the direct vicinity of the acetabulum. The deeper part of the subchondral layer becomes sub-normally loaded (stress-shielded). The extent of stress shielding depends on the flexibility of the implant. Stresses increase at the superior edge of the subchondral bone. Stresses in the trabecular bone in the superior acetabular wall are also higher than for normal load transfer. The stress patterns in the cortical shell of the pelvic bone are only marginally affected by an acetabular reconstruction.

Comparison of the results of this study with findings from two-dimensional and axisymmetric finite element models performed earlier shows that the latter types of models are not very suitable to describe pelvic mechanics realistically. Especially the alleged mechanical advantage of a stiff backing to reduce stress peaks in the cement mantle and the subchondral bone, which was based on findings from these kind of models, could not be confirmed. In fact, the opposite was found, implying an increased risk of cement failure and interface loosening for cemented metal-backed cups relative to cemented full-polyethylene cups.

Introduction

For acetabular prostheses, aseptic loosening is the most frequent type of failure (Charnley, 1979; Stauffer, 1982; Sutherland *et al.*, 1982). However, no relation between unnatural pelvic load transfer and implant failure has been established so far. Yet, it is the acetabular component which becomes the restrictive factor in the life-span of a total hip arthroplasty in the long run. Long-term follow-up shows that, initially, acetabular components are less susceptible to aseptic loosening, but after eight to ten years post-operatively, the survival rate of acetabular cups suddenly shows a sharp decrease, whereas survival curves for femoral stems decrease more gradually (Stauffer, 1982; Sutherland *et al.*, 1982; García-Cimbrelo and Munuera, 1992; Malchau *et al.*, 1993). This characteristic difference in survival rates between femoral and acetabular components has led some authors to suggest that the actual mechanisms governing femoral and acetabular aseptic loosening are different. In a retrieval study Schmalzried *et al.* (1992) observed a characteristic progress in loosening of acetabular cups: a front of bone resorption and membrane formation always occurs first near the rim of the cement mantle and gradually extend towards the dome of the acetabulum. Histologic analysis revealed that this process is fueled by small polyethylene particles, while they could not find any evidence in support of mechanical failure of the fixation. Therefore, they proposed that, unlike aseptic loosening of femoral stems, which is initiated by mechanical factors, the primary causes for aseptic loosening of acetabular cups are biological. In their immunohistochemical studies, Andrew *et al.* (1992), however, found that membranes from around loosened femoral and acetabular implants are identical in their cellular composition, and they therefore reject the hypothesis that femoral and acetabular loosening are subject to different mechanisms.

The actual changes in load transfer across the pelvic bone due to an acetabular prosthesis are not fully understood yet. Compared to a stem inserted in the femur, the mechanical effects of an acetabular cup may be restricted to a much smaller area and also the difference in the flexibility of the implant and the bone, which actually causes femoral stress shielding, may be less prominent for an acetabular cup. This does not necessarily imply, however, that the performance of acetabular implants is less dependent on mechanics.

There have been a few finite element (FE) and strain-gage studies in which direct comparisons were made between stress distributions in normal and reconstructed pelvic bones. Vasu *et al.* (1982) studied the stress distributions in the acetabular region before and after total joint replacement, using a two-dimensional FE model. They found an increase in the stresses in the cancellous bone immediately superior to the cup and in the medial cortical shell. Furthermore, they found that the cup tended to grip the head of the femoral component as it was pressed between the medial and lateral walls of the ilium. Oonishi *et al.* (1983) examined the effect of a ceramic acetabular socket and used a three-dimensional FE model. In comparison to a normal pelvic bone, they found no substantial changes in the stress distributions on the outer surface of the bone. Near the implant, the amount of bone deformation had decreased

relative to the normal situation, while the stresses had increased. Finlay *et al.* (1986) used strain gages to study the efficacy of metal-backed cups. They found that the stresses in the cortical shell due to a non-backed or a metal-backed cup did not change substantially relative to the normal situation, provided that the relatively stiff subchondral bone layer was not removed. Because of the nature of strain-gage techniques, however, they were not able to study changes in load transfer in the acetabulum itself. Using two-dimensional contact finite element analyses, Rappoport *et al.* (1987) could shed more light on this issue. They found significantly different stress distributions in the subchondral bone when an uncemented porous ingrowth cup was implanted than in the natural hip. Especially an increase was seen in the compressive stresses. These stresses were predicted to decrease in due time, due to both ingrowth of the implant or fibrous tissue formation between implant and bone. Finally, Huiskes (1987) found in his axisymmetric finite element study on non-cemented threaded cups, that relative to a normal pelvic bone, the superior trabecular bone is stress-shielded, and more load is transferred through the lateral cortical shell in case of a reconstructed acetabulum.

Most FE studies on pelvic mechanics have been performed using two-dimensional and axisymmetric models. The efficacy of these models, however, may be questioned, because both approaches seriously limit a realistic description of the geometry and loading of the pelvic bone. Through the recent use of three-dimensional models, more insight was obtained in the load-transfer mechanism of a normal pelvic bone (Goel *et al.*, 1978; Koenenman *et al.*, 1989; Dalstra and Huiskes, 1990; Dalstra and Huiskes, 1992; Landjerit *et al.*, 1992; Renaudin *et al.*, 1992). The purpose of this study was to investigate the mechanical effects of the placement of an acetabular prosthesis using a realistic finite element model (Dalstra *et al.*, 1992), and see how the load transfer and stress distributions in the pelvic bone change once a cup is present. To examine whether the flexibility of the cup plays any role in this, both a relatively flexible and a relatively stiff cup were analyzed. The results are compared to those earlier, simplified FE models, for the purpose of assessing their validity.

Method

For this study, two FE models were used; a mesh of a normal pelvic bone and a mesh of a reconstructed pelvic bone. The reconstruction consisted of a cemented hemispherical cup. The subchondral bone layer was assumed to be left intact. The inner diameter of the cup was 28 mm, the outer diameter 48 mm and the cement mantle had a uniform thickness of 2 mm. Additionally, a TiAl6V4- (Young's modulus 110 GPa) and a CoCrMo-backed (Young's modulus 210 GPa) variant of this cup were included in the analyses. The model of the normal pelvic bone consisted of 1,361 elements and the reconstruction model of 1,506 elements. Figure 1 shows both models in a lateral view. Eight-node brick elements were used to represent trabecular bone, subchondral bone, the cement mantle and the prosthesis. The cortical shell was represented by 4-node membrane elements. For the model of the reconstructed bone,

interface conditions between both cement and cup, and bone and cement were assumed to be bonded, representing a stable postoperative situation. To ensure a realistic introduction of the hip-joint force into the acetabulum, parts of the femoral heads (the head of the femoral stem in case of the reconstructed bone) were represented as well (Huiskes, 1987). Gap elements were placed between this head and the acetabulum (or acetabular cup) in order to allow interaction only in case of compressive contact.

The Young's moduli of the elements representing trabecular bone and subchondral bone were based on the results of quantitative computer tomography measurements (Dalstra *et al.*, 1992). For the trabecular bone, the Young's moduli ranged from 1 MPa to 132 MPa; for the subchondral bone, the range was 186 MPa to 2,155 MPa. Examination of the material properties of pelvic trabecular bone has shown that it is not highly anisotropic (Dalstra *et al.*, 1993). Therefore, assuming isotropy for these elements seems justified. That same study showed that 0.2 is a reasonable approximation for the Poisson's ratio of pelvic trabecular bone. In the FE model, the thin cortical shell of the pelvic bones is represented by membrane elements. The thickness of these elements was based on computer tomography measurements as well (Dalstra *et al.*, 1992) and ranged from 0.7 to 3.2 mm with an average of about 1.5 mm. Young's moduli and Poisson's ratios for these elements were assumed to be 17 GPa and 0.3 respectively. Contact between femoral head and the acetabulum was modeled by 60 gap elements, ensuring that only compressive forces could be transmitted. This contact was assumed to be frictionless. The model was previously verified in simulations of strain-gage experiments and its results have shown good agreement with the experimental findings (Dalstra *et al.*, 1992).

Setting the kinematic boundary conditions for the FE models, the nodes situated in the sacro-iliac joint areas and the pubic support areas were kept fixed to simulate sacral and pubic support of the pelvic bones. The loading conditions for the models simulated the beginning of the one-legged stance phase in a walking cycle. At this particular phase, the most prominent of the external forces working on the pelvic bone, the hip-joint force, reaches its maximal value of around 3.5 times body weight (Bergmann *et al.*, 1990). In this case, a body weight of 650 N was assumed. Apart from the hip-joint force, fifteen muscle forces were included in the model. Table 1 gives an overview of these muscles and their magnitudes. Actually, more than fifteen muscles are attached to the pelvic bone, but EMG-data by Crowninshield and Brand (1981) shows that at this particular phase of the walking cycle only the muscles considered have a contribution. The directions of the muscle forces were determined by subtracting the coordinates of their distal and proximal insertions (Dostal and Andrews, 1981).

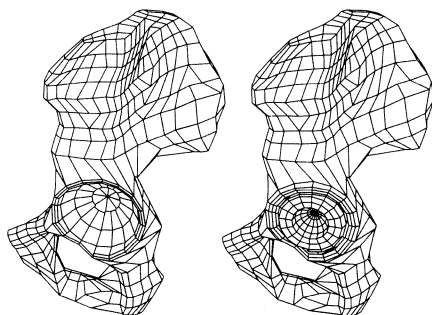


Fig. 1: Lateral views of the FE model of a normal (left) and a reconstructed pelvic bone (right).

Load	Magnitude (N)
hip-joint force	2158
m. gluteus maximus	930
m. gluteus medius	1053
m. gluteus minimus	140
m. tensor fasciae latae	132
m. sartorius	88
m. semimembranosus	368
m. semitendinosus	140
m. biceps femoris longus	202
m. adductor longus	88
m. adductor brevis	114
m. obturator internus	123
m. piriformis	175
m. quadratus femoris	96
m. superior gemellus	88
m. rectus femoris	123

Table 1: Magnitudes of the various external forces, accounted for in the model.

The individual stress components and the equivalent Von Mises stress in the various materials and at their interfaces were calculated. The FE analyses were performed using the MARC/MENTAT FEM and pre- and postprocessing codes (MARC Analysis Corporation, Palo Alto, CA, USA) running on the EX-60 mainframe computer (Hitachi Data Systems, Bells Hill, Bucks., U.K.) of the University of Nijmegen.

Results

During one-legged stance, the hip-joint force is the largest of the external forces working on the pelvic bone, and its influence on the stress distributions throughout the pelvic bone, and particularly in the acetabular region, is evident. Its introduction into the acetabulum takes place in the anterosuperior quadrant of the acetabulum and from there the main stress transfer takes place in the cortical shell, directed towards the sacro-iliac joint along the superior acetabular rim. A smaller portion is transferred to the pubic symphysis. After an acetabulum has been reconstructed, this overall load-

transfer mechanism hardly changes. Figure 2 shows the Von Mises stress distribution in both the cortical shell of a normal pelvic bone and a pelvic bone with a non-backed reconstruction. There are only marginal differences in both stress distributions, and these are restricted to the immediate vicinity of the acetabulum. In

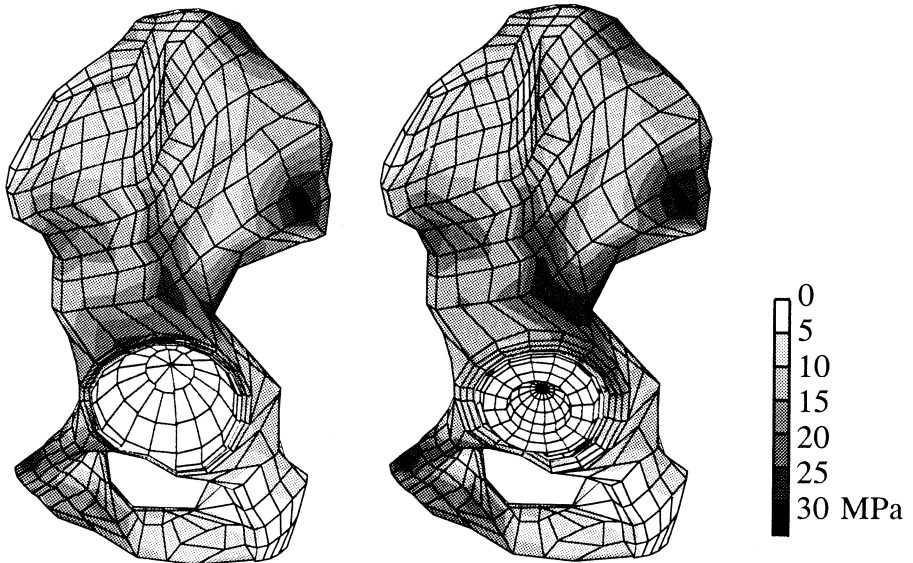


Fig. 2: Von Mises stresses in the cortical shell of a normal pelvic bone (left) and a pelvic bone with a cemented non-backed cup (right) during one-legged stance.

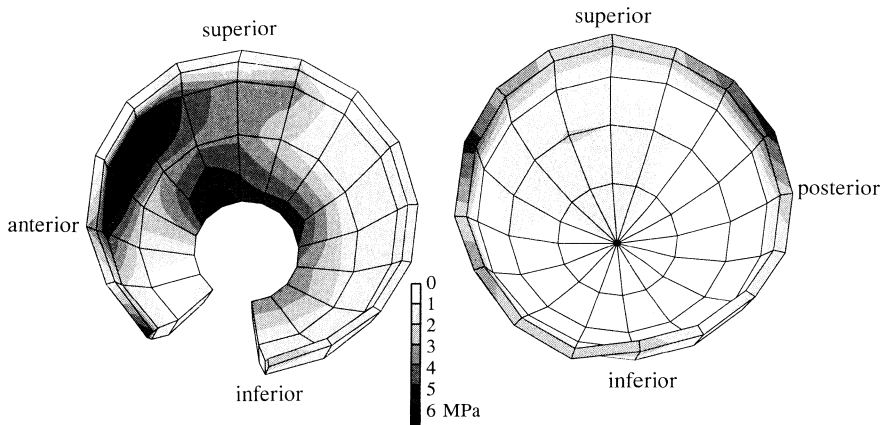


Fig. 3: Von Mises stresses in the subchondral bone layer of a normal bone (left) and a pelvic bone with a cemented non-backed cup (right).

the superior acetabular rim, the load transfer has shifted slightly to posterior after reconstruction. For the subchondral and the trabecular bone in the acetabular region,

the changes are more substantial. In the intact case, the highest stresses in the subchondral bone occur in the anterosuperior quadrant of the acetabulum. In the reconstructed case, stresses in the subchondral bone have not only reduced considerably, but also a shift has taken place from the dome area towards the edges (in particular the posterosuperior edge). This leaves the deeper areas in the acetabulum 'stress-shielded' (Figure 3). In the underlying trabecular bone, this situation is more or less reversed; as can be seen in Figure 4. The stresses in the trabecular bone in the superior wall are higher in the reconstructed case. At the lower anterior side of the ilium and the pubic bone, stresses decrease slightly after reconstruction.

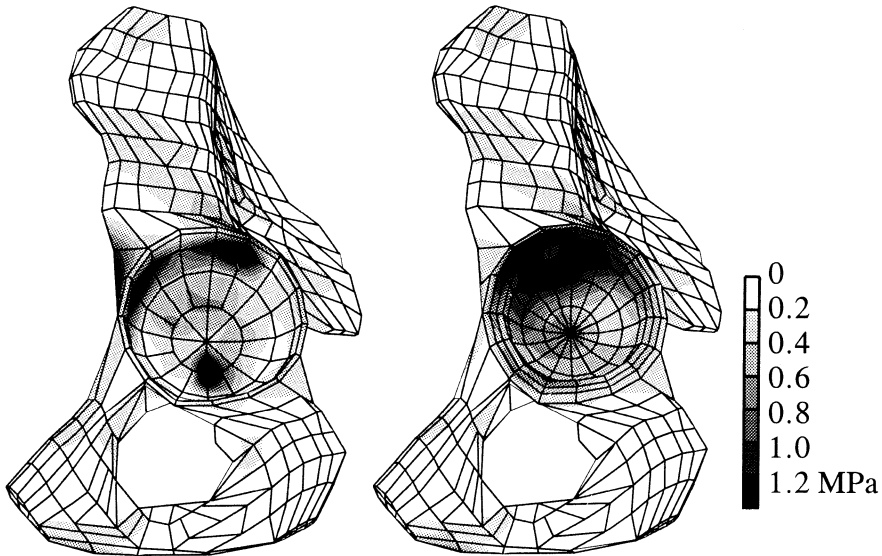


Fig. 4: Von Mises stresses in the trabecular bone of a normal bone (left) and a pelvic bone with a cemented non-backed cup (right).

Obviously, the presence of a metal backing makes the implant more rigid. As the backing restricts the deformations in the polyethylene, the stresses reduce. Figure 5 shows the compressive radial stresses in the polyethylene cup of both the non-backed and the titanium-backed case. Near the dome of the articulating surface of the cup, the stress distributions are almost identical, but near the anterosuperior edge, the stresses are higher for the non-backed cup. The highest values of this stress component are 6.4 MPa for the non-backed cup and 5.2 MPa for the titanium-backed cup. Furthermore, it can be seen that along its perimeter the metal-backed polyethylene insert has over 80 percent compressive contact with the backing (the cup is pressed into the backing), while the non-backed cup has barely 50 percent compressive contact with the cement mantle.

In contrast to previous FE studies (Carter *et al.* 1982; Pedersen *et al.*, 1982), we find that the stress peaks in the cement increase by the presence of a metal backing when compared to the non-backed case. The Von Mises stress distributions in the

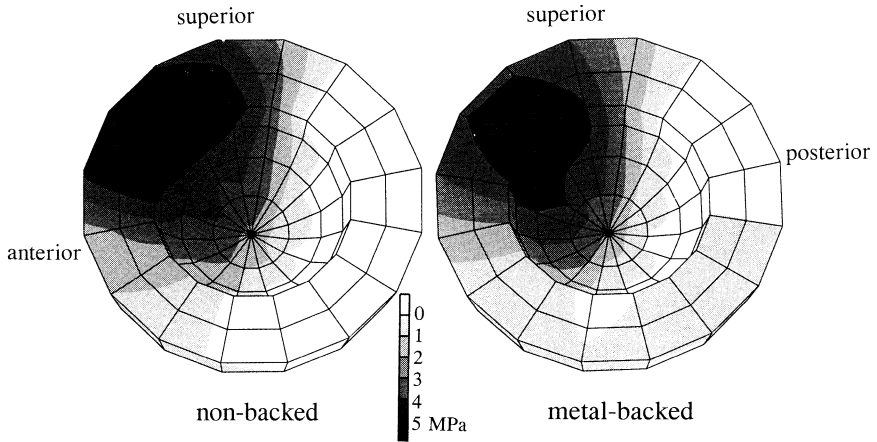


Fig. 5: Compressive radial stresses in the polyethylene cup for a non-backed (left) and a metal-backed implant (right). Note that the white areas denote tensile stresses.

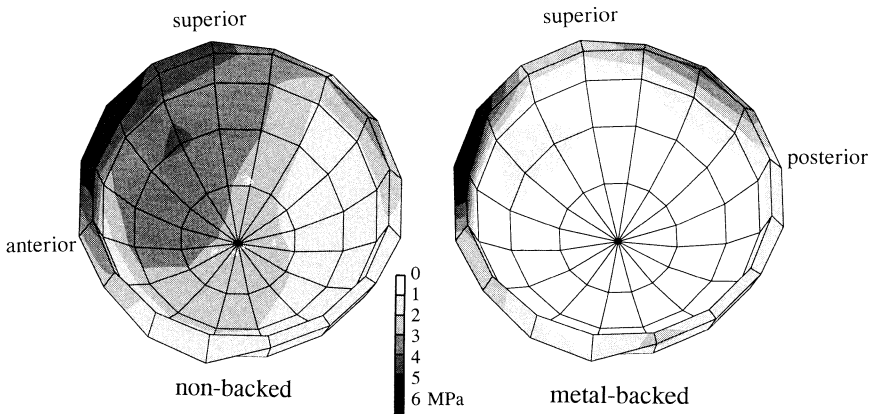


Fig. 6: Von Mises stresses in the cement mantle for a non-backed case (left) and a metal-backed case (right).

cement mantle (Figure 6) reveal that for a metal-backed cup, load transfer takes place predominantly in a small strip along the edge. Not only are the peak values 30 percent higher for the metal-backed cup (8.0 MPa vs. 6.1 MPa), higher stress gradients occur as well. Although for a non-backed cup stresses also increase towards the edge, they are more evenly distributed. This discrepancy with the results of the earlier FE studies led us to simulate the load transfer of these models by directing the hip-joint force more to posterior and also slightly more towards the dome of the cup, in accordance with the loads assumed in these earlier analyses. In this case, metal-backing indeed caused a reduction of the stresses. The stress peaks at the antero-superior edge, seen in Figure 6, have now disappeared. Because of the relatively low

stiffness of the acetabulum near its dome, the polyethylene in the non-backed case is allowed to bulge in the direction of the hip-joint force, resulting in the stress pattern for the cement mantle as seen in Figure 7.

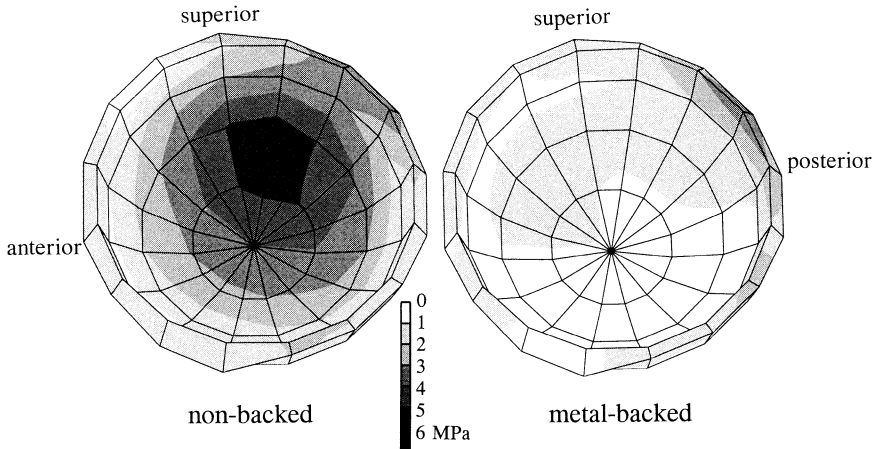


Fig. 7: Von Mises stresses in the cement mantle for a non-backed case (left) and a metal-backed case (right), while simulating 'two-dimensional' loading conditions.

Additionally, the cup and cement mantle are more or less pinched or squeezed, as compression in the posterosuperior direction results in a closing of the anterosuperior and posteroinferior edges of the acetabular wall. A stiff backing will obviously reduce this, and therefore results in lower stresses. The stress peaks are now 3.8 MPa vs. 5.4 MPa for the titanium-backed and non-backed respectively. For the more physiological loading, when the hip-joint force is directed anterosuperiorly, this pinching or squeezing mechanism plays a much lesser role; because of the geometry of the pelvic bone, the anteroinferior and the posterosuperior part of the acetabular wall are inhibited in moving towards one another, and consequently a stiff backing has no real use now.

For the performance of an implant, interface stresses are very important. Generally, three stress components can be identified at an interface between two materials; a direct stress, normal to the interface, and two perpendicular shear stress components in the plane of the interface. Due to the hemispherical shape of the interfaces in this particular case, these stress components are a radially directed normal stress, a circumferentially directed shear stress, tending to rotate the two interacting bodies relative to one another (torsional shear), and a longitudinally directed shear stress with the tendency to tilt the interacting bodies relative to one another (tilting shear). Of these stress components, the shear stresses and the tensile normal stress endanger the integrity of the interface in particular, because they tend to disrupt the connection between the surfaces. In Table 2, the peak values of these particular stress components, at both the cup/cement interface and the cement/bone interface, are given for a non-backed cup, a titanium-backed cup and a CoCrMo-alloy-backed cup. There is not much difference between the latter two. It can be seen that for the metal-backed cups

the shear stresses are higher at both interfaces. At the cup/cement interface, these stresses are even more than three times higher. In all cases, the torsional component of the shear stress is about twice as high as the tilting component.

	non-backed	Ti-backed	CoCrMo-backed
tensile normal stress (cup/cement)	0.51	1.01	1.13
torsional shear stress (cup/cement)	0.93	3.64	3.62
tilting shear stress (cup/cement)	0.57	1.72	1.81
tensile normal stress (cement/bone)	3.17	2.74	2.85
torsional shear stress (cement/bone)	2.79	3.66	3.65
tilting shear stress (cement/bone)	0.98	1.37	1.41

Table 2: Peak values (in MPa) of the 'disruptive' interface stress components.

Figure 8 shows how the shear stresses at the cement/bone interface are distributed. In this case the vector sums of the torsional and tilting shear stresses are shown. For both the non-backed cup and the metal-backed cups the patterns are very similar; shear stress 'hot-spots' appear at the anterosuperior, the posterosuperior and the inferior edges. This suggests that, should loosening occur, the process will start at the edge rather than near the dome of the cup. Tensile normal stresses at the cup/cement interface are also higher for metal-backed cups, while for a non-backed cup this stress component is higher at the cement/bone interface.

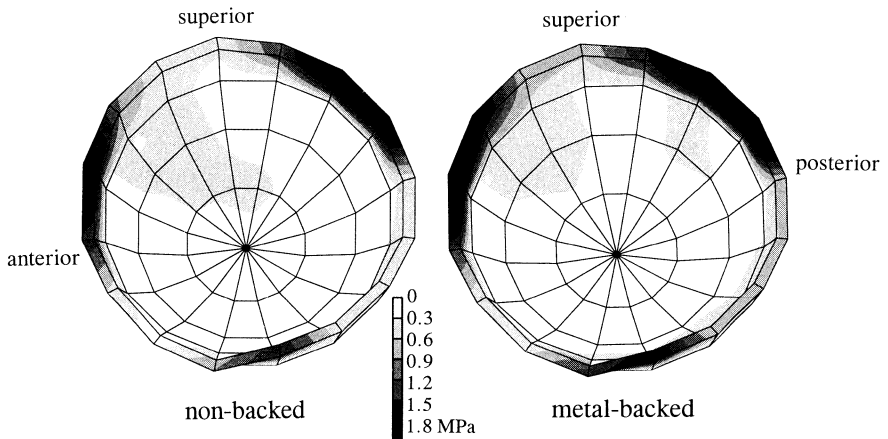


Fig. 8: Shear stress patterns at the cement/bone interface for a non-backed (left) and a metal-backed cup (right).

Discussion

Reconstructing an acetabulum with an acetabular cup introduces a mechanically 'unnatural' situation for the remaining part of the pelvic bone. Compared to the femoral side, the changes in load transfer may be restricted to a smaller area, but can not be overlooked. In this study, we compared load transfer in a normal pelvic bone to that in a bone with an acetabular reconstruction. Due to the presence of the prosthesis, the stresses in the remaining part of the subchondral bone layer were found to decrease, while in the underlying trabecular bone stress concentrations occur in the superior acetabular wall. This decrease of the subchondral stresses corresponds with the findings of Rappaport *et al.* (1987). They also reported a stress concentration near the edge of the bone/implant interface and identified this as a possible initiator for mechanical loosening. The present study shows that this stress concentration is found along the superior edge in particular. In connection with this, it is interesting that the characteristic development of a fibrous membrane, reported by Schmalzried *et al.* (1992) as the cause for aseptic loosening of cemented cups, also starts at the intraarticular margin and from there progresses towards the dome of the cup. Hence, the onset of this biological mechanism might have been caused by mechanical failure, creating a route for wear debris to enter the interface. The sub-normal loading of the deeper subchondral bone, which may be considered as a form of stress shielding, is a matter of concern as well, especially for stiffer cups. It may lead to local bone resorption and in this light it is worth mentioning the process of focal osteolysis behind the cup, which has been reported lately in combination with metal-backed implants (Santavirta *et al.*, 1990; Pierson and Harris, 1993).

Because of its 'sandwich' behavior, the main load transfer across the pelvic bone takes place in the cortical shell (Jacob *et al.*, 1976; Dalstra and Huiskes, 1990). Stress distributions in this cortical shell, however, are hardly affected by the placement of an acetabular cup. This is in accordance with the findings of Finlay and co-workers (1986). In their strain-gage experiments they did not find substantial differences in the stresses in the cortical shell of normal pelvic bones and bones with cups implanted; even metal backing had no effect. The stresses in a reconstructed bone in our study, however, do show a slight decrease at the superior acetabular rim and shift towards the posterior edge. At the medial cortex stresses reduce slightly as well. This can be explained by the placement of an acetabular cup, which increases the amount of material within the acetabulum. Therefore, the transfer of the antero-superiorly directed hip-joint force towards the posterosuperiorly directed support of the sacroiliac joint already takes place within cup and cement, instead of in the subchondral layer and the lower ilium, as in the normal case.

The increase in stresses in the cancellous bone near the dome of the cup and in the medial cortex found by Vasu *et al.* (1982) in their two-dimensional model, can not be confirmed by our results. This must be attributed to the differences in external loading between the two types of models. In their model, Vasu and co-workers only considered a hip-joint force directed almost towards the dome of the cup. They found an acetabular deformation mode by which the femoral head is pressed between the

medial and lateral wall of the ilium. In our case, the hip-joint force is not pointing so deep into the acetabulum and, more importantly, it is not directly pointed towards the support areas of the pelvic bone. Thus, squeezing of the femoral head between both sides of the acetabular wall does not occur. Instead, the hip-joint force rather tends to tilt the whole acetabulum towards anterosuperior, rotating it around an axis going through the sacro-iliac joint and the pubic symphysis. Muscles attached to the pelvic bone, especially the powerful gluteus muscles, prevent this, and the hip-joint force is transferred through the superior acetabular wall towards the support areas of the pelvic bone. Obviously, this can not be described in a two-dimensional model, which puts the efficacy of these models to question. Oonishi *et al.* (1983) studied stress distributions in a normal bone and one with a ceramic acetabular implant. Like the present results, their analysis showed almost no changes in the cortical stresses of the normal and the reconstructed bone. Because they assumed that the implant would replace all of the subchondral bone, their finding of increased trabecular stresses can not be related to the present results.

Although initially designed for easy replacement of the polyethylene insert by Harris (1971), use of metal-backed cups was encouraged, as these were considered to be mechanically superior to non-backed cups. The idea was that a stiff backing would not only reduce stress levels in the polyethylene insert, but also in the cement mantle and the underlying bone. This assumption was mainly based on finite element studies by Carter *et al.* (1982) and Pedersen *et al.* (1982), who demonstrated large stress reductions, especially near the dome of the cup. However in these geometrically simplified models the stress distributions are governed by different deformation modes than in the three-dimensional situation. When we mimicked the external loads of these two-dimensional and axisymmetric models studied earlier in our three-dimensional model, metal backing was indeed seen to perform better than a polyethylene cup. When using a more realistic loading, however, the alleged advantages of metal backing diminished. Only the stresses in the polyethylene liner were less for a metal-backed cup than for a full-polyethylene one, and this may be associated with a reduction of polyethylene wear (although no direct relationship between the stresses in the polyethylene and polyethylene wear has been reported). Maximal stresses in the cement mantle and its interfaces increased by about 30 percent relative to the non-backed case. At the interface between cup and cement, stress peaks were even more than three times higher for a metal-backed cup. The question may be raised whether this is important, because the stresses occur at different kind of contacts: metal /cement versus polyethylene/cement. It depends on the strength of these interfaces if and when loosening will occur, and the former may be stronger than the latter. There is clinical evidence, however, that metal-backed cups are more susceptible to loosening-related complications than non-backed cups (Ritter *et al.*, 1990). The stresses at the cement/bone interface are better comparable, as here identical interface conditions exist. Metal-backed cups were found to generate higher shear stresses, while a non-backed cup generates higher tensile stresses. The increase in the shear stresses for metal-backed cups is relatively higher, but actual rupture of the ce-

ment/bone interface depends on its strength in shear and tension respectively. Increasing the stiffness of the cup by using a CoCrMo-backing instead of titanium had little effect on the stresses in cement and bone. Apparently, a titanium backing is already so stiff in relation to the other materials, that it may be assumed to act almost as a rigid body; increasing the stiffness further has hardly any effect.

We have seen that the normal mechanical situation in the pelvic bone becomes disturbed when an acetabular implant is placed. Some clinical observations concerning the performance of acetabular cups might be associated with the transformations in stress patterns due to this newly created, 'unnatural' situation. Just like for femoral stems, the degree of stress shielding in the bone is largely determined by the flexibility of the implant. In this study, we have only considered a relatively flexible and a relatively stiff cup. Varying parameters like the thickness of the cement mantle or the thickness of the polyethylene is likely to result in more subtle changes in the pelvic load transfer.

References

- Andrew, S.M., Andrew, J.G., Wroblewski, B.M., Freemont, A.J. (1992) Is there a difference in the role of inflammatory cells in aseptic loosening of femoral and acetabular components of hip arthroplasties? *Trans. Europ. Orthop. Res. Soc.*, **2**, 64.
- Bergmann, G., Graichen, F., Rohlmann, A. (1990) Instrumentation of a hip joint prosthesis. In: *Implantable telemetry in orthopaedics.*, eds. G. Bergmann, F. Graichen, A. Rohlmann, Freie Universität Berlin, pp. 35-63.
- Carter, D.R., Vasu, R., Harris, W.H. (1982) Stress distributions in the acetabular region - II. Effects of cement thickness and metal backing of the total hip acetabular component. *J. Biomech.*, **15**, 165-170.
- Charnley, J. (1979) *Low friction arthroplasty of the hip.*, New York, Springer-Verlag.
- Crowninshield, R.D., Brand, R.A. (1981) A physiologically based criterion of muscle force prediction in locomotion. *J. Biomech.*, **14**, 793-801.
- Dalstra, M., Huiskes, R. (1990) The pelvic bone as a sandwich construction; a three dimensional finite element study. *Proc. Europ. Soc. Biomech.*, **7**, B32.
- Dalstra, M., Huiskes, R. (1992) Load-transfer in pelvic cortical bone. *Proc. Europ. Soc. Biomech.*, **8**, 60.
- Dalstra, M., Huiskes, R., van Erning, L. (1992) Development and validation of a three-dimensional finite element model of the pelvic bone. *J. Biomech. Eng.*, accepted.
- Dalstra, M., Huiskes, R., Odgaard, A., van Erning, L. (1993) Mechanical and textural properties of pelvic trabecular bone. *J. Biomech.*, **26**, 523-535.
- Dostal, W.F., Andrews, J.G. (1981) A three-dimensional biomechanical model of hip musculature. *J. Biomech.*, **14**, 802-812.
- Finlay, J.B., Bourne, R.B., Landsberg, R.P.D., Andreac, P. (1986) Pelvic stresses in vitro - II. a study of the efficacy of metal-backed acetabular prostheses. *J. Biomech.*, **19**, 715-725.
- García-Cimbrelo, E., Munuera, L. (1992) Early and late loosening of the acetabular cup after low-friction arthroplasty. *J. Bone Joint Surg.*, **74-A**, 1119-1129.
- Goel, V.K., Valliappan, S., Svensson, N.L. (1978) Stresses in the normal pelvis. *Comput. Biol. Med.*, **8**, 91-104.
- Harris, W.H. (1971) A new total hip implant. *Clin. Orthop.*, **81**, 105-113.
- Huiskes, R. (1987) Finite element analysis of acetabular reconstruction. *Acta Orthop. Scand.*, **58**, 620-625.
- Jacob, H.A.C., Huggler, A.H., Dietschi, C., Schreiber, A. (1976) Mechanical function of subchondral bone as experimentally determined on the acetabulum of the human pelvis. *J. Biomech.*, **9**, 625-627.

- Koeneman, J.B., Hansen, T.M., Beres, K. (1989) Three dimensional finite element analysis of the hip joint. *Trans. Orthop. Res. Soc.*, **14**, 223.
- Landjerit, B., Jacquard-Simon, N., Thourot, M., Massin, P.H. (1992) Physiological loadings on human pelvis: a comparison between numerical and experimental simulations. *Proc. Europ. Soc. Biomech.*, **8**, 195.
- Malchau, H., Herberts, P., Ahnfelt, L., Johnell, O. (1993) Prognosis of total hip replacement. Results from the national register of revised failures 1979-1990 in Sweden - a ten year follow-up of 92,675 THR. *Scientific exhibition 61st AAOs*, february 18-23, 1993, San Francisco, USA.
- Oonishi, H., Isha, H., Hasegawa, T. (1983) Mechanical analysis of the human pelvis and its application to the articular hip joint - by means of the three dimensional finite element method. *J. Biomech.*, **16**, 427-444.
- Pedersen, D.R., Crowninshield, R.D., Brand, R.A., Johnston, R.C. (1982) An axisymmetric model of acetabular components in total hip arthroplasty. *J. Biomech.*, **15**, 305-315.
- Pierson, J.L., Harris, W.H. (1993) Extensive osteolysis behind an acetabular component that was well fixed with cement - a case report. *J. Bone Joint Surg.*, **75-A**, 268-271.
- Rapperport, D.J., Carter, D.R., Schurman, D.J. (1987) Contact finite element stress analysis of porous ingrowth acetabular cup implantation, ingrowth, and loosening. *J. Orthop. Res.*, **5**, 548-561.
- Renaudin, F., Lavaste, F., Skalli, W., Pecheux, C., Scmitt, V. (1992) A 3D finite element model of pelvis in side impact. *Proc. Europ. Soc. Biomech.*, **8**, 194.
- Ritter, M.A., Keating, E.M., Faris, Ph.M., Brugo, G. (1990) Metal-backed acetabular cups in total hip arthroplasty. *J. Bone Joint Surg.*, **72-A**, 672-677.
- Santavirta, S., Hoikka, V., Eskola, A., Kontinen, Y.T., Paavilainen, T., Tallroth, K. (1990) Aggressive granulomatous lesions in cementless total hip arthroplasty. *J. Bone Joint Surg.*, **72-B**, 980-984.
- Schmalzied, Th.P., Kwong, L.M., Jasty, M., Sedlacek, R.C., Haire, T.C., O'Connor, D.O., Bragdon, Ch.R., Kabo, J.M., Malcolm, A.J., Path, M.R.C., Harris, W.H. (1992) The mechanism of loosening of cemented acetabular components in total hip arthroplasty. *Clin. Orthop. Rel. Res.*, **274**, 60-78.
- Stauffer, R.N. (1982) Ten-year follow-up study of total hip replacement with particular reference to roentgenographic loosening of the components. *J. Bone Joint Surg.*, **64-A**, 983-990.
- Sutherland, Ch.J., Wilde, A.H., Borden, L.S., Marks, K.E. (1982) A ten-year follow-up of one hundred consecutive Müller curved-stem total hip-replacement arthroplasties. *J. Bone Joint Surg.*, **64-A**, 970-982.
- Vasu, R., Carter, D.R., Harris, W.H. (1982) Stress distributions in the acetabular region - I. before and after total joint replacement. *J. Biomech.*, **15**, 155-164.

Prestresses around the acetabulum generated by screwed cups

M. Dalstra, R. Huiskes

Biomechanics Section, Institute of Orthopaedics, University of Nijmegen

Submitted to Clinical Materials

Abstract: *Screwed acetabular cups, applied in total hip replacements, generate stresses in the surrounding bone during implantation (prestresses). The effect of these prestresses on the endurance of the hip replacement are unknown. The prestresses in the acetabulum were examined both experimentally, using strain-gage techniques, and numerically, using the finite element method. It was found that the prestresses were on the same order of magnitude, if not larger, than the stresses due to the hip reaction force during one-legged stance. In some cases, the prestresses even approximated the ultimate tensile strength of cortical bone. The prestresses seemed to have a strong dependence on the outer shape of the cup, rather than on the flexibility of the cup or whether the cup had a self-cutting thread or not. Furthermore, it was found that the prestresses are not very susceptible to stress relaxation due to the viscoelastic behavior of bone. This means that prestresses will remain present over long periods of time. So even when a patient has resumed normal daily activities, the prestresses will still play an important role in the overall stress distributions around the acetabulum. Due to the interaction of prestresses and stresses due to normal loading, the primary stability of a metal backed screwed cup is better guaranteed than the primary stability of a full-polyethylene cup.*

Introduction

As cemented acetabular components proved to be less successful than their femoral counterparts (DeLee and Charnley, 1976; Charnley, 1979; Huiskes, 1980; Stauffer, 1982; Eriksson, 1984), several cementless fixation techniques were developed, one of which is the screwed cup (Mittelmeier, 1976; Weill, 1982; Lord and Bancel, 1983). Screwed acetabular cups are designed to generate stresses in the surrounding bone upon insertion to guarantee a good initial stability (Ungethüm and Blömer, 1986). Depending on the actual design of the cup, secondary stability may be realized by different principles, like the fit of the screw thread in the surrounding bone or bone ingrowth, but generating initial stresses or prestresses, as they are called, is inherent for all types of screwed cups. In stress analyses of screwed cups reported (Huiskes, 1987; Huiskes and Slooff, 1987), these prestresses were not considered, simply because hardly anything was known about them. Yet, if the magnitudes of these prestresses are substantial, their presence may greatly influence the stress patterns during physiological loading and may even lead to fractures in the bone. The purpose of this study was to obtain more information about the magnitudes and distributions of these prestresses and to examine how they interact with the stresses due to normal loading of the hip.

The study consisted of both *in vitro* strain-gage experiments and finite element analyses. The types of screw cups used in this study were a solid polyethylene (PE) cup, requiring pre-tapping of the thread, and a metal backed (MB) cup with self-cutting thread. Owing to these differences, the possible effects of the cup's flexibility and the type of thread on the prestresses could be examined, as well. The cups were implanted in acetabula of several cadaver pelvic bones and strains were recorded during insertion and subsequent loading in a material's testing machine, simulating the hip-joint force. As strain gages can only measure strains on the surface, the finite element method (FEM) was used to study the stress patterns within the bone around the acetabulum.

Materials and Methods

Strain-gage experiments

Six embalmed hemipelves were available for the experiments. They were mounted upside down in a block of acrylic bone cement with the iliac wing submerged. Each bone was fitted with six rectangular rosette strain gages. Three of these gages were placed on the posterior acetabular rim, one on the anterior side of the rim and two on the medial cortex, just underneath the acetabulum. The locations of the gages are shown in Figure 1.

Two types of cups were used. The first one was a pre-tapped solid polyethylene cup (Endler), the second was a self-cutting TiAl6V4-backed cup with a polyethylene liner (Zweymüller). On the outside, both cups had identical trapezoidal taper shapes. Each type of cup was implanted in three hemipelves. Before insertion, each acetabulum was prepared according to the manufacturer's guidelines (Allo Pro AG,

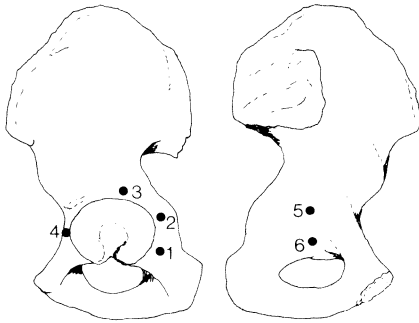


Fig. 1: The locations of the six rosette strain gages projected on a left hemipelvis.

Baar, Switzerland). For screwing the cup into the acetabulum, a torque wrench was used in order to have good control over the insertion torque. The strains in the gages were measured at torques of 10, 20 and 30 Nm and beyond this value at every increment of 5 Nm. This continued until the cup was judged to have the right fit. From the measured strains, the principal stresses were calculated, assuming a Young's modulus of 17.0 GPa (Reilly *et al.*, 1974), and a Poisson's ratio of 0.3 for the cortical bone. The hemipelves were left untouched after the final torque was applied and strains were measured again after

50 and 100 minutes to see if any stress relaxation had occurred in the bone.

After inserting the cups, the hemipelves were mounted in an MTS-based loading machine (DSTS Engineering & Electronics, Zoetermeer, the Netherlands) and a force was applied to the cup, simulating the hip reaction force during the one-legged stance phase, when the hip reaction force reaches its maximal magnitude of about 3.5 to 5 times bodyweight (Bergmann *et al.*, 1990). At each increment of 500 N up to 2500 N, the strains in the gages were recorded and again the corresponding principal stresses were calculated.

FEM analyses

An axisymmetric finite element model was used. The mesh is shown in Figure 2 and in Table 1 the Young's moduli of the various materials are given. All materials were assumed to be linear elastic, homogeneous and isotropic, with the distribution of the bone elastic constants according to Pedersen and co-workers (1982). The elements used in the analyses are axisymmetric with quadrilateral cross section and eight nodal points (isoparametric quadratic displacement). For the loads, an external hip contact stress distribution was directly prescribed as a distributed load over the inner cup boundary over a globular region measuring 60 degrees across. Towards the edges the magnitude of the distributed load decreased to half of its value in the center. Because the FE model can only simulate static or quasi-static loading, the actual process of inserting the cup could not be modelled directly. Therefore, to simulate the generation of the prestresses, the elements constituting the cup were expanded by using the thermal expansion procedure of the FE code (MARC, MARC Analysis Corporation, Palo Alto, CA, USA). The surrounding bone deformed by this increase of volume in a similar manner as if a cup was inserted and the stresses thus generated represent the prestresses. To be assured of a resulting stress pattern in the bone with a good resemblance to the actual stress patterns in the experiments, several calculations were performed for both types of cup, each time varying a group of elements

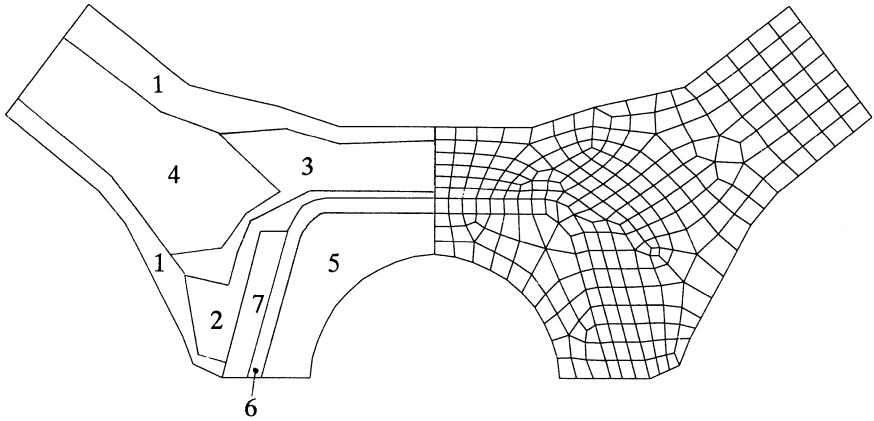


Fig. 2: The FE mesh (right) with the regions of the different materials (left).

involved in the expansion procedure. Then two points in the mesh were chosen; the first one corresponding to the locations of gages 1 or 4, the second one to the locations of gages 5 or 6. In the analysis, the ratio of the total shear strains, occurring in these points was calculated and compared to the same ratio as found in the experiments. Only the analysis which compared best to the actual ratio was considered further. For this particular analysis, scaling was applied, such that the total shear strain in the point on the lateral cortex equalled the average value of the total shear strain at the gage locations 1 and 4 in the experiments.

region	material	Young's modulus (GPa)
1	cortical bone	17.0
2	cancellous bone	3.0
3	cancellous bone	1.5
4	cancellous bone	1.0
5	polyethylene	0.7
6(PE)	polyethylene	0.7
6(MB)	titanium-alloy	110.0
7(PE)	screw thread/bone	11.0
7(MB)	screw thread/bone	32.0

Table 1: Materials and their Young's moduli, used in the FE model.

Results

Strain-gage experiments

Due to individual differences in bone quality of the cadaver hemipelves used in the experiments, there was a large scatter in the values of the strains and the applied torque needed to insert the cups. Yet some consistent differences between the insertion of the full-polyethylene (PE) and the metal-backed (MB) cups could be observed. The maximal torque needed to screw the cup into the acetabulum was significantly higher for the MB cups. The mean value, averaged over the three pelvic bones, was 51.3 Nm with a standard deviation of 12.3 Nm. For the PE cups these values were 29.0 Nm and 5.9 Nm, respectively. This difference can be explained by the fact that the MB cup has self-cutting thread and thus has to overcome much more resistance than the PE cup, for which the thread has already been cut in the preparation phase.

A positive correlation was found between the magnitude of the torque applied and the values of the strains measured in each case. The torque-strain relationships showed considerable variations, even in the same series of implants, probably due to intraspecimen variations. However, the strain values at maximal torque were qualitatively very similar, regardless of the type of implant inserted. In the Figures 3 and 4, the principal strains, averaged over the three bones, are graphically displayed. For this purpose, the magnitudes and the directions of these principal strains have been averaged separately to ensure that the average maximal and average minimal principal strains remain perpendicular to one another.

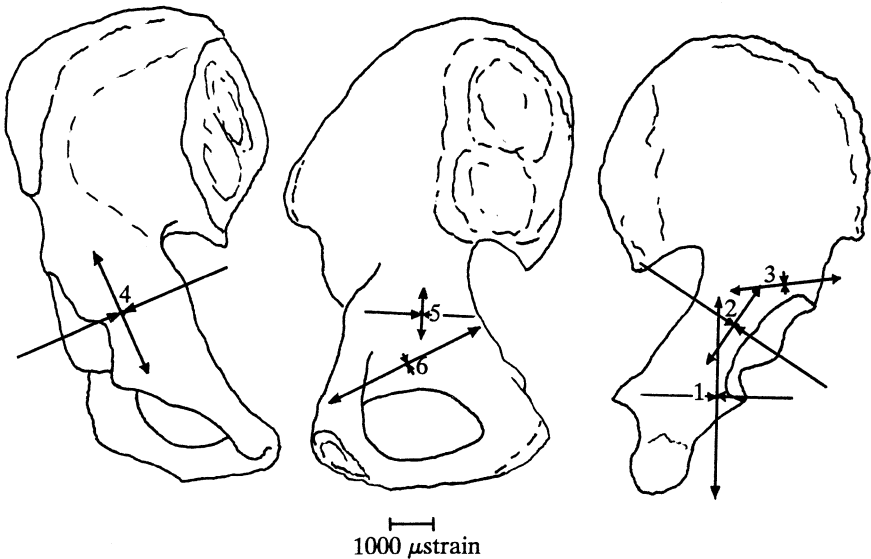


Fig. 3: Average principal strains at the strain-gage locations due to inserting a PE cup.

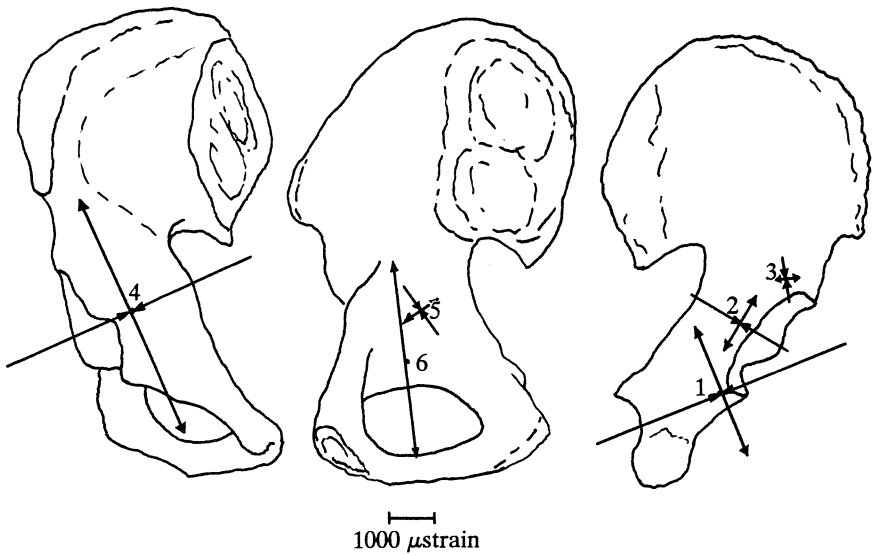


Fig. 4: Average principal strains at the strain-gage locations due to inserting a MB cup.

In Table 2, the accompanying values for the principal and the Von Mises stresses at the individual gage locations are given for each type of cup, averaged over the three pelves. The Von Mises stresses can be seen as a measure for the stress intensity. Despite large standard deviations, it is evident that for both types of cups, the gages 1 and 4 are the most highly strained and gages 3 and 5 the least.

gage	non-backed (PE) cup			metal-backed (MB) cup		
	σ_{\max}	σ_{\min}	σ_{Mss}	σ_{\max}	σ_{\min}	σ_{Mss}
1	14.9 (10.9)	-63.9 (24.4)	73.6 (16.8)	33.4 (29.3)	-20.4 (16.3)	51.3 (21.1)
2	16.5 (10.1)	-22.1 (5.3)	34.2 (7.1)	6.1 (9.8)	-43.5 (31.9)	48.1 (30.4)
3	5.8 (2.5)	-6.2 (2.7)	10.6 (2.5)	22.0 (27.3)	2.8 (20.7)	27.0 (18.1)
4	35.8 (28.1)	-44.5 (26.4)	74.0 (15.7)	14.4 (28.2)	-41.6 (10.5)	54.7 (14.7)
5	4.2 (3.1)	-10.9 (10.1)	14.3 (7.8)	2.5 (0.5)	-21.5 (8.8)	22.9 (8.5)
6	43.7 (11.4)	14.9 (10.0)	39.0 (8.8)	36.3 (7.9)	5.3 (14.2)	35.9 (5.9)

Table 2: Average values and standard deviations (between brackets) of the principal stresses and the Von Mises stresses (in MPa) at the individual gages for both PE and MB cups for maximal applied torque.

Furthermore, it was observed that for the gages on the acetabular rim, tension occurred circumferential to the rim and compression perpendicular to it. On the medial cortex tension occurred more or less in the direction of the foramen obturatum

and again compression perpendicular to it. This deformation mode shows that the cups are acting as wedges, trying to force the acetabulum open by hinging it around an axis from the ilium to the incisura acetabuli.

Due to the viscoelastic behavior of bone, the strains and stresses, caused by inserting a cup, will reduce after a while. To estimate the order of magnitude of this relaxation, the Von Mises stresses were considered just after insertion, and 50 and 100 minutes later. The maximal decrease in value that occurred was 6.5 percent after 50 minutes and 8.0 percent after 100 minutes. If an exponential function is assumed to describe this relaxation process in time, it can be calculated that the Von Mises stresses will never drop below 91.5 percent of their original values. This means that the major parts of the prestresses remain, even after an infinitely long period of time, assuming of course that no biological relaxation effect, like bone remodeling, takes place.

After inserting the cups, the pelvic bones were placed in a testing machine to simulate the hip reaction force. As should be expected, linear relations between the stresses and the load magnitude were observed, but due to the intraspecimen variations the magnitudes of the stresses again varied from case to case. In Table 3, the principal and the Von Mises stress values at the individual gage locations are given at the maximal load value, averaged over the three pelvis.

non-backed (PE) cup				metal-backed (MB) cup		
gage	σ_{\max}	σ_{\min}	σ_{Mss}	σ_{\max}	σ_{\min}	σ_{Mss}
1	14.8 (0.9)	-27.3 (2.6)	37.0 (1.8)	12.4 (9.9)	-10.4 (12.0)	22.6 (5.7)
2	11.0 (6.9)	-23.5 (7.9)	31.4 (2.3)	4.7 (5.4)	-7.7 (7.3)	12.6 (2.7)
3	15.0 (10.3)	-16.9 (15.7)	30.5 (4.7)	22.1 (5.6)	-10.0 (19.4)	31.7 (12.9)
4	5.8 (6.2)	-12.0 (1.0)	16.5 (3.3)	27.3 (9.4)	4.0 (6.0)	25.9 (8.3)
5	61.3 (37.9)	7.5 (7.7)	58.0 (34.5)	22.8 (14.7)	3.1 (5.4)	21.7 (12.7)
6	0.7 (19.8)	-44.2 (15.7)	47.8 (5.2)	3.5 (1.5)	-20.4 (10.4)	22.5 (10.0)

Table 3: Average values and standard deviations (between brackets) of the principal stresses and the Von Mises stresses (in MPa) at the individual gages for both PE and MB cups for a load of 2500 N.

Compared to the values during insertion (Table 2), the standard deviations were smaller, suggesting a more uniform response of the bone to this kind of loading. It was observed for the gages on the acetabular rim that the average direction of tension had shifted about 90 degrees relative to the one during insertion of the cup. So now compression occurred more or less circumferential to the rim, except for the gages 2 and 4 in case of a PE cup, where tension remained circumferential. This shift of 90 degrees causes the tensile stresses due to inserting the cup to be somewhat neutralized by the compressive stresses due to loading and vice versa, when the two loading

situations are superimposed. The direction of the principal stresses in the medial cortex is less clear. For the PE cups, the direction of tension was pointing towards the ischial bone and for the MB cups the direction of tension was pointing towards the foramen obturatum at gage 6 and perpendicular to this at gage 5.

The results of superpositioning the two loading cases (Tables 2 and 3), are summarized in Table 4. Comparing the ranges of the principal stresses during insertion (Table 2) to those after insertion with a physiological load (Table 4), it appears that for the MB cups the combined range is for the greater part based on the prestresses and only slightly enlarged by the stresses due to loading. For the PE cups, the high tensile stresses due to loading are tempered by the prestresses, while for compression the stress peaks of inserting and loading seem to add up.

gage	non-backed (PE) cup			metal-backed (MB) cup		
	σ_{\max}	σ_{\min}	σ_{Mss}	σ_{\max}	σ_{\min}	σ_{Mss}
1	5.9 (4.7)	-67.5 (34.2)	71.0 (31.3)	33.5 (26.6)	-17.8 (9.7)	45.9 (29.8)
2	-0.7 (0.2)	-13.9 (0.8)	13.6 (0.7)	9.5 (3.8)	-48.5 (37.1)	54.3 (35.7)
3	16.4 (12.3)	-21.2 (10.2)	34.6 (0.9)	42.5 (32.9)	-7.0 (40.2)	56.6 (21.0)
4	9.0 (16.5)	-51.7 (32.9)	59.8 (21.4)	38.9 (23.5)	-35.6 (6.6)	65.7 (20.2)
5	49.3 (25.2)	7.9 (6.9)	46.0 (22.3)	12.6 (9.3)	-5.4 (11.8)	18.3 (8.5)
6	24.9 (15.8)	-9.5 (1.5)	31.0 (16.1)	26.0 (12.1)	-1.3 (9.0)	27.5 (13.8)

Table 4. Average values and standard deviations (between brackets) of the principal stresses and the Von Mises stresses (in MPa) at the individual gages for both PE and MB cups in the combined load case.

FEM analyses

As already shown in Figures 3 and 4, a prominent component of the prestresses around the acetabulum are the hoop stresses, which, because of the stretching of the acetabular rim, are tensile by nature. Figure 5 shows the values of this stress component in the bone for both types of cup from the FE analyses simulating the insertion of the cup. Because of symmetry, only half of the meshes are shown. In accordance with the experimental findings, the distributions of this stress component are very similar for both types of cup. In the acetabular rim and at the medial cortex, right underneath the cups' domes, the highest values occur and these stresses are indeed tensile. In fact, all along the cup/bone interface, hoop stresses are tensile. In Figure 6, the hoop stresses and the other stress components are combined in the Von Mises stress. Like the hoop stresses, the Von Mises stress distributions are also very similar for both types of cups. High stresses occur particularly in the bone directly around the cups and in the cortical shells.

When subject only to external loading, the major part of the load is transferred straight through the dome of the cup onto the medial cortex for both MB and PE

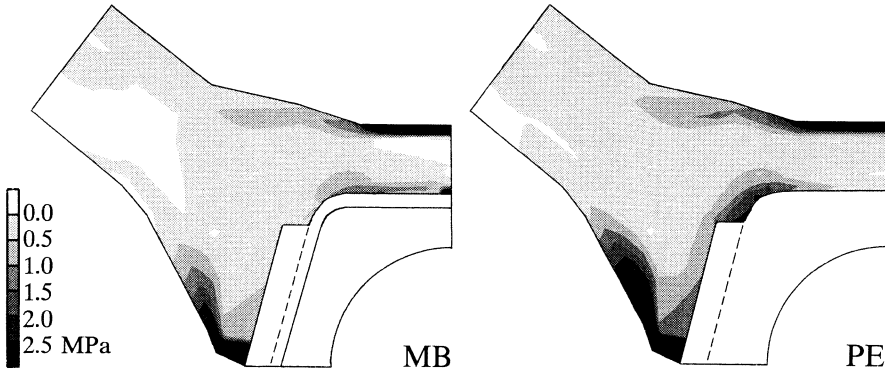


Fig. 5: Tensile hoop stress distributions due to inserting the cup for both MB and PE cups. White areas denote compressive hoop stresses.

cups. Due to the stiff backing, however, the MB cup is able to direct a small part of the load to the lateral cortex, while for the PE cup, the lateral cortex is hardly loaded at all.

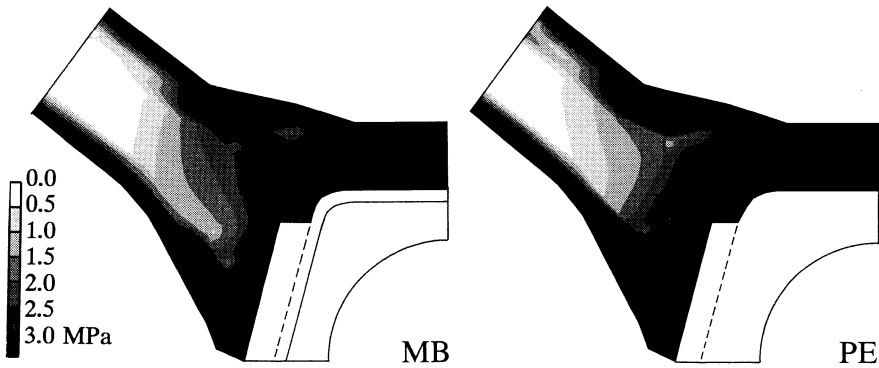


Fig. 6: Von Mises stress distributions due to inserting the cup for both MB and PE cups.

The Von Mises stress patterns resulting from only the hip-joint force, without prestresses, are shown in Figure 7. Unlike in the experiments, the stresses due to hip-joint loading are now much smaller than the prestresses. Because of this, the prestress patterns seem hardly affected by the hip reaction force, when both loading modes are combined. The resulting Von Mises stress distributions are shown in Figure 8. For both cups, a slight attenuation in the medial cortex is observed, but the high prestresses around the implant remain fully present. The combination of prestresses and stresses due to loading resulted in a decrease of the (tensile) hoop stresses and an increase in the (compressive) parallel stresses in the acetabular rim for both types of

cups. The decrease in the hoop stress for the PE cup, however, was somewhat larger than for the MB cup.

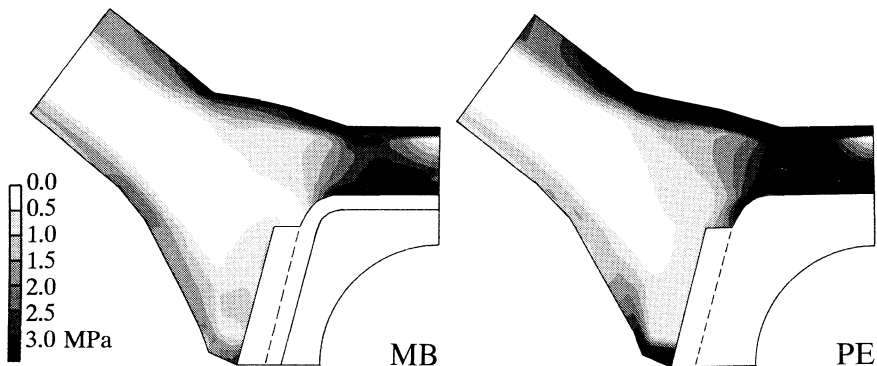


Fig. 7: Von Mises stress distribution due to the hip-joint force for both MB and PE cups.

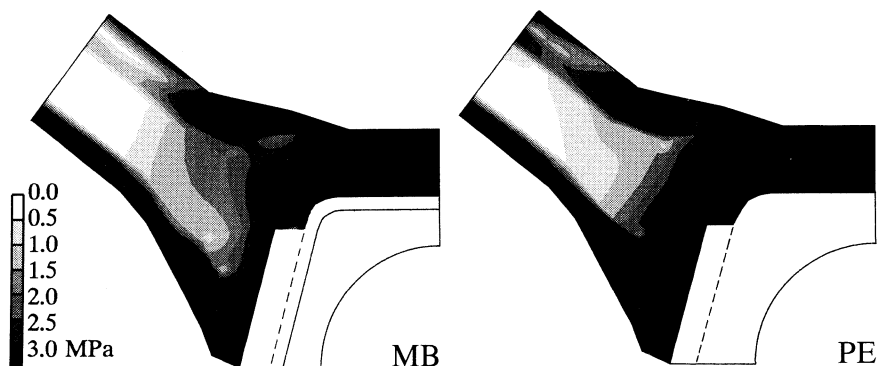


Fig. 8: Von Mises stress distributions in the combined case for both MB and PE cups.

Discussion

Screwed acetabular cups obtain a press-fitted primary fixation by generating prestresses in the surrounding bone upon insertion. Hardly any quantitative data on these prestresses were available. The present study was performed to provide quantitative information about prestresses and to analyze the interaction of these prestresses with the stresses due to normal loading. For this purpose two different types of acetabular cups were selected in order to be able to study the effects of the cup flexibility characteristics and the type of screw thread on the prestresses, as well.

Strain measurements during inserting both the metal backed (MB) and the solid polyethylene (PE) cups in cadaver pelvic bones, revealed peak values of about 5,000 microstrain (both tensile and compressive). The values of the corresponding stresses were about the same for both cups (Table 2), suggesting that the prestresses are not so much dependent on either the cup's flexibility or the method of implantation (pre-tapped or self-cutting thread). In some cases, these prestresses were even on the same order of magnitude as the ultimate tensile strength of human compact bone (Reilly and Burstein, 1975). This means that cracks in the acetabular rim might easily occur, so it requires both care and experience on behalf of the orthopaedic surgeon to decide whether he can tighten the cup a bit more or not. He should also pay attention to the bone quality around the acetabulum, for we found in our experiments a large intraspecimen variation, which will surely also show up in the reality of an operating room. This variety in bone quality has a great influence on the magnitude of the prestresses and thus makes them somewhat unpredictable. Despite these variations, however, the MB and PE cups showed the same trend in the prestress patterns they generated in the surrounding bone. At the strain-gage locations 1 to 4, tensile stresses occurred circumferentially and compressive stresses were found perpendicular to this. The compressive stresses tended to be somewhat larger in magnitude than the tensile stresses. These locations also showed to have the highest stresses in an absolute sense. In the bone underneath the acetabulum (locations 5 and 6), tensile stresses occurred in the direction of the foramen obturatum and the pubic bone with compressive stresses perpendicular to this. These stresses suggest a deformation mode in which the acetabulum is 'hinged open' along a line perpendicular to the foramen obturatum. This is caused by a structural weakening of the acetabular wall by the incisura acetabuli.

Measurements show that some degree of relaxation of the prestresses occurs during the first few hours after implantation, due to viscoelastic effects. However, they remain at about 90 percent of their initial value over a long period of time. These measurements were performed using embalmed bone material, so it may well be that for fresh bone the results would be different. Adaptive bone remodeling will certainly also affect these stresses *in vivo*. As the prestresses constitute an unphysiological loading, the affected bone will remodel in such a way, that these stresses reduce. This effect, however, was not further evaluated in this study.

During loading of the pelvic bones in the testing machine, the stresses in the bones implanted with PE cups were almost twice as high as the stresses in the bones implanted with MB cups. This is caused by the deformation restraints which the metal backing imposes on the underlying bone. The stresses were on the same order of magnitude as the prestresses, suggesting that the prestresses are quite substantial in relation to the stresses due to normal activities. However, the presence of prestresses does not necessarily mean that the bone will be stressed additionally; theoretically, both stress states can level each other out. This all depends on the directions and magnitudes of the principal stresses. When there is no or only a minor shift in the directions of the maximal principal stresses as a result from the insertion and due to physiological loading, the stresses will amplify each other. However, if that shift is

about 90 degrees, then compressive and tensile stresses will be neutralized. In our experiments, a decrease in the overall stress level in the acetabular rim was observed in the case of a PE cup, while with a MB cup the stresses increased around the acetabulum.

Because the strain-gage experiments can give only information about the strains and stresses on the outside of the bone, numerical simulations (FEM) of these experiments were made to obtain data on the stresses within the bone. FE analyses of the pelvic bone have been reported by several authors. For modeling the acetabular region, there are three basic possibilities; two-dimensional (2-D) models (Carter *et al.*, 1982; Vasu *et al.*, 1982; Rappoport *et al.*, 1985), semi 3-D axisymmetric models (Pedersen *et al.*, 1982; Crowninshield *et al.*, 1983; Huiskes, 1987; Huiskes and Slooff, 1987), and 3-D models (Goel *et al.*, 1978; Oonishi *et al.*, 1983; Dalstra and Huiskes, 1991). Unlike finite element models of the femoral reconstruction (Verdonschot and Huiskes, 1990), however, the similarity between 2-D, axisymmetric and 3-D pelvic models of acetabular reconstruction is not very good. Obviously, a 3-D model has the best potential to produce the most realistic results. A 2-D model tends to underestimate the real acetabular stiffness, because it takes no account of the out-of-plane part of the acetabular wall. Therefore stresses, calculated from a 2-D pelvic model are usually too high. Conversely, an axisymmetric model tends to overestimate the real stiffness. This means that 2-D and axisymmetric pelvic models should, therefore, rather be interpreted in a qualitative sense.

The same trends in the experimental findings were also found in the FE analyses. As far as the prestresses are concerned, both types of cup generated similar stress patterns. The stresses due to the hip-joint force showed a difference in the load-transfer characteristics between a metal backed and a non-backed cup. The metal backing seems to take over the mechanically important role of the subchondral bone (Jacob *et al.*, 1976; Charnley, 1979), and spreads the load transfer from cup to bone more evenly along the interface. In 3-D FE analyses, however, it appears that this results in a concentrated load transfer along the acetabular rim (Dalstra and Huiskes, 1991). The present FE analyses confirmed the experimental finding that the interaction of prestresses and stresses due to normal loading leads to a decrease of the stresses in the acetabular wall when PE cups are used. In particular, the tensile hoop stress, which is the 'containing' component for the cup, decreases. This suggests that the primary stability of full-polyethylene screwed cups may suffer more relative to metal-backed screwed cups, once normal loading is resumed. At the end of the eighties, use of the full-polyethylene Endler cup has led to a high number of loosening, in fact so many that further production of the cup was stopped (Slootman, 1993). Apparently, the cups had badly suffered from micromotions, because upon revision the polyethylene which had been in contact with bone showed much wear. Load transfer predominantly takes place in the first and last screw thread (Huiskes, 1987), resulting in high stress concentrations locally at the interface between cup and bone. Gross migrations, following from disruption of this interface, are not an all unfamiliar problem for fully-threaded cups (Snorrason and Kärrholm, 1990). Early loss of initial stability, as this study has demonstrated, may have accelerated the

process of loosening, leading to the dramatic performance of the Endler cup.

References

- Bergmann, G., Graichen, F., Rohlmann, A. (1990) Instrumentation of a hip joint prosthesis. In: *Implantable telemetry in orthopaedics.*, eds. G. Bergmann, F. Graichen & A. Rohlmann. Freie Universität Berlin, pp. 35-63.
- Carter, D.R., Vasu, R., Harris, W.H. (1982) Stress distributions in the acetabular region II; Effects of cement thickness and metal backing of the total hip acetabular component. *J. Biomech.*, **15**, 165-170.
- Charnley, J. (1979) *Arthroplasty of the hip, theory and practise.*, New York, Springer Verlag.
- Crowninshield, R.D., Brand, R.A., Pedersen, D.R. (1983) A stress analysis of acetabular reconstruction in protrusio acetabuli. *J. Bone Joint Surg.*, **65-A**, 495-499.
- Dalstra, M., Huiskes, R. (1991) The influence of metal backing in cemented cups. *Trans. Orthop. Res. Soc.*, **16**, 272.
- DeLee, J.B., Charnley, J. (1976) Radiological demarcation of cemented sockets in total hip replacement. *Clin. Orthop. Rel. Res.*, **121**, 20-23.
- Eriksson, A.R. (1984) *Heat-induced bone tissue injury.*, dissertation, University of Göteborg, Sweden, 1984.
- Goel, V.K., Valliappan, S., Svenson, N.L. (1978) Stresses in the normal pelvis. *Comput. Biol. Med.*, **8**, 91-104.
- Huiskes, R. (1980) Some fundamental aspects of human joint replacement. *Acta Orthop. Scand.*, **51**, Suppl. 185.
- Huiskes, R. (1987) Finite element analysis of acetabular reconstruction; noncemented threaded cups. *Acta Orthop. Scand.*, **58**, 620-625.
- Huiskes, R., Slooff, T.J. (1987) Stress transfer across the hip joint in reconstructed acetabuli. In: *Biomechanics: Basic and applied research.*, eds. G. Bergmann, R. Kölbl, A. Rohlmann. Dordrecht, Martinus Nijhoff Publishers, pp. 333-340.
- Jacob, H.A.C., Huggler, A.H., Dietschi, C., Schreiber, A. (1976) Mechanical function of subchondral bone as experimentally determined on the acetabulum of the human pelvis. *J. Biomech.*, **9**, 625-627.
- Lord, G., Bancel, P. (1983) The madreporic cementless total hip arthroplasty. New experimental data and a seven year clinical follow up study. *Clin. Orthop.*, **176**, 67-76.
- Mittelmeier, H. (1976) Anchoring hip endoprostheses without bone cement. In: *Advances in artificial hip and knee joint technology.*, eds. M. Schaldach, D. Hohmann. Berlin, Springer Verlag.
- Oonishi, H., Isha, H., Hasegawa, T. (1983) Mechanical analysis of the human pelvis and its applications to the artificial hip joint - by means of the three dimensional finite element method. *J. Biomech.*, **16**, 427-444.
- Pedersen, D.R., Crowninshield, R.D., Brand, R.A., Johnston, R.C. (1982) An axisymmetric model of acetabular components in total hip arthroplasty. *J. Biomech.*, **15**, 495-499.
- Rapperport, D.J., Carter, D.R., Schurman, D.J. (1985) Contact finite element stress analysis of the hip joint. *J. Orthop. Res.*, **3**, 435-446.
- Reilly, D.T., Burstein, A.H., Frankel, V.H. (1974) The elastic modulus for bone. *J. Biomech.*, **7**, 271-275.
- Reilly, D.T., Burstein, A.H. (1975) The elastic and ultimate properties of compact bone tissue. *J. Biomech.*, **8**, 393-405.
- Slootman, R. (1993) Personal communication (Allo Pro Nederland BV, Eindhoven).
- Snorrason, F., Kärrholm, J. (1990) Primary migration of fully-threaded acetabular prostheses. *J. Bone Joint Surg.*, **72-B**, 647-652.
- Stauffer, R.N. (1982) Ten-year follow-up study of total hip replacement. *J. Bone Joint Surg.*, **64-A**, 983-990.
- Ungethüm, M., Blömer, W. (1986) Biomechanische Aspekte Zementfreier Hüftpfannenimplantate mit Schraubverankerung. *Med. Orthop. Tech.*, **6**, 194-197.
- Vasu, R., Carter, D.R., Harris, W.H. (1982) Stress distributions in the acetabular region I; Before and after total joint replacement. *J. Biomech.*, **15**, 155-164.

- Verdonschot, N., Huiskes, R. (1990) FEM analyses of hip prostheses: validity of the 2-D side-plate model and the effects of torsion. *Proc. Europ. Soc. Biomech.*, 7, A20.
- Weill, D. (1982) Les prothèses de hanche non cimentées. Premiers résultats. A propos d'une série personnelle de 166 implantations. *Ann. Orthop. Traumatol. Est.*, V, 9-21.

Differences in pelvic load transfer due to variations in acetabular cup design

M. Dalstra, R. Huiskes, J.E. Bechtold*, R.F. Kyle*, R.B. Gustilo*

Biomechanics Section, Institute of Orthopaedics, University of Nijmegen

*Orthopaedic Biomechanics Laboratory, Hennepin County Medical Center

Submitted to the Journal of Arthroplasty

Abstract: *The load-transfer mechanism in the acetabular part of total-hip replacement is poorly understood. As a result, little is known about the effects of surgical and design parameters on the probability of mechanical failure. In this study three design features of acetabular cups were evaluated concerning their influence on the load transfer across the pelvic bone. Using an anatomic three-dimensional finite element model, the effects of acrylic cement thickness, metal backing and thickness of polyethylene on the stress distributions in the various materials and interfaces were investigated.*

The mechanical influence of an acetabular cup on the pelvic bone is restricted to the acetabular region. Hence, differences in cup design only work through in the subchondral bone and the underlying trabecular bone, while the stress distributions in the cortical shells are hardly affected. The mechanical requirements for acetabular cups are subject to incompatible design goals. Increasing the stiffness of the cup, either by adding cement, a metal backing or a thicker polyethylene layer, results in a decrease of the stresses in the polyethylene liner, which might result in less wear of the polyethylene. However, a stiffer cup also means that in the subchondral bone and the cement mantle (if present) stresses become more concentrated in the periphery, while in the dome area of the acetabulum stress shielding takes place. Possible consequences of this (increased risk for interface failure at the periphery and bone resorption in the dome area) correspond well to clinical observations. This shift in the stress distributions is most prominent for metal-backed cups. In fact, the highest stresses between implant and bone were found for cementless, metal-backed cups. Therefore, the present study can not confirm the alleged mechanical advantage of metal backing put forward by earlier finite element studies.

Introduction

Most acetabular cups in total hip replacement are of a hemispherical shape. Individual designs vary in size or in thickness of polyethylene. They may have metal backing or not and different fixation methods for attachment to the bone, such as acrylic cement, screw fixation or pegs. The underlying design philosophies behind many of these features, however, are often based on subjective information or fashion, rather than on quantitative data. At this stage, it is hard to decide which type of acetabular cup performs best. The ultimate test of a prosthesis is its clinical performance, but follow-up studies of the newer designs have generally been short.

It is known that cemented cups show sharply increasing failure rates after a period of eight to ten years (Sutherland *et al.*, 1982; Mulroy and Harris, 1990). This is usually attributed to the effects of polyethylene wear particles (Wroblewski, 1986; Schmalzried *et al.*, 1992), although other causes were also reported (Kelley and Johnston, 1992). Excessive polyethylene debris has also led to abandonment of the concept of cementless uncoated polyethylene cups (Wilson-MacDonald *et al.*, 1990).

Pre-clinical testing of acetabular prostheses may produce valuable information on the mechanical effects of design features. Examples of methods are *in-vitro* strain-gage experiments or finite element studies. To extrapolate the results from pre-clinical testing to the *in vivo* situation, the model must be adequately precise, a condition which was not always fulfilled. Metal backing, for example, was initially designed to allow easy replacement of the polyethylene insert by Harris (1971), but it gained wider use after finite element studies had shown that a stiff backing in an acetabular prosthesis was mechanically favorable, as stresses in the cement mantle and the underlying bone would be reduced (Carter *et al.*, 1982; Pedersen *et al.*, 1982). This apparent advantage, however, did not bear out in clinical practice. Ritter *et al.* (1990) have shown that in a well-matched series of metal-backed and full-polyethylene cups, the latter showed much better results. Radiolucency, loosening and revision were two to three times as frequent in the metal-backed series as in the full polyethylene ones, which led the authors to advise against their further use. Re-evaluating metal backing in a three-dimensional finite element model, Dalstra and Huiskes (1991) found higher stresses in the cement mantle and at its interfaces than in non-backed reconstructions. Whether these increased stress levels are the direct cause for the inferior performance of metal-backed cups or that this must be attributed to additional polyethylene wear from the polyethylene/backing interface can not be answered at this stage, but the fact remains that earlier simplified finite element models produced erroneous information.

Using more precise three-dimensional, validated finite element models, this study was meant to investigate the effects of acetabular design features on pelvic load transfer and to see whether clinical observations regarding failure of acetabular cups can be explained with a better understanding of the mechanics of a cup *in situ*. Design variations studied include the cementless versus cemented and full-polyethylene versus metal-backed cups. The influence of the thickness of the polyethylene socket was evaluated as well.

Method

A three-dimensional finite element model of a left pelvic bone was developed. The outer geometry of the bone was established by digitizing 8 mm thick slices of an actual pelvic bone, which had been sectioned previously. Within the spatial boundaries set by the contours of these slices, a distribution in elements was made. In the acetabulum additional elements were placed to represent the implant configuration, a hemispherical acetabular prosthesis. In positioning the prosthesis, a thin layer of (relatively stiff) subchondral bone was assumed to be still present. The total mesh consisted of 1,506 elements. For trabecular bone, subchondral bone and the prosthesis 8-node brick elements were used. The cortical shell covering the entire pelvic bone was in most locations too thin to use brick elements, and therefore 4-node membrane elements were used instead. The femoral head of the stem was also included in the model, to guarantee smooth load transfer at the articulation. Gap elements were used to allow only compressive contact between the head and the polyethylene liner. The implant was assumed to be fully bonded to bone and cement.

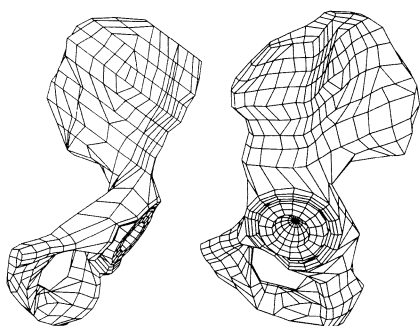


Fig. 1: Frontal and lateral view of the basic model.

A frontal and a lateral view of the mesh are given in Figure 1. Table 1 shows the values of the Young's moduli of the various materials. The values for the Young's moduli of the individual elements representing pelvic trabecular and subchondral bone, as well as the local thickness of the cortical shell, were based on values taken from dual-energy CT-scans (Dalstra *et al.*, 1992).

The loads applied in the model simulate the beginning of the one-legged stance phase of a normal walking cycle. Previous analyses (Dalstra and Huiskes, 1992) have shown that in this particular phase the highest stresses in the pelvic bone are generated. The individual

forces include the hip-joint force and 15 muscle forces. The direction and magnitude of the hip-joint force was based on data by Bergmann and co-workers (1990). The magnitude of the muscle forces was taken from data by Crowninshield and Brand (1981), while the direction of the muscle forces was calculated from the coordinates of the proximal and distal insertion areas of the muscles given by Dostal and Andrews (1981).

The following variations of the acetabular cup configuration were included in the analyses. First a division was made between cementless and cemented cups. In the latter case, a cement mantle with a uniform thickness of 2 mm was assumed. For each of these two groups, both a full-polyethylene and a TiAl6V4-backed variant were studied. Finally, for all these cases either a 6 mm or a 10 mm thick polyethylene liner were considered. The difference in thickness was realized by increasing the outer diameter of the cup. In all cases, a 28 mm sized head was

assumed. The variations resulted in eight different cases which are listed in Table 2. The finite element meshes were adjusted accordingly to account for these configurations.

material	Young's modulus (GPa)	Poisson's ratio
trabecular bone	0.001 - 0.132	0.2
subchondral bone	0.186 - 2.155	0.3
cortical bone	17.0	0.3
polyethylene	0.7	0.3
acrylic cement	2.3	0.3
TiAl6V4	110.0	0.3
ceramic	420.0	0.3

Table 1: Values of the Young's moduli and Poisson's ratios for the different materials used in the analyses.

cementless	full-polyethylene	6 mm PE	model 1
		10 mm PE	model 2
	Ti-backed	6 mm PE	model 3
		10 mm PE	model 4
cemented	full-polyethylene	6 mm PE	model 5
		10 mm PE	model 6
	Ti-backed	6 mm PE	model 7
		10 mm PE	model 8

Table 2: Overview of the variations in the eight different models.

In this study, the emphasis lies on comparing the stress distributions in the various materials and at their respective interfaces. With the interfaces often being the mechanically weakest link in a prosthesis/bone configuration, the interface stresses are of particular interest when evaluating an implant. Three individual stress components can be identified at an interface, a direct stress, normal to the interface and two perpendicular shear stresses in the plane of the interface. For a hemispherically shaped geometry like the acetabulum, the latter two can be defined as torsional shear, having a tendency to circumferentially rotate the implant in the acetabulum, and tilting shear, with a tendency to tangentially rotate the implant out of the acetabulum.

The FE analyses were performed using the MARC/MENTAT FEM and pre- and postprocessing codes (MARC Analysis Corporation, Palo Alto, CA, USA) running on the EX-60 mainframe computer (Hitachi Data Systems, Bells Hill, Bucks., U.K.) of the University of Nijmegen.

Results

The materials particularly affected by the design characteristics of the cup are the cup itself, the cement mantle (if present), the subchondral bone and the trabecular bone in the acetabular wall. The overall load transfer across the pelvic bone, which takes place predominantly in the cortical shell, is hardly affected. The stress distributions in the cortical shell show hardly any difference between the cases considered. This is illustrated in Figure 2, where the Von Mises stresses are shown for a thin cementless full-polyethylene cup and a cemented metal-backed cup with a thick liner.

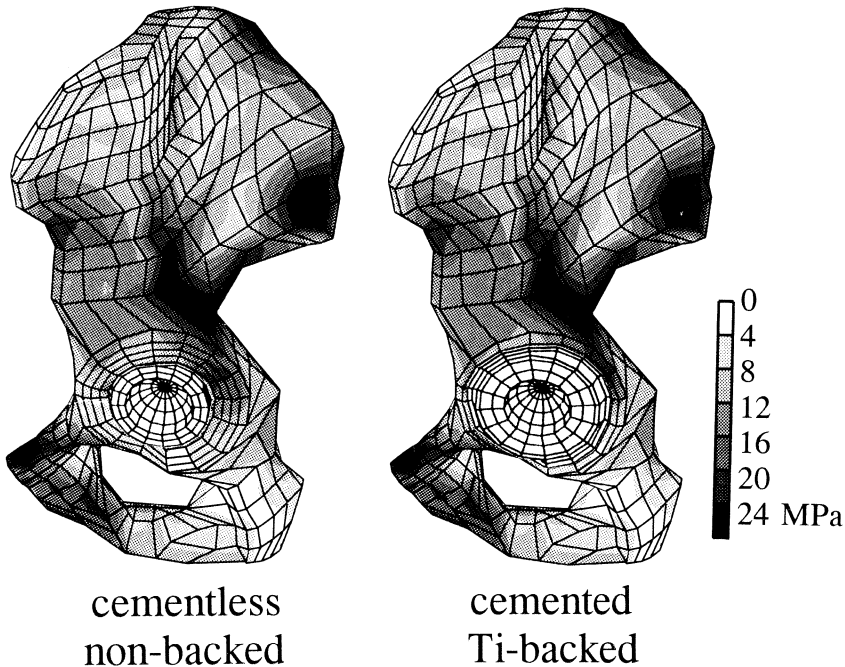


Fig. 2: Von Mises stresses in the cortical shell of a bone implanted with a thin cementless full-polyethylene cup (model 1; left) and a bone with a cemented Ti-backed cup with a thick liner (model 8; right).

These two cases are the two most extreme in terms of stiffness of the implant configuration which were considered in the present analyses. This means that for further evaluation of the different design characteristics, only the immediate vicinity of the acetabulum need to be examined.

Cementless versus cemented

The stress distributions in the cup and surrounding bone of both cementless and cemented cups strongly depend on whether the cups are metal-backed or not. The Von Mises stress peaks in the polyethylene of cementless cups during the load case considered (one-legged stance), for instance, range from 8.1 MPa for metal-backed cups with a thick liner to 13.8 MPa for thin full-polyethylene cups. For cemented cups, these values are 7.3 MPa and 11.0 MPa, respectively. For full-polyethylene cups, the cement mantle acts as a reinforcement for the cup itself. The deformation of the polyethylene reduces, which decreases the stresses with about 20 percent. At the cement/bone interface, cemented cups show lower compressive interface stresses than the cementless cups at the implant/bone interface, but the tensile interface stresses and the interface shear stresses are higher. For metal-backed cups, the reinforcement function of the cement is taken over by the metal backing. Although the stresses in the polyethylene liner of metal-backed cups are also reduced when cement is used, these reductions are less than for non-backed cups.

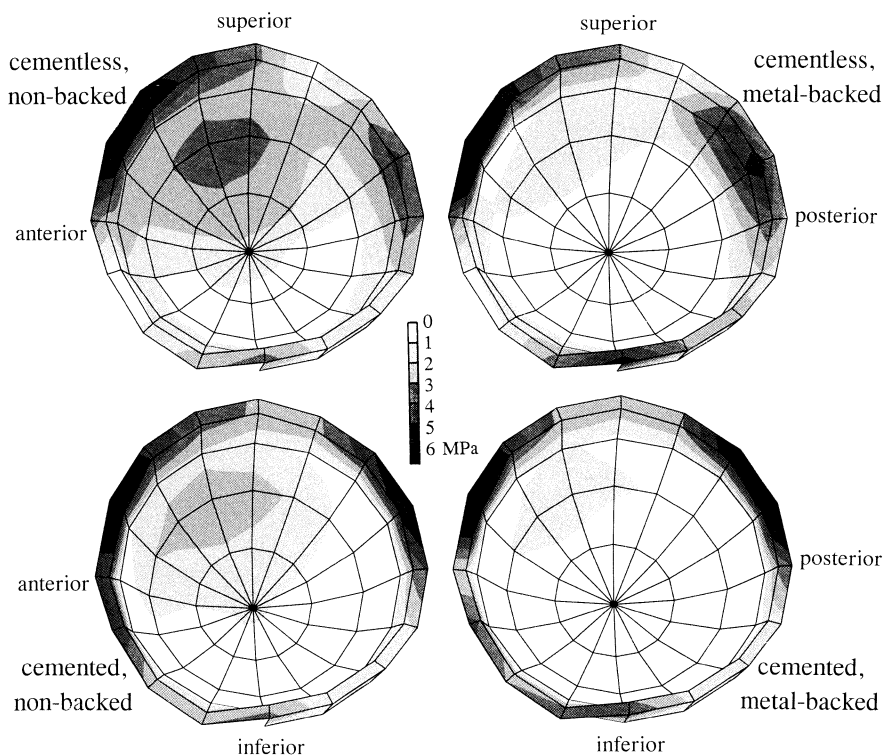


Fig. 3: Von Mises stresses in the subchondral bone layer for cementless full-polyethylene (top left) and Ti-backed cups (top right), and cemented full-polyethylene (bottom left) and Ti-backed cups (bottom right).

The addition of acrylic cement causes the stresses in the subchondral bone to be concentrated in the periphery of the acetabulum. This happens for metal-backed and non-backed cups alike, which is illustrated in Figure 3.

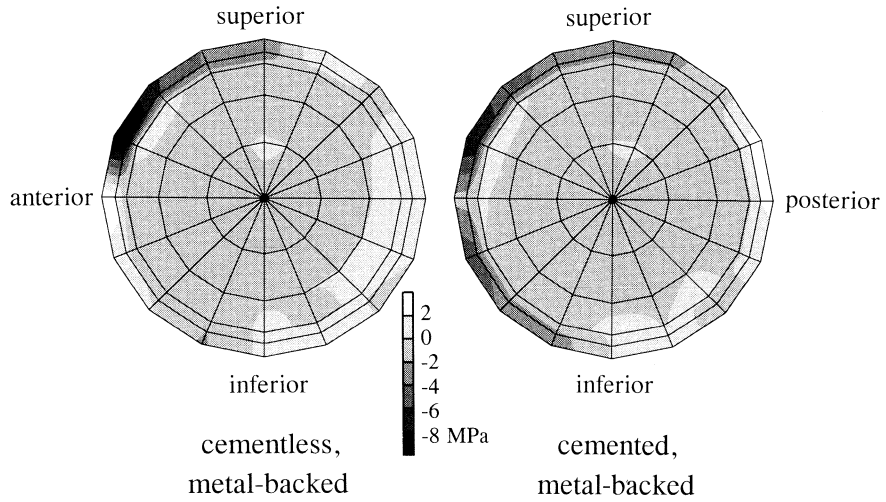


Fig. 4: Normal stresses at the prosthesis/bone interface for cementless and cemented Ti-backed cups.

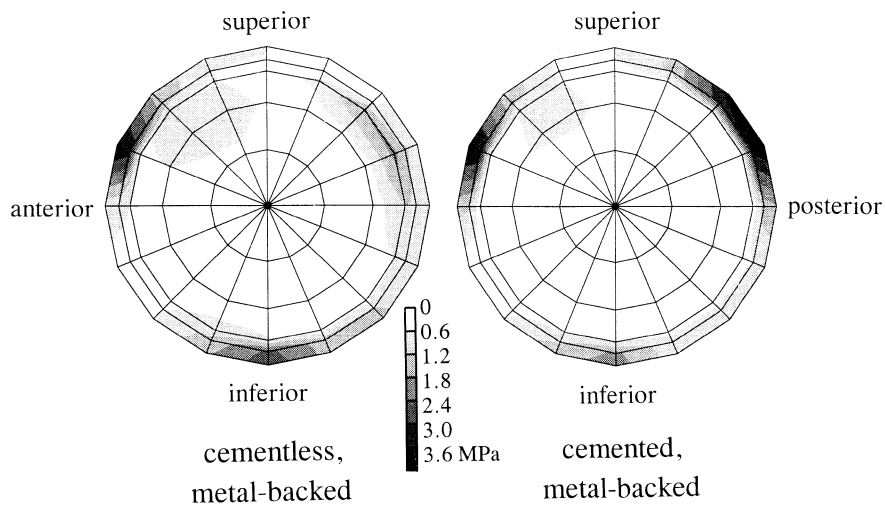


Fig. 5: Resultant shear stresses at the prosthesis/bone interface for cementless and cemented Ti-backed cups.

For cementless cups the maximal stresses in the subchondral bone occur at the anterosuperior edge. For cemented cups stress concentrations also develop at the posterosuperior edge. For metal-backed cups this shift of the stresses towards

posterior results in a decrease of the maximal stress in the subchondral bone by 20 percent. At the cement/bone interface, a 40 percent reduction of the peak values of the interface normal stresses (both compressive and tensile) and a 20 percent increase of the peak values of the interface shear stresses occur relative to a cementless metal-backed design. Figure 4 shows the distribution of the normal component of the interface stresses.

These stresses are mostly compressive, meaning that the implant configuration is pushed into the acetabulum. At the posterior edge an area of tensile stresses is found. This area is smaller in the cemented cases, but the stress values are higher. The distribution of the shear component of the interface stresses is shown in Figure 5. Actually, the vector sums of the two individual shear stress components (torsional and tilting) are taken. Shear stresses are mainly focussed around the edges. In the cemented cases, they become even more concentrated, especially in the postero-superior region.

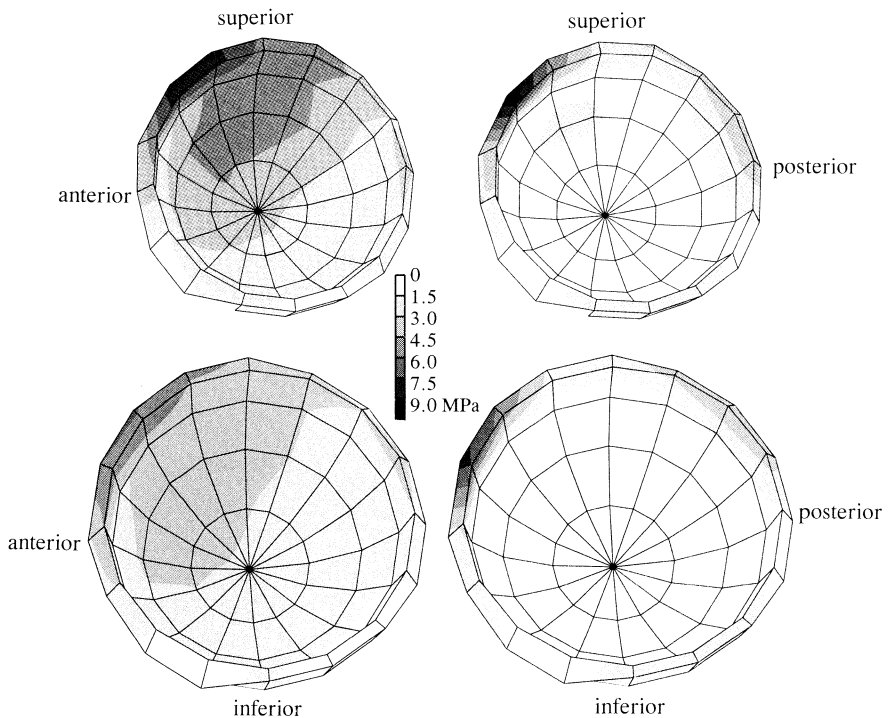


Fig. 6: Von Mises cement stresses for a full-polyethylene cup with a thin liner (top left), a full-polyethylene cup with a thick liner (bottom left), a Ti-backed cup with a thin liner (top right), and a Ti-backed cup with a thick liner (bottom right).

Full-polyethylene versus metal-backed

Metal backing greatly influences load transfer in the acetabular area. First of all, it restricts deformations of the polyethylene, leading to stress reductions of up to 40 percent. Because a metal-backed cup is so stiff relative to the materials it is contained in (bone and cement), it acts as a rigid body and stresses are mostly transferred along the edge of the acetabulum. Figure 6 shows the Von Mises stress distributions in the cement mantle for the models 5 to 8. With the hip-joint force directed towards the anterosuperior quadrant of the acetabulum, the highest stresses are found in this region for both non-backed and metal-backed cases. However, in the latter case an entirely different load transfer is generated. The dome of the cement mantle remains virtually unloaded, and the stresses become concentrated around the edge. For the cementless cases a similar situation occurs in the subchondral bone layer, leading to stress shielding of the bone deeper in the acetabulum. Due to these stress concentrations around the acetabular edge, the interface stresses here are also increased locally. Especially for cementless metal-backed cups, the shear stresses at the implant/bone interface are three to four times higher than the non-backed cases.

Thickness of the polyethylene liner

Increasing the thickness of the polyethylene from 6 mm to 10 mm results in reduced stress peaks in all materials. For the polyethylene itself these reductions are about 25 percent for non-backed cups and 10 percent for metal-backed cups. Figure 7 shows the Von Mises stress distributions in the polyethylene for the non-backed

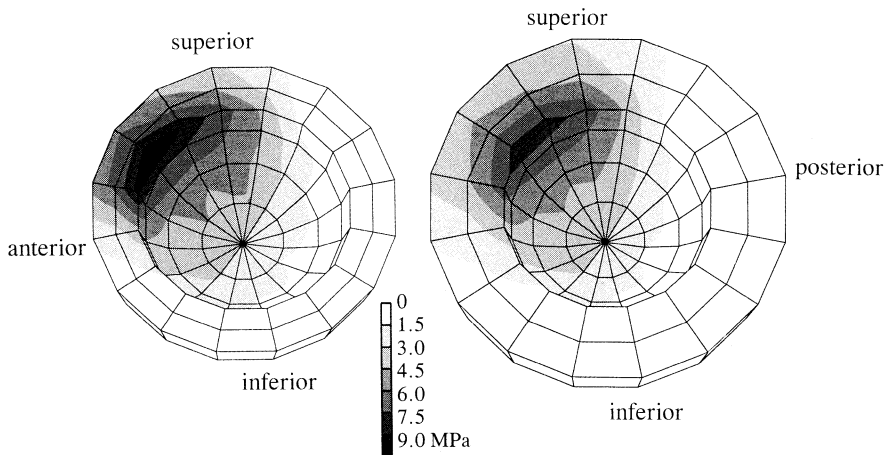


Fig. 7: Von Mises stresses in the polyethylene cup for a full-polyethylene cup with a thin liner (left) and a full-polyethylene cup with a thick liner (right).

cemented cups. In the deeper areas the same stress patterns are found for both the thin and the thick cup. At the anterosuperior edge, stresses are considerably higher

for the thinner cup. For the cementless and the metal-backed cases, similar results were found. The stress levels in the subchondral and the underlying trabecular bone decrease up to 30 percent when a 10 mm liner is placed instead of a 6 mm one, but unlike the changes due to cementing and metal backing, the stress distributions remain qualitatively similar. The interface stresses between implant and bone are also lower for a thicker liner. Only for cemented full-polyethylene cups the interface shear stresses between cement mantle and cup increase when a thicker cup is used.

Overall, the highest stresses in the polyethylene are found in thin, cementless, non-backed cups. The highest cement stresses are generated by thin metal-backed cups, and these also cause the highest interface stresses between implant and cement. The highest normal stresses at the bone interface (both tensile and compressive) are generated by cementless metal-backed cups with a thin liner. The highest shear stresses at this interface occur for cemented metal-backed cups with a thin liner. An overview of the peak values in the various stress components is given in Table 3.

	cementless				cemented			
	non-backed		Ti-backed		non-backed		Ti-backed	
	6 mm PE	10 mm PE	6 mm PE	10 mm PE	6 mm PE	10 mm PE	6 mm PE	10 mm PE
Von Mises stress cup	13.8	10.4	9.3	8.1	11.0	8.5	8.0	7.3
normal stress head/cup	-10.2	-7.6	-7.0	-5.9	-8.3	-6.4	-6.2	-5.2
normal stress cup/cement (tens.)	-	-	-	-	0.5	0.5	1.0	1.0
normal stress cup/cement (comp.)	-	-	-	-	-6.9	-5.2	-9.4	-6.3
shear stress cup/cement	-	-	-	-	1.1	1.4	4.3	3.8
Von Mises stress cement	-	-	-	-	8.5	6.1	10.4	8.1
normal stress implant/bone (tens.)	2.5	1.2	4.3	2.7	3.3	3.2	2.8	2.7
normal stress implant/bone (comp.)	-8.1	-6.1	-12.0	-8.4	-7.0	-4.6	-8.2	-5.1
shear stress implant/bone	1.2	1.0	3.7	3.5	3.4	2.8	4.3	3.7

Table 3: Peak values (in MPa) of various stress components in the cup, the cement mantle and at their respective interfaces.

Discussion

This study deals with variations in the load transfer across the pelvic bone induced by different designs of acetabular cups. Using three-dimensional finite element models, the influences of a cement mantle, metal backing and polyethylene thickness were investigated. These anatomic models have been experimentally validated and were seen to be capable to describe the mechanics of a reconstructed bone realistically (Dalstra *et al.*, 1992). Because of the comparative nature of the present analyses,

we only considered one load case, representing the one-legged stance in gait. This particular phase was chosen, because previous analyses had shown that in this case the highest stresses in the acetabular region occur (Dalstra and Huiskes, 1992). The interfaces between the various materials were assumed to be fully bonded. This may not always be realistic, but in this way we get an impression of how the load transfer from cup to bone takes place in the idealized case.

It was found that the different types of cups considered do affect the stress distributions in the subchondral and underlying trabecular bone, while the stresses in the cortical shell are virtually independent of the type of implant. Strain-gage experiments by Finlay *et al.* (1986) confirm this. They showed that, unless the subchondral bone layer was removed, pelvic bones implanted with metal-backed or non-backed cups displayed no major changes in the cortical stresses. With their three-dimensional finite element model, Oonishi *et al.* (1983) also found only minimal changes in overall load transfer across the pelvic bone before and after reconstruction of the acetabulum with a ceramic cup. This implies that the influences of the different design features remain restricted to the immediate vicinity of the acetabulum.

The stresses in the polyethylene strongly depend on the stiffness of the entire implant configuration. In a thin, cementless, full-polyethylene cup the maximal stresses are almost twice as high as in the thick liner of a cemented, metal-backed one. This is caused by the larger deformations a more flexible cup undergoes when it is compressed between the head of the femoral stem and the acetabulum, resulting in higher contact pressures between the head of the femoral stem and the polyethylene. It is therefore likely that polyethylene wear will be less of a problem for stiffer cups, although no direct relationship between the amount of wear and the magnitude of polyethylene stresses has been reported as yet.

In general, a stiff cup is less beneficial for the stresses in the bone. When a stiff cup is used, stress transfer tends to shift from the acetabular dome towards the superior acetabular wall. Consequently, this leads to higher stresses in this area while in the deeper region of the acetabulum stress shielding occurs. The stiffer the cup, the more prominent this phenomenon is. Obviously, the higher stresses are more likely to cause mechanical failure of the materials and their interfaces, but this stress shielding mechanism is also a serious matter. By the process of adaptive bone remodeling, it could eventually cause local resorption of the bone behind the cup. It is interesting that a number of cases of focal osteolysis have been reported in combination with metal-backed cups (Santavirta *et al.*, 1990; Pierson and Harris, 1993). Although the authors blamed polyethylene wear particles as its primary cause, it is remarkable that the osteolytic areas developed behind the cup rather than at the acetabular wall. The case study by Pierson and Harris (1993) answers perfectly to how the bone is expected to remodel, given the stress distributions for cemented metal-backed cups: extensive osteolysis behind the cup, while the bone/cement interface around the edge was still intact. In this particular case the cup showed no sign of migration, but the phenomenon itself does raise concern.

Of the three variations that were evaluated in this study, the presence of a cement mantle had the least influence on the stress levels in the polyethylene. With a Young's modulus of 2.3 GPa, acrylic cement approximates the stiffness of the subchondral bone plate (values for the Young's modulus of subchondral bone, used in the model, go up to 2.2 GPa). Because in the analyses fully bonded interfaces were assumed, the cement mantle in the models can be considered as mechanically equivalent to a thicker subchondral layer. In reality, however, the interfaces may debond in the course of time.

A definite choice between cementless or cemented fixation for acetabular cups can not be made on the basis of this study alone. With respect to the stresses in the polyethylene, cemented cups are to be preferred. Interface stresses between bone and implant are also generally higher for cementless cups. Actual failure of the interface, however, depends on its strength. The large variety of fixation techniques used for cementless cups (e.g. porous-coated, hydroxyapatite-coated, threaded cups, fixation with pegs or screws) also causes variety in the strength of the implant/bone interfaces. Experimental data on the strengths of these different connections are required to judge whether these increased interface stresses are indeed a matter of concern.

Metal backing was found to be the most influential of the three design concepts that were studied. Both for cemented and cementless cups, metal backing resulted in considerable stress reductions in the polyethylene. As described above, this may imply less wear of the polyethylene, but on the other hand fretting between the backing and the liner is also considered an additional source of polyethylene wear particles. The mechanical advantage of metal backing for cemented cups which was claimed in early finite element studies (Carter *et al.*, 1982; Pedersen *et al.*, 1982), could not be confirmed in this study. The present analyses predict higher maximal cement stresses when a metal backing is present, as was also found in an earlier study (Dalstra and Huiskes, 1991) This also enlarges the risk for cement failure. In the subchondral bone maximal stresses were also found to increase. For cementless cups, the addition of metal backing almost doubles the peak values of the stresses there. In fact, the highest interface stresses between implant and bone are found in the case of cementless metal-backed cups. However, just as for the cemented versus the cementless cups, this does not necessarily mean that this particular interface has a higher chance of disintegration; this depends on the actual strength of the interface, which is no doubt higher for a metal/bone connection than for a polyethylene/bone connection. For cemented cups metal backing was also found to increase stresses at the bone interface. Particularly the high shear stresses endanger the integrity of the bone/cement interface. Schmalzried *et al.* (1992) found a characteristically developing front of bone resorption and membrane forming around cemented cups, starting at the intraarticular margin and from there progressing towards the dome of the cup. Micro-morphology and histologic analysis revealed that this process is fueled by polyethylene wear particles. It is quite possible, that the onset of this is caused by mechanical failure and thus creating a route for the wear debris to enter the interface.

Combined with the aforementioned possibility of focal osteolysis developing behind the cup, this will certainly have contributed to the worse clinical performance of the metal-backed cups in the study described by Ritter *et al.* (1990). They found that in a well-matched series of full-polyethylene and metal-backed cups the latter had a rate of loosening twice as high as the former.

This leads to the conclusion that a metal backing with a uniform thickness is not a very good option. Perhaps non-uniform backings (Huiskes *et al.*, 1990) or partial backing to locally reinforce the cup may prove to be more successful.

A thick polyethylene liner is mechanically favorable. In reality, however, there is not much room for variation. On the one hand, there is a restriction on the articular side. A standard diameter of the femoral head and the size of the patient's acetabulum restrict the choice of the cup's thickness. To avoid high stresses in the polyethylene very thin cups should be avoided. A smaller sized femoral head could also be an option to gain polyethylene thickness, but this also leads to higher stresses in the polyethylene (Bartel *et al.*, 1986; Hoeltzel *et al.*, 1989). On the other hand, there is a restriction on the bone side. The subchondral bone plate should be retained, because removal would mean a substantial loss of structural stiffness of the whole pelvic bone and increases in all stresses.

In summary, the mechanical requirements for acetabular cups are subject to incompatible design goals. Geometrically a design is bounded by retainment of the subchondral bone plate on the one side, and by an adequately large femoral-head diameter on the other. From the viewpoint of wear-particle generation it requires a minimal number of interfaces, hence a minimal number of separate components. To avoid excessive polyethylene stresses the cup should be adequately stiff; to avoid excessive interface stresses and stress shielding of trabecular bone it should be adequately flexible. There is no obvious escape from these dilemmas with the materials presently available. Certainly design optimization methods could be applied to find the optimal stiffness configuration (Kuiper, 1993). But this also requires more realistic data on the interface strength of the various materials.

References

- Bartel, D.L., Bicknell, V.L., Wright, T.M. (1986) The effect of conformity, thickness, and material on stresses in ultra-high molecular weight components for total joint replacement. *J. Bone Joint Surg.* **68-A**, 1041-1051.
- Bergmann, G., Graichen, F., Rohlmann, A. (1990) Instrumentation of a hip joint prosthesis. In: *Implantable telemetry in orthopaedics*. Bergmann, Graichen, Rohlmann (eds.), Freie Universität Berlin, pp. 35-63.
- Carter, D.R., Vasu, R., Harris, W.H. (1982) Stress distributions in the acetabular region - II. Effects of cement thickness and metal backing of the total hip acetabular component. *J. Biomech.*, **15**, 165-170.
- Crowninshield, R.D., Brand, R.A. (1981) A physiologically based criterion of muscle force prediction in locomotion. *J. Biomech.*, **14**, 793-801.
- Dalstra, M., Huiskes, R. (1991) The influence of metal backing in cemented cups. *Trans. Orthop. Res. Soc.*, **16**, 272.
- Dalstra, M., Huiskes, R. (1992) Load-transfer in pelvic cortical bone. *Proc. Europ. Soc. Biomech.*, **8**, 60.

- Dalstra, M., Huiskes, R., van Erning, L. (1992) Development and validation of a pelvic finite element model. *J. Biomech. Eng.*, accepted.
- Dostal, W.F., Andrews, J.G. (1981) A three-dimensional biomechanical model of hip musculature. *J. Biomech.*, **14**, 802-812.
- Finlay, J.B., Bourne, R.B., Landsberg, R.P.D., Andreae, P. (1986) Pelvic stresses in vitro - II. a study of the efficacy of metal-backed acetabular prostheses. *J. Biomech.*, **19**, 715-725.
- Harris, W.H. (1971) A new total hip implant. *Clin. Orthop.*, **81**, 105-113.
- Hoeltzel, D.A., Walt, M.J., Kyle, R.F., Simon, F.D. (1989) The effects of femoral head size on the deformation of ultrahigh molecular weight polyethylene acetabular cups. *J. Biomech.*, **22**, 1163-1173.
- Huiskes, R., van der Venne, R., Spierings, P.T.J. (1990) Numerical shape optimization applied to cemented acetabular cup design in THA. *Trans. Orthop. Res. Soc.*, **15**, 255.
- Kelley, S.S., Johnston, R.C. (1992) Debris from cobalt-chrome cable may cause acetabular loosening. *Clin. Orthop. Rel. Res.*, **285**, 140-146.
- Kuiper, J.H. (1993) *Numerical optimization of artificial hip joint designs.*, dissertation, University of Nijmegen, the Netherlands.
- Mulroy, R.D., Harris, W.H. (1990) The effect of improved cementing techniques on component loosening in total hip replacement. *J. Bone Joint Surg.*, **72-B**, 757-760.
- Oonishi, H., Isha, H., Hasegawa, T. (1983) Mechanical analysis of the human pelvis and its application to the articular hip joint - by means of the three dimensional finite element method. *J. Biomech.*, **16**, 427-444.
- Pedersen, D.R., Crowninshield, R.D., Brand, R.A., Johnston, R.C. (1982) An axisymmetric model of acetabular components in total hip arthroplasty. *J. Biomech.*, **15**, 305-315.
- Pierson, J.L., Harris, W.H. (1993) Extensive osteolysis behind an acetabular component that was well fixed with cement - a case report. *J. Bone Joint Surg.*, **75-A**, 268-271.
- Ritter, M.A., Keating, E.M., Faris, Ph.M., Brugo, G. (1990) Metal-backed acetabular cups in total hip arthroplasty. *J. Bone Joint Surg.*, **72-A**, 672-677.
- Santavirta, S., Hoikka, V., Eskola, A., Kontinen, Y.T., Paavilainen, T., Tallroth, K. (1990) Aggressive granulomatous lesions in cementless total hip arthroplasty. *J. Bone Joint Surg.*, **72-B**, 980-984.
- Schmalzried, Th.P., Kwong, L.M., Jasty, M., Sedlacek, R.C., Haire, T.C., O'Connor, D.O., Bragdon, Ch.R., Kabo, J.M., Malcolm, A.J., Path, M.R.C., Harris, W.H. (1992) The mechanism of loosening of cemented acetabular components in total hip arthroplasty. *Clin. Orthop. Rel. Res.*, **274**, 60-78.
- Sutherland, Ch.J., Wilde, A.H., Borden, L.S., Marks, K.E. (1982) A ten-year follow-up of one hundred consecutive Müller curved-stem total hip-replacement arthroplasties. *J. Bone Joint Surg.*, **64-A**, 970-982.
- Wilson-MacDonald, J., Morscher, E., Masar, Z. (1990) Cementless uncoated polyethylene acetabular components in total hip replacement. *J. Bone Joint Surg.*, **72-B**, 423-430.
- Wroblewski, B.M. (1986) 15-21-year results of the Charnley low-friction arthroplasty. *Clin. Orthop. Rel. Res.*, **211**, 30-35.

Towards a mechanically optimized acetabular cup?

M. Dalstra, J.H. Kuiper, R. Huiskes

Biomechanics Section, Institute of Orthopaedics, University of Nijmegen

Abstract: *Metal backing has become widely used in acetabular cup design. Its function is controversial though: it decreases stresses in the polyethylene, while at the same time it increases stresses in the cement mantle (if present), the underlying bone and at the interfaces at the periphery, and causes stress shielding in the bone in the acetabular dome region. In this study a numerical optimization method is employed in combination with the finite element method to find possible solutions for a non-uniform metal backing, which would to keep the stresses in the polyethylene low, while generating smooth stress distributions in the cement and underlying bone as well.*

The analyses predict that a backing, answering these requirements, should only have a relatively high stiffness in the anterosuperior periphery. At other locations, it should be so flexible that the backing might as well be absent. In this way, the large deformations occurring at the edge of the polyethylene are restricted by the backing, while deeper in the acetabulum load transfer from cup to cement and underlying bone remains possible.

Introduction

One of the most prominent design features of acetabular prostheses is metal backing. It is seen in most cementless cup designs and also in a number of cemented cup types. For cementless cups, metal backing is primarily used because the combination of metal and bone provides better fixation than polyethylene and bone. This fixation can be achieved in a number of ways, e.g. by providing the backing with a hydroxyapatite or a porous coating or screw thread. Yet, because of its high stiffness, metal backing was also believed to provide a better load transfer across the reconstructed acetabulum by reducing peak stresses in the bone behind the cup. And due to this alleged stress-reducing capability, it is also used in some cemented cup designs.

The concept of using a metal backing for acetabular implants was introduced by Harris (1971). The initial concept had nothing to do with pelvic mechanics, but was a solution to a practical problem: a metal backing with a snap-fit polyethylene insert would make a revision of this insert, once it was worn, much easier. The use of metal backing was boosted in the eighties by the results of finite element analyses, which showed that a metal backing would be mechanically favorable as well. Stiffening of the implant would result in a reduction of the stress peaks in the cup, the cement mantle and the underlying bone (Carter *et al.*, 1982, Pedersen *et al.*, 1982). Clinical studies, however, have shown lately that the concept of metal backing is not as favorable as one would expect from those finite element studies. Ritter *et al.* (1990) reported on a well matched, retrospective study of both non-backed and metal-backed cups and found that the results of metal-backed cups were inferior where it concerned radiolucency, loosening and revision. They explicitly advised against the use of metal-backing.

Recent finite element studies with more realistic models relative to the representation of the three-dimensional acetabular geometry, boundary conditions, loading and bone properties, however, provided very different information than the earlier simplified finite element studies (Dalstra and Huiskes, 1990; Dalstra *et al.*, 1993). It was shown that because of the three-dimensional character of the load-transfer mechanism across the pelvic bone, the effect of a metal backing is different from that found in the aforementioned studies. In earlier analyses, bending of the acetabulum was the predominant deformation mode, which is restricted by a stiff cup, thus reducing the stresses. The later three-dimensional analyses show that this bending mode plays a lesser role, and the implant reconstruction is in fact pushed against the superior acetabular wall. From here the greater part of the load is transferred through the lateral cortical shell of the iliac bone. A metal-backed cup behaves almost like a rigid body and thus directly transfers the load onto this lateral cortex, which results in a concentration of the load transfer along the periphery of the acetabular rim. Here the stresses in the cement mantle (if present) and the subchondral bone are actually higher than for a non-backed cup. The interface stresses between cup, cement and bone in this region are higher as well, which implies an increased risk for loosening of the implant. Furthermore, the bone deeper in the acetabulum becomes stress-shielded. According to adaptive bone remodeling theory, disuse will lead to bone

resorption, so this local stress shielding may be associated with the process of focal osteolysis, which is reported particularly to occur behind metal-backed cups (Santavirta *et al.*, 1990; Pierson and Harris, 1993). So, the mechanical advantage of a metal backing lies solely in a reduction of the stresses in the polyethylene insert. Huiskes *et al.* (1990) showed that instead of the traditional backing with a uniform thickness, interface stresses would be reduced with a backing which is thicker near its dome and thinner near the edge. However, this finding was obtained from analyses with an axisymmetric model and we now know that these kind of models are not very well suited to describe pelvic mechanics, so it might be recommendable to verify these findings with a more realistic model.

Recently, a technique has been developed to numerically optimize the material properties within a femoral stem with respect to the load transfer from prosthesis to the bone (Kuiper and Huiskes, 1992; Kuiper, 1993). With this technique, it was shown that for an uncemented femoral stem to have low interface stresses combined with a low degree of bone resorption, it should be stiff in the proximal region and decreasing in stiffness towards distally. It is the purpose of this study to implement this routine in a pelvic finite element model to find an optimal stiffness distribution for the backing of a cemented acetabular cup with the objective to avoid the inhomogeneous load transfer across the cement mantle which is seen to occur for traditional metal-backed cups. The results of these optimization studies may be translated into more practical designs.

Method

The finite element model used in this study is a three-dimensional mesh of a left pelvic bone with a hemispherically shaped acetabular prosthesis with an inner and outer diameter of respectively 28 and 48 mm. In positioning the prosthesis, a thin layer of subchondral bone is assumed to be still present. The total mesh consists of 1,506 elements. For the trabecular bone, the subchondral bone and the prosthesis 8-node brick elements are used, while for the cortical shell covering the entire pelvic bone, 4-node membrane elements are used instead. A frontal and a lateral of the mesh are given in Figure 1. The values for the Young's moduli of the individual elements representing pelvic trabecular and subchondral bone, as well as the local thickness of the cortical shell are based on values taken from dual-energy CT-scans (Dalstra *et al.*, 1992). Validation of the model had been done by simulating a loading experiment and comparing the numerically calculated stresses with the actual stresses calculated from strain-gage data (Dalstra *et al.*, 1992). The interfaces between

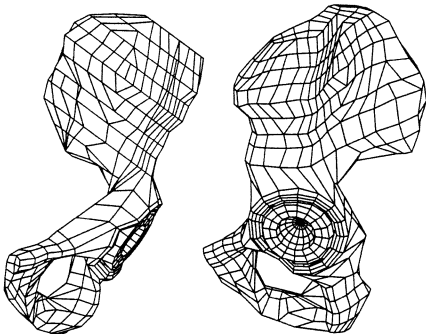


Fig. 1: Frontal and lateral view of the FE mesh.

implant and bone were assumed rigidly bonded. The loads applied in the model include the hip-joint force and 15 muscle forces. Actually, two load cases from a normal walking cycle are simulated: the beginning of the one-legged stance phase and the beginning of the swing phase.

Between the elements representing the cup and the elements representing the cement mantle a 2 mm thick layer of elements is located, which represents the backing which design characteristics (stiffness) are subject to optimization. Throughout this group of elements a grid of equally spaced points is defined and the Young's moduli at these points are the so-called design variables which are varied in the optimization process. The actual Young's modulus for an individual element in the backing is obtained by interpolating the values of the Young's moduli from the points in the grid. The upper and lower boundaries of the values of the design variables are set to 110 GPa and 0.7 GPa, respectively; these being the Young's moduli of titanium and polyethylene. This means that the two most extreme cases represent either a 2 mm thick titanium-alloy (TiAl6V4) backing or a 2 mm thicker full-polyethylene cup.

The optimization process was developed (Kuiper, 1993) as an interaction between two commercially available core routines: the actual optimization routine, in this case a sequential quadratic programming algorithm (NCONG; IMSL Math/Library, Houston, TX, USA 1987) and the finite element code (MARC; MARC Analysis Corporation, Palo Alto, CA, USA). A schematic representation of this interaction is shown in Figure 2. For a certain design, the finite element program not only calculates the stresses and strains, but also the adjoint stresses and strains. These quantities are used to calculate the objective function and its gradient relative to the design variables (Yang *et al.*, 1984; Haug *et al.*, 1986). The objective function and its gradient are returned to the optimization routine, which then determines the most effective adjustments to the design variables, and the adjusted model is again used as input for the finite element program. This loop continues until the optimal value of the objective function is reached; the accompanying distribution of the design variables then represents the optimized design.

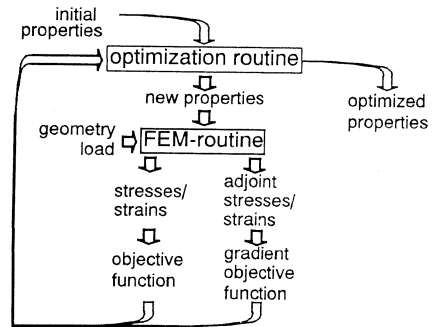


Fig. 2: Schematic representation of the interaction between the finite element program and the numerical optimization routine (adapted from Kuiper and Huiskes, 1992).

The objective function ($F(\mathbf{b})$) in the optimization process is given by:

$$F(\mathbf{b}) = C \sum_{i=1}^n (U_i(\mathbf{b}))^m \quad (1)$$

where:

- \mathbf{b} = vector of design variables; in this case the Young's moduli in the backing, $0.7 \text{ GPa} < b_j < 110 \text{ GPa}$
- C = scaling constant
- $U_i(\mathbf{b})$ = strain energy density in cement element i , depending on design variables \mathbf{b}
- m = peak value attenuation parameter.

The strain energy density itself is defined as:

$$U = \frac{1}{2} \boldsymbol{\sigma} \boldsymbol{\varepsilon} \tag{2}$$

where:

- $\boldsymbol{\sigma}$ = stress tensor
- $\boldsymbol{\varepsilon}$ = strain tensor.

So, the objective function represents the sum of the strain energy densities raised to the power m in all elements of the cement mantle. The exponent m amplifies the contribution of the peak values in the objective function.

To test the consistency of the solution of the optimization process, a number of parameter variations were performed. First, the density of the grid of design variables was increased step-wise from 4 by 4 to 6 by 6. Then the exponent m in eq. (1) was increased from 4 to 16. These variations are summarized in Table 1.

Case	exponent m (eq. 1)	number of design variables
A	4	16
B	4	25
C	4	36
D	16	36

Table 1: Overview of the peak value attenuation parameter (m) in the objective function and the number of design variables for the cases A, B, C and D.

In these analyses the starting value for the Young's moduli in the backing was 1.5 GPa. In the possible range of 0.7 to 110 GPa, this is rather low. An additional analysis with 110 GPa as starting value (representing a full metal backing) was performed to test the influence of the starting condition on the solution. Finally, four designs of titanium reinforcements for the acetabular cup were analyzed. Although the shapes of these reinforcements were derived from the results of the optimization analyses, their Young's moduli were not variable. The elements representing the backing were given a Young's modulus of either titanium or polyethylene. These four designs include a ring-shaped reinforcement around the entire periphery of the cup,

two quadrant-shaped backings (one covering the anterosuperior quadrant, the other the superior quadrant) and a 'tripod'-shaped reinforcement, covering the superior edge of the cup and from there extending from three sides to the dome of the cup. The shapes of these reinforcements are shown in Figure 3.

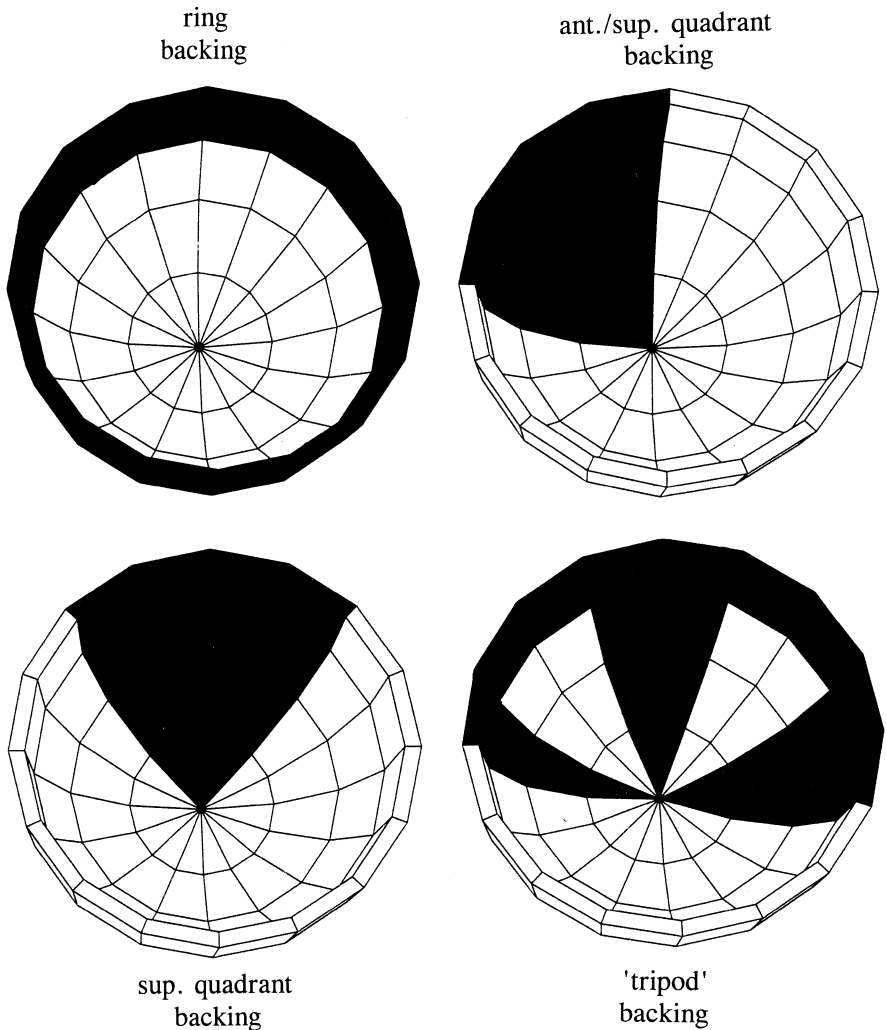


Fig. 3: Four designs for metal reinforcement of acetabular cups, derived from the optimization results.

Results

The problem with a traditional metal-backed cup is the inhomogeneous load transfer it generates in the cement mantle and the underlying subchondral bone.

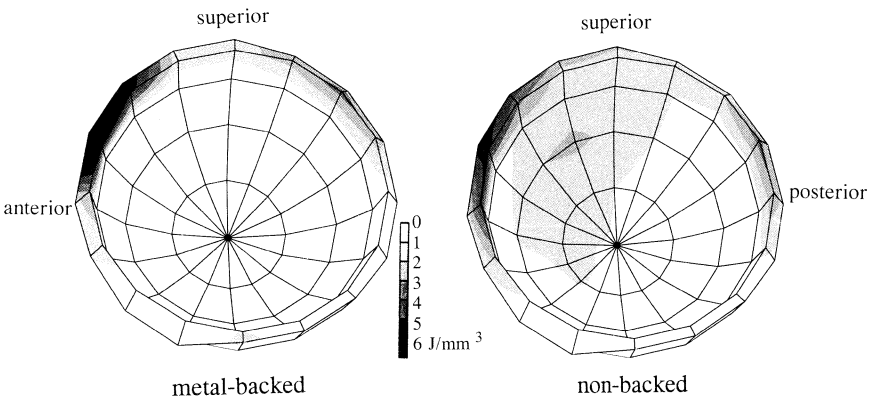


Fig. 4: Strain energy density distribution in the cement mantle of the model with a traditional metal backing (left) and the non-backed case (right).

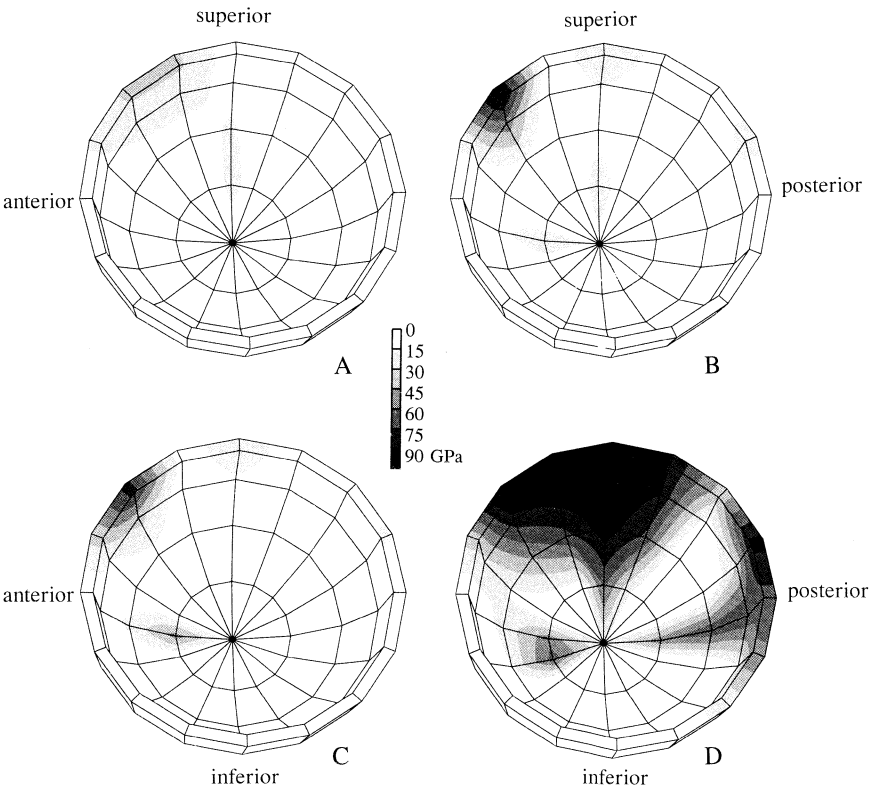


Fig. 5: Optimal distributions of the Young's modulus in the backing for the cases A to D (Table 1).

Relative to a non-backed cup, stress transfer from cup to bone intensifies predominantly along the superior acetabular rim, which leads to increased stresses in this area, while the material in the dome-region of the acetabulum becomes stress-shielded. This also applies to the strain energy density, the quantity which determines the objective function considered in the optimization analyses. Figure 4 shows the strain energy density distribution in the cement mantle for both a traditional metal-backed cup and a non-backed cup during one-legged stance. The optimization analyses show that in order to minimize the objective function considered, the greater part of the backing should have a low Young's modulus, in fact the lowest value possible. Only a small area with high stiffness is required at the anterosuperior edge. As can be seen in Figure 5, increasing the number of design variables (the cases A to C from Table 1) enables a more detailed distribution of the Young's moduli in this particular area. However, there is not much difference between a 5 by 5 grid (case B) and a 6 by 6 grid (case C). Also, when looking at the distributions of the strain energy density in the cement mantle, almost the same patterns are generated in the

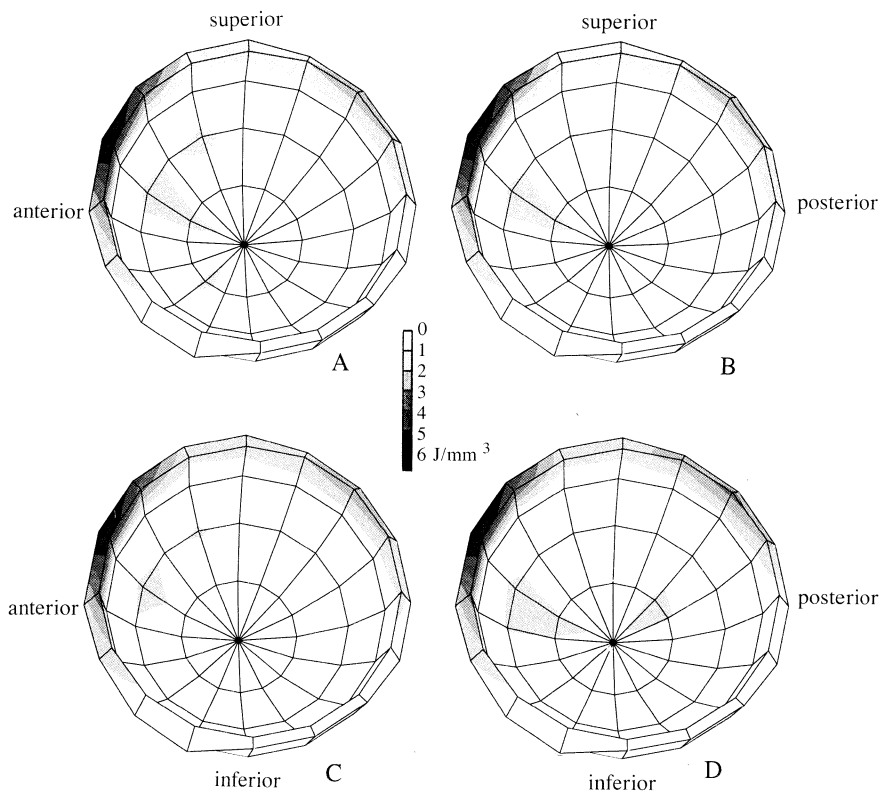


Fig. 6: Distributions of the strain energy density in the cement mantle in case of optimized backings for the cases A to D (Table 1).

cases A to C (Figure 6). This is an indication that a grid of 6 by 6 equally spaced points should be sufficiently refined for the current problem. Relative to the strain energy densities in the cement mantle of a traditional metal-backed cup, peak values have decreased by 40 percent for the optimized backing, but there is still a considerable concentration at the anterosuperior edge. To emphasize the influence of these high values, the exponent m in the objective function was increased from 4 to 16. This results in an enlargement of the area of stiff material at the superior edge of the backing (Figure 5D). However, this has hardly any effect on the distribution of the strain energy densities (Figure 6D).

When instead of a low starting value for the Young's modulus in the backing, a high value is taken, the final solution is not the same. There are certain locations in the backing where the influences of the design variables on the objective function are only marginal and as a consequence the design variables at these locations will hardly change from their initial values. For the load case of one-legged stance, this happens at the posterosuperior quadrant. As illustrated in Figure 7, starting the optimization process with a high initial value results in a solution in which high-stiffness material is still present in this quadrant. In the anterosuperior quadrant, the stiffness distribution is similar to the one obtained with low starting values, however.

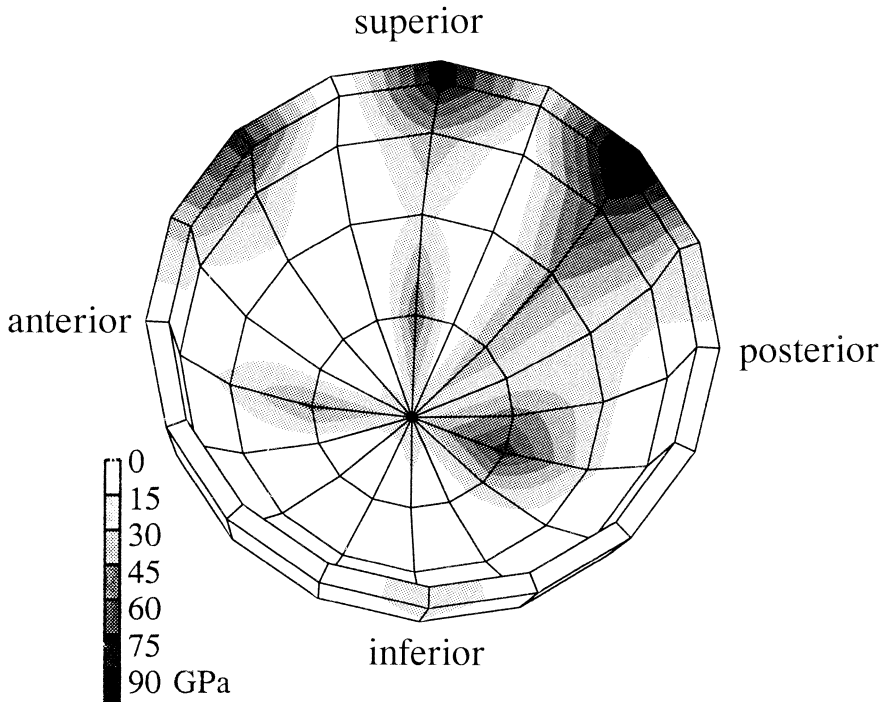


Fig. 7: Optimized distribution of the Young's modulus in the backing for case C with full Ti-backing as starting condition.

So far, loading in the analyses simulated one-legged stance. To see whether the outcome of the optimization changes when a different load case is considered, an additional optimization was performed with the optimal distribution of the Young's modulus presented in Figure 5C as a starting condition, while the load case applied simulates the beginning of the swing phase. The solution displays a slight increase of the stiffness in the dome area and at the posterior rim. The high-stiffness area at the anterosuperior rim remains unchanged (Figure 8).

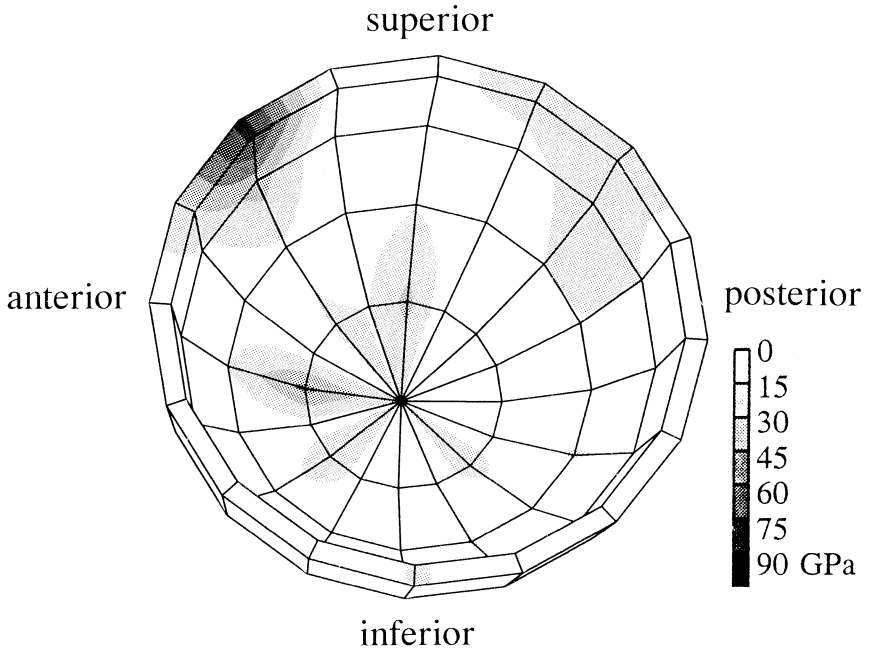


Fig. 8: Optimized distribution of the Young's modulus in the backing for case C for a load case simulating the swing phase during the walking cycle.

The optimizations have shown that in order to achieve minimal stressing of the cement mantle only a partial backing should be present, and as such it might be better to speak of a 'reinforcement' rather than a 'backing'. The four designs of such reinforcements presented in Figure 3 were based on the finding that at least at the anterosuperior rim high-stiffness material should be present. The stress transfer for each of these four designs strongly depends on the shape of the reinforcement. The material directly behind this reinforcement is stress-shielded. This is illustrated in Figure 9, which shows the distribution of the Von Mises stresses in the cement mantles of these four cases during one-legged stance.

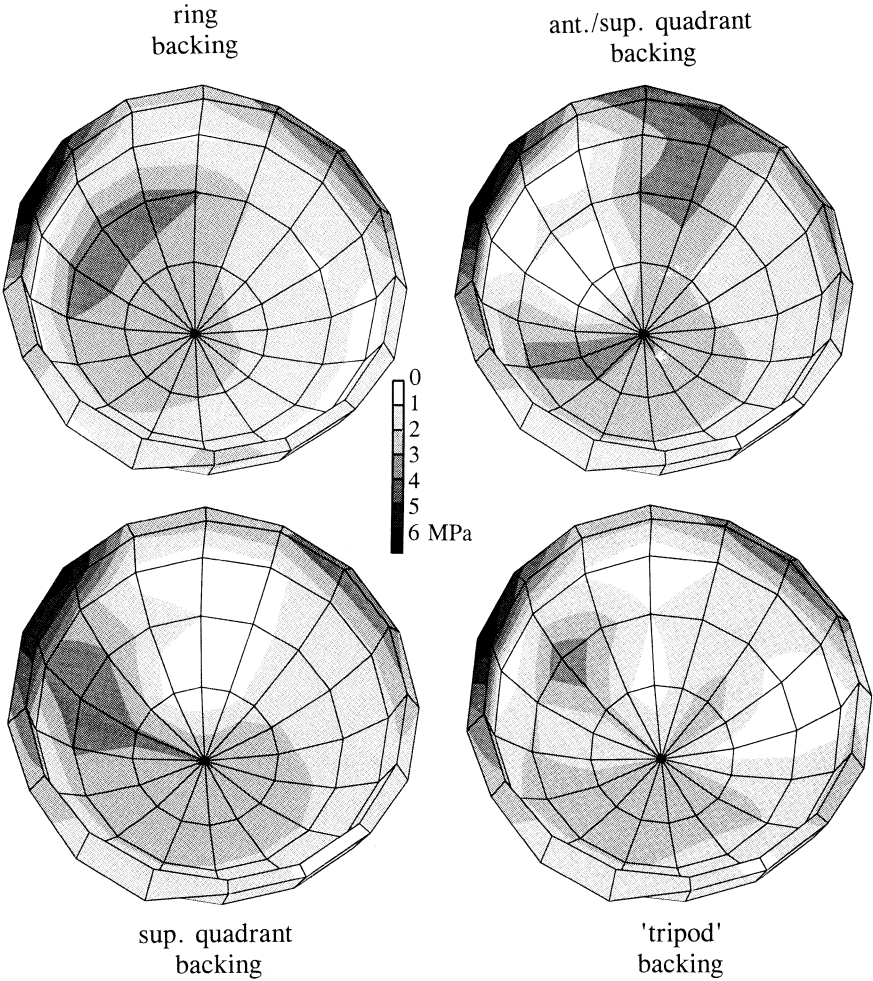


Fig. 9: Von Mises stresses in the cement mantle of the models with the four considered designs of cup reinforcement.

Compared to the stress distributions in the cement mantles of a full-titanium-backed cup, it can be seen that the deeper areas are now more loaded and the stress levels here are comparable to those of a non-backed cup. In Table 2, the stress peaks in both cement and polyethylene cup are summarized for the four designs, as well as a full-titanium-backed cup and a non-backed cup. For all four reinforcement designs, the maximal stresses in the cement mantle are decreased relative to the full-backed cup, but are still higher as the stress peak for the non-backed cup. The maximal stresses in the polyethylene cup are increased relative to the full-backed cup, but not as high as for the non-backed cup. This leveling of stresses is also observed for the

interface stresses between cup and cement, and cement and bone. For instance, the maximal tensile stress and the maximal shear stress at the cement/bone interface are 2.7 and 3.9 MPa for a full-backed cup and 3.2 and 3.0 MPa for a non-backed cup. For the four reinforcements, the maximal tensile stress varied between 2.8 and 3.0 MPa, while the maximal shear stress varies between 3.1 and 3.9.

backing	peak stress cement (MPa)	peak stress cup (MPa)
ring-shaped	7.4	8.2
ant./sup. quadrant	6.8	7.9
sup. quadrant	6.6	8.2
'tripod'	7.0	8.1
uniform backing	8.0	7.3
non-backed	6.1	8.5

Table 2: Von Mises stress peaks in the cement mantle and the cup for the four considered designs of cup reinforcement, the uniform metal backing and the non-backed case.

Discussion

In this study, a numerical optimization technique was applied to find a mechanically optimal design for the backing of acetabular cups. However, a single optimal design does not exist; it depends on the objective for optimization. For acetabular cups there are many possible, sometimes even contradictory objectives, and optimizing each one of these leads to a different solution. For example, it would be conceivable to minimize shear stresses at the cement/bone interface to reduce the risk of disruption of this interface, minimize tensile stresses in the cement mantle to reduce the risk of cracking of the cement or minimize stressing of the polyethylene cup with regard to wear. In this particular study, however, we wanted to reduce the high stress concentrations in the cement and subchondral bone at the superior edge of the acetabular wall, which are found with traditional metal-backed cups. If this can be achieved, the interface stresses between cup, cement and bone in this area will also become less concentrated and consequently reduce in magnitude.

Optimization was performed by varying the stiffness (Young's modulus) throughout the backing, rather than the shape of the backing. Although the latter approach would have yielded a more practical, ready-to-implement design, it requires remeshing of the finite element input for each increment of the numerical optimization process, which is rather cumbersome. Varying the Young's modulus of the backing does give an indication about the design concept, however. It shows where the backing should be stiff and where it should be flexible, and this can later be

translated into a more practical design.

The actual solutions predicted by the optimization analyses were dependent on the number of design variables and their initial values, the parameters in the objective function and external loading. However, all solutions showed the same characteristic distribution of Young's moduli throughout the backing: at most locations the moduli should be very low and only at the anterosuperior edge some high-modulus material should be present. In this way, the cup/backing configuration is both flexible enough to allow stress transfer near the dome of the cup and stiff enough to restrict large deformations of the cup at its anterosuperior edge due to the hip-joint force. This immediately brings us to the paradox of contradicting objectives which is encountered when trying to find an optimal backing: a cup with full metal backing incurs high peak stresses in the cement and bone, but has low stresses in the polyethylene, while a non-backed cup has a more evenly distributed stress pattern in the cement mantle, but high stresses in the cup itself. The coupling between these stresses in cup and cement is much more direct than between the magnitude of the interface stresses between femoral stem and bone and the amount of bone resorption, on which Kuiper (1993) based his optimization of the femoral stem, and therefore, the design space for a backing is more limited. This explains why the gains for an optimized backing are not so spectacular. Looking at Table 2, we see that the designs of reinforcements, which were based on the results of the optimizations do result in lower stresses in the cement mantle relative to the full backing. The actual reductions, however, are only marginal.

The present optimization analyses emphasize once more the difference between modeling the pelvic bone with a two-dimensional or axisymmetric model and a three-dimensional model. Also minimizing loading of the cement, Huiskes *et al.* (1990) found that an optimal backing should be thick at the dome and become thinner near the edges. This optimization was performed with an axisymmetric model. In these models bending of the acetabulum is the most prominent loading mode, and an increased thickness near the dome of the backing is then a logical solution, because it restricts bending. In the present three-dimensional pelvic model, this bending has shifted to the pubic bone and plays almost no role in the acetabulum itself. Instead loading of the acetabulum is predominantly determined by the acetabular cup being pushed against the superior acetabular wall. As a result, the optimized backing found in the present analyses turns out to be nearly the opposite of the backing proposed by Huiskes and co-workers.

What is the significance of the present results for the actual design of acetabular cups? Although in this study only cemented cups were considered, theoretically the results have validity for cementless cups as well, because the overall load transfer is not very much affected by the cement mantle (Dalstra *et al.*, 1993). The same high stress concentrations, which are seen at the superior edge of the cement mantle for cemented metal-backed cups are seen in the same region in the subchondral bone for cementless metal-backed cups. For cementless cups the objective for optimization would then be to reduce these high stresses in the subchondral bone instead of in the

cement mantle. We have seen that to achieve this, the metal backing as such should disappear and be replaced by a small reinforcement along the superior edge of the cup. This, however, might lead to practical problems. For normal metal backing, fretting of the polyethylene at sharp edges of the backing as a consequence of micro-motions of the liner relative to the backing is seen with growing concern as an additional source of wear particles. For a small partial reinforcement, a tight fixation to the liner is an even greater problem than for a full backing; so micro-motions between cup and reinforcement are not inconceivable. For cemented cups, it may therefore be more practical to realize superior stiffening of the implant by locally increasing the thickness of the polyethylene or thickening of the cement mantle. For cementless cups, the latter can obviously not be done. But in this case also a different problem is created when a reinforcement is used instead of a full backing. For cementless cups, it is often the metal backing which provides the basis for the fixation of the cup to the bone, as direct contact between polyethylene and bone is not considered to be favorable. And if loss of strength of the interface between cup and bone would be the result of using a reinforced cup instead of a fully backed cup, this might be worse than the occurrence of high stress peaks in the first place.

References

- Carter, D.R., Vasu, R., Harris, W.H. (1982) Stress distributions in the acetabular region - II. Effects of cement thickness and metal backing of the total hip acetabular component. *J. Biomech.*, **15**, 165-170.
- Dalstra, M., Huiskes, R., van Erning (1992) Development and validation of a pelvic finite element model. *J. Biomech. Eng.*, accepted.
- Dalstra, M., Bechtold, J.E., Kyle, R.F. (1993) Changes in pelvic load transfer due to variations in acetabular cup design. *Trans. Orthop. Res. Soc.*, **18**, 442.
- Harris, W.H. (1971) A new total hip implant. *Clin. Orthop.*, **81**, 105-113.
- Haug, E.J., Choi, K.K., Komkov, V. (1986) *Design sensitivity analysis of structural problems.*, New York, Academic Press.
- Huiskes, R., van der Venne, R., Spierings P.T.J. (1990) Numerical shape optimization applied to cemented acetabular-cup design in THA. *Trans. Orthop. Res. Soc.*, **15**, 255.
- Kuiper, J.H., Huiskes, R. (1992) Numerical optimization of hip-prosthetic material. In: *Recent advances in computer methods in biomechanics & biomedical engineering.*, eds. J. Middleton, G.N. Pande, K.R. Williams. Swansea, Books & Journals International Ltd., pp. 76-84.
- Kuiper, J.H. (1993) *Numerical optimization of artificial hip joint designs.*, dissertation, University of Nijmegen, the Netherlands.
- Pedersen, D.R., Crowninshield, R.D., Brand, R.A., Johnston, R.C. (1982) An axisymmetric model of acetabular components in total hip arthroplasty. *J. Biomech.*, **15**, 305-315.
- Pierson, J.L., Harris, W.H. (1993) Extensive osteolysis behind an acetabular component that was well fixed with cement - a case report. *J. Bone Joint Surg.*, **75-A**, 268-271.
- Ritter, M.A., Keating, E.M., Faris, Ph.M., Brugo, G. (1990) Metal-backed acetabular cups in total hip arthroplasty. *J. Bone Joint Surg.*, **72-A**, 672-677.
- Santavirta, S., Hoikka, V., Eskola, A., Konttinen, Y.T., Paavilainen, T., Tallroth, K. (1990) Aggressive granulomatous lesions in cementless total hip arthroplasty. *J. Bone Joint Surg.*, **72-B**, 980-984.
- Yang, R.J., Choi, K.K., Crowninshield, R.D., Brand, R.A. (1984) Design sensitivity analysis: a new method for implant design and a comparison with parametric finite element analysis. *J. Biomech.*, **17**, 849-854.

Summary and conclusion

Total hip arthroplasties have seen an enormous development over the last two decades. New insight brought forth by fundamental research and clinical feedback have led to improved implant designs and operative techniques. Yet, most attention was given to the femoral component. As a result, we now know that mechanical factors play an important role in the clinical performance of femoral prostheses and may even be decisive for the ultimate success or failure of a particular type of implant. For the acetabular component, such insights are less well developed and as a result no consensus exists with regard to which factors determine the success of a design. The studies described in this dissertation were designed to learn more about the basic mechanics of the pelvic bone and how this is affected after an acetabular reconstruction. Topics include the mechanical properties of pelvic trabecular bone, the load transfer and stress distributions in both normal and reconstructed pelvic bones, and the mechanical consequences of different designs of acetabular cups. In these studies, both experimental methods and computer simulations have been used, but the emphasis lies on the development and use of a realistic three-dimensional finite element model of the pelvic bone.

Summary of the Chapters I to VII

Apart from a thin cortical shell, the pelvic bone consists entirely of trabecular bone. Mechanical properties, such as stiffness and strength, of this type of bone are found in a wide range and depend on its location in the skeleton and its mechanical function. On the mechanical properties of pelvic trabecular bone, however, virtually no data existed. Therefore, in Chapter I the mechanical and textural properties of pelvic trabecular bone are studied. Dual Energy Quantitative Computer Tomography (DEQCT) reveals that the density of pelvic trabecular bone on the whole is relatively low. Highest densities were found in the superior part of the acetabular wall, but volume fractions are still well below 20 percent. The stiffness of the bone is largely dependent on the density. Consequently, the elastic moduli, measured in non-destructive tests for small cubic specimens, are also very low. For most specimens the Young's moduli do not exceed 100 MPa, while values of 2000 MPa are not exceptional for trabecular bone of femoral or tibial origin. Although not measured, this also implies that the strength of trabecular bone in the pelvis is relatively low. Therefore, the subchondral bone plate should never be completely removed when an acetabular cup is placed.

To be able to analyze the three-dimensional stress distributions in the pelvic bone adequately, a realistic finite element model of the pelvic bone is needed. Chapter II

describes the development of such a model. Again DEQCT is used; this time to correlate the actual local bone densities from the scans with the Young's moduli of the respective elements. From the CT-scans, the local thickness of the cortical shell is also measured and used as input for the model. Validation of the model is done by simulating a loading experiment of a pelvis in a testing machine. In the actual experiment, the pelvic bones are fitted with strain gages. Numerical and experimental results agree well enough to use the developed model to assess more realistic load cases. This is done in Chapter III, where the load transfer in a normal pelvic bone is evaluated. Eight phases in a normal walking cycle are simulated by assuming realistic values for the hip-joint force and twenty two muscle forces. The cortical shell carries the bulk of the load and, as such, the pelvic bone behaves like a so-called 'sandwich' construction. The most important external load acting on the pelvic bone is the hip-joint force. Although the magnitude of this force varies considerably during walking, its direction remains pointed into the anterosuperior quadrant of the acetabulum. Therefore, in the transfer mechanism of this load the superior acetabular wall plays an important role. Muscle forces have a stabilizing effect on the stress distributions; analyses without muscle forces show that at some locations stresses are actually higher than when muscle forces are included.

Now having a fair idea of the way in which the different parts of the pelvic bone are loaded in the normal case, Chapter IV describes the mechanical consequences of an acetabular reconstruction. The analyses show that the global load transfer through the cortical shell is hardly affected by the presence of an acetabular implant. Locally, changes in the stress patterns do occur in the subchondral bone plate and in the underlying trabecular bone. The deeper part of the subchondral bone becomes sub-normally loaded (stress-shielded), while along the superior edge of the acetabular wall stresses increase. The degree of the shift increases with the stiffness of the cup.

One of the options for cementless fixation of acetabular prostheses is the use of screwed cups. These cups derive their primary stability from generating prestresses in the acetabular wall upon insertion. There were, however, no quantitative data on these stresses, nor was it known how these stresses interact with stresses due to normal loading of the hip joint. In Chapter V, these prestresses are determined both experimentally and in a finite element model for two different types of screwed cups. One had self-cutting thread, the other required pre-tapping. Although the torque needed to insert the cup is twice as high for the former type, this has no influence on the magnitude of the prestresses generated by both types of cups. In some cases the magnitude of these prestresses even approximated the ultimate strength of cortical bone, which implies that a surgeon should always be on his guard against fracturing the bone when inserting a screwed cup. Comparison of the interaction of the prestresses and the stresses due to physiological loading for both types of cups suggests that the primary stability of a metal-backed screwed cup is better guaranteed than the primary stability of a full-polyethylene cup.

The present acetabular cups show a large variety in designs and each of these has its own characteristic influence on the pelvic load transfer. Chapter VI describes the effect of a number of design features on the stress distributions in the various

materials and interfaces. By comparing cementless versus cemented cups, metal-backed versus non-backed cups and cups with thin and thick polyethylene liners, it can be concluded, that the mechanical requirements for acetabular cups are subject to incompatible design goals. Increasing the stiffness of the cup, either by using acrylic cement and/or a metal backing or by having a thicker polyethylene layer, results in a decrease of the stresses in the polyethylene liner, which might result in less wear of the polyethylene. However, a stiffer cup also means more stress shielding in the bone at the dome of the acetabulum together with stress rises around the edge of the acetabular wall, as was already described in Chapter IV. Possible consequences of this are an increased risk for interface failure and bone resorption in the dome area. Analyses using the three-dimensional model show that metal-backed cups will be the most affected by this. Therefore, the alleged mechanical advantage of metal backing, put forward by earlier finite element studies, can not be confirmed.

Because of the controversy in the mechanical function of metal backing for acetabular cups described in Chapter VI, a numerical optimization method is employed in Chapter VII to find possible solutions for an optimal distribution of local stiffnesses in a (metal) backing. The aim is to find a backing, which would keep the stresses in the polyethylene low, while generating smooth stress distributions in the cement and underlying bone as well. The analyses predict that a backing answering these requirements should only have a relatively high stiffness in the anterosuperior periphery. Everywhere else, it should be so flexible that the backing might as well be absent. So, with regard to generating optimal loading conditions in the cement and the underlying bone, a partial reinforcement of the polyethylene cup might be a good solution. However, in practical terms there are perhaps other ways of local stiffening which are more preferable, like a variable thickness of the cement mantle or the polyethylene.

Conclusion

The pelvic bone is a fine example of a natural 'sandwich' construction. Its trabecular structure of low-density material and its thin cortical shell, which carries the bulk of the load, make it a very efficient mechanical structure, able to transfer loads of many times body weight. Because of its irregular geometry, loading of the pelvic bone is typically three-dimensional in nature. Stress distributions for various load cases show that certain locations are consistently higher loaded than others. Especially the anterosuperior acetabular wall and the incisura ischiadaca region play an important role in the load transfer across the pelvic bone. As a consequence, the cortical shell is thicker and the trabecular bone is more dense (and thus stiffer and stronger) at these locations. The overall load transfer through the cortical shells is hardly affected by the placement of an acetabular prosthesis. Yet, locally in the acetabular region, the load transfer becomes different from the normal situation. Just like a femoral stem, an acetabular cup also causes stress shielding in the surrounding bone. And just like for a femoral stem, the degree of this stress shielding is

dependent on the flexibility of the implant. Stiffer cups have the tendency to shift the load transfer from the dome of the acetabulum towards the superior edge of the acetabular wall. This involves local stress increases relative to more flexible cups. It is therefore suggested that metal backing for acetabular cups should be carefully reconsidered. There is still a general opinion that a metal backing reduces the stresses in the cement and the underlying bone, which is largely based on results from studies with geometrically simplified models. The more realistic models show just the opposite. Although the higher interface strength between bone and metal, relative to bone and polyethylene, may justify the use of metal backing for cementless designs, metal backing should not be considered for cemented cups. However, a stiff cup generates lower stress levels in the polyethylene, which suggests that wear of the polyethylene might be less. Because polyethylene wear particles are considered an important contributor to tissue reactions around both femoral and acetabular components, which may ultimately lead to aseptic loosening of the implant, there is also evidence in favor of metal backing. This shows that the mechanical requirements for acetabular prosthesis are in fact subject to incompatible design goals. Therefore, a better insight in the clinical/biological factors playing a role in the failure of acetabular prostheses will be required before it can be decided which road should be taken next.

Samenvatting en conclusie

De totale heup arthroplastiek heeft de laatste twee decennia een enorme ontwikkeling doorgemaakt. Nieuwe inzichten, voortgekomen uit fundamenteel onderzoek en klinische evaluatie, hebben geleid tot verbeterde ontwerpen en operatie technieken. De meeste aandacht werd hierbij besteed aan het femorale deel met als gevolg dat wij nu weten dat mechanische factoren een belangrijke rol spelen in het klinisch functioneren van femorale prothesen. Deze factoren kunnen zelfs beslissend zijn voor het uiteindelijke succes of falen van het implantaat. Voor het acetabulaire deel zijn dergelijke inzichten echter minder ontwikkeld, waardoor er nog geen consensus is bereikt aangaande de factoren die een succesvol ontwerp bepalen. De studies welke beschreven staan in dit proefschrift zijn bedoeld om een beter beeld te krijgen van de mechanica van het heupbeen en hoe deze wordt beïnvloed wanneer een acetabulaire reconstructie is uitgevoerd. De behandelde onderwerpen omvatten de mechanische eigenschappen van trabeculair bot in het heupbeen, belastingsoverdracht en spanningsverdelingen in zowel een normaal heupbeen als een gereconstrueerd heupbeen en de mechanische consequenties van verschillende ontwerpen van acetabulaire cups. In deze studies zijn zowel experimentele methoden als computer simulaties gebruikt, maar de nadruk ligt op de ontwikkeling en het gebruik van een realistisch driedimensionaal eindige elementen model van het heupbeen.

Samenvatting van de Hoofdstukken I tot VII

Afgezien van een dunne corticale schil, bestaat een heupbeen geheel uit trabeculair bot. Mechanische eigenschappen van dit type bot, zoals stijfheid en sterkte, kennen een grote variatie en hangen af van de plaats in het skelet en de mechanische functie. Over de mechanische eigenschappen van het trabeculaire bot in het heupbeen zijn echter nagenoeg geen kwantitatieve gegevens bekend. Daarom worden in Hoofdstuk I de mechanische eigenschappen en de structuur van dit bot bestudeerd. Dual Energy Quantitative Computer Tomography (DEQCT) laat zien dat de dichtheid van het bot in het heupbeen overwegend relatief laag is. De hoogste dichtheden worden gevonden in het superieure deel van de acetabulaire wand, maar de volume fractie ligt hier evenwel nog beneden de 20%. De stijfheid van trabeculair bot wordt voor een groot deel bepaald door de dichtheid met als gevolg dat de elasticiteitsmoduli, gemeten aan kleine blokjes bot in non-destructieve testen, ook erg laag uitvallen. Voor de meeste proefstukjes blijft deze waarde ruim beneden 100 MPa, terwijl waarden van 2000 MPa niet uitzonderlijk zijn voor trabeculair bot uit het femur of de tibia. Ofschoon niet gemeten, valt het te verwachten dat de sterkte van het trabeculaire bot in het heupbeen dan ook relatief laag is. Daarom zou de subchondrale botplaat nooit geheel

verwijderd mogen worden wanneer een acetabulaire cup wordt geplaatst.

Een realistisch eindige elementen model van het heupbeen is nodig om de drie-dimensionale spanningsverdelingen goed te kunnen analyseren. In Hoofdstuk II wordt de ontwikkeling van een dergelijk model behandeld. Hierbij is opnieuw gebruik gemaakt van DEQCT; ditmaal om de lokale dichtheden, gemeten in het heupbeen, te correleren aan de elasticiteitsmodulus van het trabeculaire bot op de overeenkomstige plaats in het model. Vanaf de CT-scans wordt tevens de lokale dikte van de corticale schil opgemeten en ingevoerd in het model. Validatie van het model bestaat uit het simuleren van een belastingsexperiment van een bekken in een trekbank. In het eigenlijke experiment, zijn de heupbeenderen beplakt met rekstrookjes. De numerieke en experimentele resultaten blijken goed overeen te komen, zodat het model gebruikt kan worden voor meer realistische belastinggevallen. Dit gebeurt in Hoofdstuk III, waar de belastingsoverdracht in een normaal heupbeen wordt geëvalueerd. Acht fasen in een normale loopcyclus worden gesimuleerd, waarbij realistische waarden voor de heupreaktielkracht en tweeëntwintig spierkrachten zijn aangenomen. De corticale schil draagt het grootste deel van de belasting en als zodanig gedraagt het heupbeen zich als een zogenaamde sandwich constructie. De heupreaktielkracht is de belangrijkste externe belasting die op het heupbeen werkt. Hoewel de grootte van deze kracht aanzienlijk varieert tijdens het lopen, blijft deze gericht naar het anterosuperieure kwadrant van het acetabulum. Daarom speelt in de overdracht hiervan de superieure wand van het acetabulum dan ook een belangrijke rol. De spierkrachten hebben een stabiliserend effect op de spanningsverdelingen; analyses zonder spierkrachten laten zien dat op sommige plaatsen de spanningen zelfs hoger zijn dan wanneer de spierkrachten wel worden meegenomen.

Nu het bekend is in welke mate de verschillende delen van een heupbeen in het normale geval belast worden, wordt in Hoofdstuk IV beschreven wat de mechanische gevolgen zijn van een acetabulaire reconstructie. De analyses laten zien dat de globale belastingsoverdracht niet of nauwelijks beïnvloed wordt door de aanwezigheid van een acetabulaire prothese. Lokaal treden er echter wel degelijk veranderingen op in de spanningen in de subchondrale laag en het onderliggende trabeculaire bot. Het dieper gelegen deel van het subchondrale bot wordt namelijk minder zwaar belast dan normaal, terwijl de spanningen langs de superieure wand van het acetabulum juist toenemen. De mate van deze verschuiving neemt toe met de stijfheid van de cup.

Eén van de opties voor cementloze fixatie van acetabulaire prothesen is het gebruik van schroefcups. Dergelijke cups ontleen hun primaire stabiliteit aan het genereren van voorspanningen in de acetabulaire wand tijdens implantatie. Er bestonden echter geen kwantitatieve gegevens over deze spanningen en bovendien was het niet bekend wat de interactie is tussen deze spanningen en de spanningen ten gevolge van het normale belastingspatroon. In Hoofdstuk V worden deze voorspanningen zowel experimenteel als numeriek bepaald voor twee verschillende types schroefcups. De ene heeft zelf-snijdende draad, voor de ander is het nodig vooraf schroefdraad in het bot te tappen. Hoewel hierdoor het benodigde aandraaimoment om de cup goed te plaatsen tweemaal zo groot is voor het eerste type, heeft dit geen invloed op de grootte van de voorspanningen. In een aantal gevallen benaderde deze

zelfs de treksterkte van corticaal bot, hetgeen betekent dat een operateur altijd op zijn hoede moet zijn voor scheurtjes in het bot tijdens het plaatsen van een schroefcup. Uit het vergelijk van de interactie van de voorspanningen en de spanningen door het normale belastingspatroon voor beide typen cups volgt dat de primaire stabiliteit van een schroefcup met metal backing beter gewaarborgd lijkt dan die van een schroefcup geheel van polyetheen.

De huidige acetabulaire cups kennen een grote variëteit in ontwerp en elk specifiek ontwerp heeft zo zijn eigen karakteristieke invloed op de belastingsoverdracht in het heupbeen. In Hoofdstuk VI wordt de invloed van een aantal ontwerp-karakteristieken op de spanningsverdelingen in de verschillende materialen en interfaces beschreven. Uit het vergelijken van gecementeerde en cementloze cups, cups met en zonder metal backing en cups met een dunne en dikke polyetheen laag, kan geconcludeerd worden dat de mechanische eisen onderhevig zijn aan onverenigbare ontwerp doelstellingen. Toename van de stijfheid van de cup, hetzij door de aanwezigheid van botcement en/of een metal backing, hetzij door een dikkere laag polyetheen, resulteert enerzijds in een afname van de spanningen in het polyetheen, hetgeen gunstig zou kunnen zijn met het oog op slijtage. Anderzijds betekent een stijvere cup echter 'stress shielding' van het bot onderin het acetabulum en een spanningstoename langs de rand van het acetabulum, zoals reeds besproken is in Hoofdstuk IV. Mogelijke consequenties hiervan zijn een verhoogde kans op het falen van de interface en botresorptie onderin het acetabulum. Analyses met het drie-dimensionale eindige elementen model voorspellen dat cups met een metal backing hieraan het meest onderhevig zijn. Hierdoor kan het algemeen veronderstelde mechanische voordeel van dergelijke cups, gebaseerd op resultaten van eerdere eindige elementen studies, niet bevestigd worden.

Vanwege de controverse in de mechanische functie van acetabulaire cups, beschreven in Hoofdstuk VI, wordt in Hoofdstuk VII een optimalisatie routine gebruikt om een mogelijke oplossing te vinden voor een optimale verdeling van de lokale stijfheid in een (metal) backing. Het is de bedoeling een backing te vinden die de spanningen in het polyetheen laag houdt, terwijl de spanningen in het cement en het onderliggende bot egaal verdeeld worden. De berekeningen laten zien dat een backing, die hieraan voldoet, alleen een hoge stijfheid dient te hebben langs de anterosuperieure rand. Op de andere plaatsen dient de backing zo flexibel te zijn, dat deze net zo goed afwezig zou mogen zijn. Hieruit volgt dat voor een optimale spanningsverdeling in het cement en het onderliggende bot een partiële versteviging van het polyetheen van de cup een goede oplossing zou kunnen zijn. In de praktijk zijn misschien echter andere manieren van lokale versteviging te prefereren, zoals een variabele dikte van de laag botcement of het polyetheen.

Conclusie

Het heupbeen is een fraai voorbeeld van een natuurlijke sandwich constructie. De trabeculaire structuur van bot met lage dichtheid en de dunne corticale schil, welke

het grootste deel van de belasting draagt, maken het tot een efficiënte mechanische structuur, die in staat is een veelvoud van het lichaamsgewicht te dragen. Door de grillige vorm is de belasting typisch drie-dimensionaal van aard. Spanningsverdelingen voor verscheidene belastingsgevallen laten zien dat bepaalde plekken consistent hoger belast worden dan andere. Met name de anterosuperieure wand en het gebied rond de incisura ischiadaca spelen een belangrijke rol in de belastingsoverdracht in het heupbeen. Als gevolg hiervan is de corticale schil hier dan ook dikker en het trabeculaire bot dichter van structuur (en dus stijver en sterker). De globale belastingsoverdracht wordt nauwelijks beïnvloed door de aanwezigheid van een acetabulaire prothese. Maar rondom het acetabulum verandert de belastingsoverdracht wel degelijk. Net als een femorale steel veroorzaakt een acetabulaire cup ook 'stress shielding' in het omliggende bot. En net als bij een femorale steel hangt de mate van 'stress shielding' in het bot af van de stijfheid van het implantaat. Stijvere cups hebben de neiging de belastingsoverdracht te verschuiven van het dieper gelegen deel van het acetabulum naar de buitenrand van de acetabulaire wand. Dit gaat gepaard met lokale spanningstoename ten opzichte van meer flexibele cups. Hierdoor zou het nut van metal backing voor acetabulaire cups heroverwogen moeten worden. Er bestaat nog steeds een idee dat deze de spanningen in het botcement en het onderliggende bot vermindert, gebaseerd op resultaten van studies met geometrisch sterk gesimplificeerde modellen. De meer realistische modellen laten echter juist het tegenovergestelde zien. Hoewel de hogere sterkte van de interface tussen bot en metaal dan die tussen bot en polyetheen het gebruik van metal backing voor cementloze ontwerpen wellicht rechtvaardigt, kan een metal backing beter niet gebruikt te worden bij gecementeerde cups. Echter bij een stijve cup zijn de spanningen in het polyetheen wel lager, hetgeen impliceert dat de slijtage van polyetheen mogelijk ook lager zal zijn. Daar slijtage deeltjes van polyetheen gezien worden als een belangrijke bijdrage aan de weefselreacties rond zowel de femorale als de acetabulaire component en zodoende uiteindelijk kunnen leiden tot het aseptisch loslaten van het implantaat, is er ook iets te zeggen voor een metal backing. Hieruit blijkt dat de mechanische eisen voor een acetabulaire prothese in wezen onderhevig zijn aan incompatibele ontwerp doelstellingen. Het is daarom noodzakelijk eerst een beter zicht te krijgen op de klinisch/biologische factoren, die een rol spelen bij het falen van acetabulaire prothesen, alvorens te kunnen bepalen welke weg ingeslagen dient te worden.

Curriculum vitae

Michel Dalstra was born on November 15, 1961 in Enschede. After graduation at the "Scholengemeenschap Zuid" highschool/college in 1980, he attended the Faculty of Mechanical Engineering of the University of Twente and it was here that he developed a special interest in biomechanics. Besides his studies, he was involved in the activities of the University's Biomedical Study Association, "Paradoks", as editor-in-chief of its magazine, "Parallaks". In the spring of 1985, he spent a three-months training period at the Bioengineering Centre of the Department of Mechanical Engineering, University College London, testing mechanical properties of plastics used in artificial limbs. His study was completed by a graduation project, entitled "The development of a computer model to simulate bone remodeling", which was performed at the Biomechanics Section of the Institute of Orthopaedics, University of Nijmegen under joint supervision of Prof. H.J. Grootenboer (University of Twente) and Prof. R. Huiskes (University of Nijmegen).

After receiving his M.Sc.-degree in the fall of 1986, he endured the mandatory fourteen months of military service being stationed at the staff of the 541st communication battalion in Deventer. In January 1988, he returned to the Biomechanics Section in Nijmegen as a research assistant. Here, he initially worked on several short-term projects which involved mechanically testing and analyzing various hip arthroplasties. In October 1988, a Ph.D.-project was started which resulted in the present dissertation. Some of the work for this was done in collaboration with the Biomechanics Laboratory of the University of Aarhus, Denmark. His affection for this institute made him decide to apply for a research position and he is, therefore, very pleased that this was granted; in December 1993, he will take up a position there as associate professor and will be working in the field of bone mechanics.

STELLINGEN

- I Het trabeculaire bot in het heupbeen heeft geen directe gewichtsdragende functie; conform de Wet van Wolff is de dichtheid van dit bot dan ook duidelijk lager dan die van het trabeculaire bot in het femur of de tibia.
- II Na het plaatsen van een totale heup arthroplastiek is, net als in het femur, de mate van *stress shielding* in het bekken afhankelijk van de stijfheid van het implantaat.
- III Zonder voorkennis van de richtingen van de hoofdasen van het materiaal is het onmogelijk de negen onafhankelijke elasticiteitsconstanten te bepalen voor een orthotroop materiaal uit een serie conventionele non-destructieve drukproeven.
- IV Aseptische loslating van implantaten is waarlijk een biomechanisch proces.
- V Het aan een *metal backing* van een acetabulum prothese toegeschreven mechanische voordeel van het verlagen van de spanningen in het onderliggende botcement en bot, is niet waar; langs de rand van het acetabulum zijn de spanningen juist hoger voor een cup met *metal backing*.
- VI In de toenemende vercommercialisering van het omroepbestel laat de BBC zien dat voor een hoge kwaliteit van televisieprogramma's reclame toch geen vereiste is.
- VII De bijdrage van adaptieve botremodellering aan het falen van orthopedische implantaten wordt nog steeds niet voldoende onderkend.
- VIII De voornaam *Bareld* bij autochtone families uit Drachten en omstreken kan via vernoeving teruggevoerd worden op één gemeenschappelijke voorvader, zijnde Bareld Allerts, boer te Ureterp in de tweede helft van de zestiende eeuw.
- IX Optimalisatie van de locale stijfheid van het implantaat is voor een acetabulaire component van een totale heup arthroplastiek minder effectief dan voor de femorale component.
- X Een schrijver is iemand die schrijven moeilijker vindt dan anderen. (Thomas Mann)
- XI Het merendeel van de publicaties, die het begrip 'totale heup arthroplastiek' of een synoniem hiervan in de titel voeren, behandelen inhoudelijk slechts de femorale component; klinische resultaten tonen echter aan dat deze desinteresse in de acetabulaire component niet terecht is.
- XII Vanwege de zeer geringe sterkte van het trabeculaire bot in het heupbeen, dient bij het implanteren van een acetabulaire cup de subchondrale laag in het acetabulum zoveel mogelijk gespaard te blijven.
- XIII Het grote publiek verwisselt de historische figuur van koning Richard III van Engeland (1450-1485) met de toneelfiguur uit het gelijknamige toneelstuk van William Shakespeare, hetgeen aantoont dat zelfs na vijfhonderd jaar de lastercampagne gelanceerd door de hem opvolgende Tudor vorsten nog steeds effect heeft.